NITRIC OXIDE-PRODRUG MEDIATED MOLECULAR AND BIOENERGETIC ALTERATIONS IN CARDIAC AND SKELETAL MYOBLASTS IN HYPERGLYCEMIA

ANAND C. R.

Ph.D. Thesis

2020

SREE CHITRA TIRUNAL INSTITUTE FOR MEDICAL SCIENCES AND TECHNOLOGY TRIVANDRUM

NITRIC OXIDE-PRODRUG MEDIATED MOLECULAR AND BIOENERGETIC ALTERATIONS IN CARDIAC AND SKELETAL MYOBLASTS IN HYPERGLYCEMIA

A THESIS PRESENTED

BY

ANAND C. R.

TO

SREE CHITRA TIRUNAL INSTITUTE FOR MEDICAL SCIENCES AND TECHNOLOGY, TRIVANDRUM
Thiruvananthapuram

IN PARTIAL FULFILLMENT OF THE REQUIREMENTS

FOR THE AWARD OF

DOCTOR OF PHILOSOPHY

2020

DECLARATION BY STUDENT

I, **Mr. Anand C. R.**, hereby certify that I had personally carried out the work depicted in the thesis entitled "**NITRIC OXIDE-PRODRUG MEDIATED MOLECULAR AND BIOENERGETIC ALTERATIONS IN CARDIAC AND SKELETAL MYOBLASTS IN HYPERGLYCEMIA"** under the direct supervision of Dr. G. Srinivas, Scientist F, Department of Biochemistry, Sree Chitra Tirunal Institute for Medical Sciences and Technology, Trivandrum, except where external help was sought and is acknowledged. No part of the thesis has been submitted for the award of any other degree or diploma prior to this date.

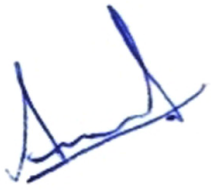

Date: 28/12/2020 ANAND C R

CERTIFICATE BY THE RESEARCH GUIDE

This is to certify that Mr. Anand C R has fulfilled the requirements prescribed for the PhD degree of the Sree Chitra Tirunal Institute for Medical Sciences and Technology, Trivandrum. The thesis entitled "**NITRIC OXIDE-PRODRUG MEDIATED MOLECULAR AND BIOENERGETIC ALTERATIONS IN CARDIAC AND SKELETAL MYOBLASTS IN HYPERGLYCEMIA**" was carried out under my direct supervision. No part of the thesis has been submitted for the award of any other degree or diploma prior to this date.

Date: 28/12/2020 Dr. G. Srinivas (Guide)

The thesis entitled

NITRIC OXIDE-PRODRUG MEDIATED MOLECULAR AND BIOENERGETIC ALTERATIONS IN CARDIAC AND SKELETAL MYOBLASTS IN HYPERGLYCEMIA

submitted by

ANAND C R

for the Degree of

Doctor of Philosophy

of

SREE CHITRA TIRUNAL INSTITUTE FOR MEDICAL SCIENCES AND TECHNOLOGY, TRIVANDRUM

Thiruvananthapuram

is evaluated and approved by

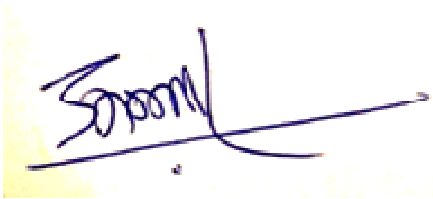

Dr. Srinivas G

(Guide)

(Dr. Suvro Chatterjee)

(Examiner)

ACKNOWLEDGEMENT

I consider myself privileged to have had the opportunity to carry out my doctoral studies in the Department of Biochemistry, Sree Chitra Tirunal Institute for Medical Sciences and Technology, Trivandrum, Kerala, India. I was fortunate to be associated with three Directors, Dr. Jagan Mohan Tharakan, Dr. Asha Kishore and last but not least, Dr. K. Jayakumar who kindly served as my DAC member as well. I am extremely grateful to them for their support and the excellent facilities at the institute. I gratefully acknowledge the fellowship awarded by CSIR (09/523(0082)/2014-EMR-1) to undertake the PhD program.

I express my extreme gratitude to my research guide, Dr Srinivas Gopala for his timely help, support and advice during my PhD course. His encouragement, constant support and contributions to my work have helped me greatly in the successful completion of my studies.

I am extremely grateful to the Deputy Registrars (former and current), Mrs. M. Radha, Dr. Santhosh Kumar B. and Dr. Sundar Jayasingh, for their constant encouragement.

I express my sincere thanks to Dr. Appukuttan P.S, Dr. N. Jayakumari, former HODs of the Department of Biochemistry, for their encouragement and advice. I also express my gratitude to Dr. Madhusoodanan U. K. and Dr. Cibin T. R., the other faculties of Biochemistry department and all other staffs. I thank Dr. Shivakumar K from the Division of Cellular and Molecular Cardiology, Sree Chitra Tirunal Institute for Medical

Sciences and Technology, for his frank assessments, suggestions and advice in my PhD work.

I also thank Dr. Renuka R Nair, DCMC, Dr. K. Jayakumar once again, former head of the Department of CVTS, SCTIMST, Dr Harikrishnan V.S, Scientist ‘E’, DLAS, BMT Wing, for serving on my Doctoral Advisory Committee.

A special thanks to Dr. S. Lakshmi from the Department of Molecular Medicine, Regional Cancer Centre, Trivandrum, for helping me with the Flow cytometry experiments and analysis. I also express my gratitude to Dr. K. A. Abdul Jaleel, Mr. A. Aneesh Kumar and Mr. Mahesh S. from the Department of Cardiovascular Diseases and Diabetes Biology of Rajiv Gandhi Centre for Biotechnology, Trivandrum, for helping me in performing the Mass-Spectrometric experiments. I also thank the staff of DLAS, staff of the Microbiology department, staff of Research & Publication Cell and students of DCMC for their support.

I would also like to thank all my lab mates and staff of Department of Biochemistry for their support throughout my PhD course. Also I extend my acknowledgement to the staff of the Molecular Genetics and Neuroimmunology Unit, for their encouraging words. I cannot end without acknowledging my parents, for their continued encouragement, unconditional support and blessings and my brother who have backed me in all my endeavors.

Contents

List of Figures

List of Tables

Synopsis

Nitric Oxide (NO) is the first gas known to act as a biological messenger. It is a free radical that plays critical roles in the regulation of a multitude of cellular processes in both health and disease conditions. When released from the endothelium, it regulates normal blood flow delivery of nutrients to tissues. The endothelial NO synthase (eNOS) is the major contributor of NO under normal physiological conditions, but the bioavailable NO from this so-called classical pathway of NO synthesis is routinely depleted during conditions pertaining to cardiovascular disease and dysfunction. Both Type 1 & Type 2 diabetic (T1DM & T2DM) patients have been found to possess a reduced ability to generate NO from L-arginine. This reduction in the bioavailability of NO is partly due to the quenching of NO molecules by superoxide anions. NO quenched by superoxides lead to the production of $ONOO^-$ that react with tyrosine residues in specific proteins and consequently nitrating them, depending upon the oxidative status of the microenvironment. Exogenous application of nitrate or nitrite can significantly enhance the systemic NO availability and has been shown to contribute to cardioprotection in experimental studies. Sodium nitrite administration provides protection against myocardial ischemia-reperfusion (I/R) injury in a pig regional ischemia model when compared to control pigs. Here, the beneficial effects included an increase in reactive oxygen species (ROS) scavenging enzymes like glutathione peroxidase (GPx), superoxide dismutase (SOD) and catalase with a concomitant rise in NO2– /NO3– levels. The preservation of mitochondrial structure and function remains the central objective in cardioprotection strategies. In the setting of T2DM, a major manifestation is the fragmentation of the cardiac mitochondrial network, which is associated with a significant downregulation of mitochondrial fusion machinery. The effect of hyperglycemia per se has been studied in neonatal rat ventricular myocytes, where high glucose-mediated mitochondrial dysfunction was linked to dynamin-related protein (Drp1)-induced mitochondrial fission and activation of pro-apoptotic pathways. In another study with cardiomyocytes, prolonged exposure to high glucose elevates ROS levels, derails the tubular network of mitochondria and subsequently induces mitochondrial permeability transition (MPT) pore opening. Consequently, there is a perturbed mitochondrial function and increased myocardial oxidative stress. The nitrite anion is reported to modulate mitochondrial fission under normoxia too; nitrite

preconditioning activates Protein kinase A (PKA), a pro-survival kinase and inactivates Drp1 thereby promoting mitochondrial fusion and renders cytoprotection on an ensuing simulated Ischemia/Reperfusion. There are reports that inorganic nitrite therapy may be involved in the regulation of glucose-insulin homeostasis and fatty acid metabolism in skeletal muscle though no studies have been done pertaining to organ-specific beneficial effects on cardiac muscle in the setting of hyperglycemia. Nevertheless, the administration of compounds those endow with bioavailable NO is delimited by several drawbacks: toxicity, tolerance, systemic hypotension (due to their inability of site-specific NO delivery) and aggravation of endothelial dysfunction. These negative effects are related to the massive production of reactive species derived from oxygen or nitrogen, which trigger oxidative and nitrosative stress. The primary scope of this study can be delineated as to analyze beneficial/detrimental alterations in mitochondrial dynamics and function in cardiac and skeletal myoblasts inflicted by nitrite or NO donor supplementation under hyperglycemia.

Methods: H9c2 myoblasts of rat embryonic heart origin were used for the majority of the experiments while some experiments were performed with C2C12 murine skeletal myoblasts also. H9c2 cells were used to study the effect of inorganic nitrite and NO donor SNAP in the presence of hyperglycemia. The myoblasts were serum-deprived for 24 h at 80% confluency and supplied with 1% FBS containing DMEM having either 5.5 mM [Normal Glucose (NG)] or 30 mM [(High Glucose (HG)] along with and without sodium nitrite (500 μM). The treatment duration was 24 h for all experiments but the respirometric analysis where 48 h time point was used. The NO donor SNAP treatment was given only for the last 4 h of the different glucose treatments owing to its short half-life. Cell viability analysis and ROS measurements were done to validate the model. Fluorescence techniques, high-resolution respirometry, and western blot were the major methods used. The in vitro effects of inorganic nitrite supplementation on mitochondrial ROS generation, dynamics and respiration and levels of antioxidant enzymes were studied in the first part under normal and high glucose (NG and HG) conditions. The second set of experiments analyzed the specific effect of the above treatments on Drp1 activity and pro-survival kinases like Akt1, GSK3β, and Pim1 that have been reported to influence the former elsewhere. In the third part, the differential effects of Drp1 silencing

over nitrite supplementation under the two glycemic levels were studied. Silencing of Drp1 was done using 50 nM Drp1 siRNA which rendered maximum reduction in Drp1 protein expression at 48 h post-transfection. The high glucose and nitrite additions were done along with respective controls at the final 24 h post-transfection for most experiments but were extended for another 24 h for the respirometric studies. In statistical analysis, multiple comparisons between groups were done using either one-way or two-way ANOVA followed by Tukey's or Dunnett's post hoc multiple comparison tests. Data represented in percentages were analyzed by Kruskal Wallis with Dunn's post hoc test. The differences among the mean values were considered significant at $p \leq 0.05$.

Major findings: Inorganic nitrite treatment reduces the intracellular ROS levels insignificantly under high glucose (HG) condition, besides decreasing the mitochondrial ROS production in particular. However, nitrite further reduces the diminished mitochondrial membrane potential inflicted by HG as indicated by less tubular mitochondria on JC1 staining. Concomitantly, nitrite treatment under HG leads to enhanced expression of mitochondrial membrane proteins, uncoupling protein 3 (UCP3) and adenine nucleotide translocase 1 (ANT1) and alterations in levels of the antioxidant enzymes GPx4 and mitochondrial SOD (SOD2). These indicate that nitrite is abrogating the high glucose-induced mitochondrial fragmentation and MPT opening albeit without a concomitant increase in ROS levels. Respirometric studies conducted with a polarographic oxygen sensor (Oroboros Oxygraph O2k) showed no significant changes in coupling efficiency by the cells treated with nitrite/SNAP under HG in comparison with their respective controls. Coupling efficiency represents the percent of oxygen consumption linked to ATP production with that linked to basal respiration of the intact cells at 37°C. Basal or routine respiration includes both the oxygen consumption driven by the ATP demand as well as by the proton leak pathways. The absence of changes in coupling efficiency even at 48 h time point suggests a maintained mitochondrial function pertaining to oxygen consumption. Immunoblot analysis showed that both nitrite and SNAP caused Akt1 inactivation (reduction in the activation phosphorylation at Ser473) under HG and a concomitant Drp1 activation leading to altered mitochondrial morphology (less reticulate mitochondria). Moreover, HG-nitrite reduced activation of Akt1 is linked with a reduction in the expression of a pro-survival kinase, Pim1 which

has been reported to increase the inactivation phosphorylation at Ser-637 residue of Drp1. Another kinase that is downstream of Akt and upstream of Drp1 is the GSK3β whose kinase domain is rendered inactive by phosphorylation at Ser-9 by an activated Akt1. Nevertheless, the Ser-9 phosphorylation was insignificantly reduced in HG-nitrite group indicating the action of other kinases on GSK3β. Optic atrophy 1 (OPA1), a regulator of inner mitochondrial membrane fusion was also not altered by either nitrite or SNAP under HG implying absence of repercussions on fusion machinery, though fission is being upregulated.

Silencing of Drp1 leads to differential effects by nitrite under NG vs. HG conditions. Drp1 silencing elevates the expression of OPA1 in normoglycemia with/without nitrite treatment whereas in HG OPA1 was already elevated that Drp1 silencing rendered an insignificant change in OPA1 expression. Nitrite supplementation enhances mitochondrial coupling efficiency of Drp1-silenced cells under NG but not under HG. On analyzing the protein levels of molecules involved in apoptosis and mitophagy, two processes that are closely related to mitochondrial fission, significant alterations were observed. Caspase 7, an effector caspase in apoptotic signaling, is downregulated in Drp1 silenced cells under HG with/without nitrite supplementation, whereas no significant change was observed under NG. However, the apoptotic marker cleaved PARP levels were not altered by Drp1 silencing under HG. Anti-apoptotic protein, Bcl2 is reduced in Drp1 silenced cells under HG with/without nitrite supplementation but not under NG. In the case of mitophagy regulators, PTEN induced kinase 1 (Pink1) is reduced in Drp1 silenced cells under both glycemic levels irrespective of nitrite treatment. Another molecule involved maintaining mitochondrial integrity and autophagy is Parkin. The Parkin levels are elevated from endogenous levels in Drp1 silenced cells only under normoglycemia with/without nitrite supplementation. The supplementation of nitrite in the presence of high glucose not only deteriorates the mitochondrial derangements pertaining to the fission machinery but also does not improve the respiratory efficiency as reported in previous literature. Moreover, downregulation of pro-survival pathways reveals the deleterious effects imparted by the anion. These observations, albeit requiring further validation, underscore the key role played by Drp1 in determining the effects of nitrite and HG on myoblasts.

Discussion: Inorganic nitrite is reported to increase mitochondrial fusion in cardiomyocytes by modulating the Drp1 activity. Subsequently, this leads to the enhancement of mitochondrial membrane potential and superoxide generation from the fused mitochondria. These events have been demonstrated under normoxic conditions where there are basal levels of ROS being generated. However, the presence of high levels of ROS in the setting of hyperglycemia exhibit a new challenge for the nitrite mediated cytoprotection. In the present study, we addressed the same and investigated the effects and mechanisms of nitrite mediated modulations on mitochondria under hyperglycemia. Interestingly, it was observed that nitrite reduces albeit insignificantly the ROS levels that are elevated in high glucose condition as opposed to the effect seen under normoxia/normoglycemia. There was a contrast in the associated events too. The mitochondrial membrane potential diminished with a simultaneous increase in mitochondrial fission. A decrease in the inhibitory phosphorylation of Drp1 and a concomitant decrease in Akt1 activity and Pim1 kinase expression bestow a possible mechanism behind the above events. Also, the studies with Drp1 silencing revealed a differential effect of nitrite on cardiomyoblasts depending on the glycemic levels highlighting the significance of Drp1 in nitrite mediated changes under hyperglycemia.

Significance of the study: Our data substantiate the need for addressing the systemic effect of nitrite/nitrate therapy covering individual organs so as to validate the reported benefits in the setting of metabolic disorders. The above findings uphold a pressing need for addressing any inexactitude of optimistic outcomes from clinical trials pertaining to cardiovascular health in metabolic syndrome. In a scenario where a dichotomy prevails in the current stance of the scientific community about the use of nitrite/nitrate as supplements to patients with metabolic syndrome, there is a need for delving deep into their molecular and biochemical targets and the changes effected by them.

“Over the long term, symbiosis is more useful than parasitism. More fun, too. Ask any mitochondria.”

— Larry Wall

I. Introduction

Nitric Oxide (NO) is the first gas known to act as a biological messenger. It is a free radical that plays critical roles in the regulation of a multitude of cellular processes in both health and disease conditions. When released from the endothelium, it regulates the normal blood flow for delivery of nutrients to tissues. The endothelial NO synthase (eNOS) is the major contributor of NO under normal physiological conditions, but the bioavailable NO from this so-called classical pathway of NO synthesis is routinely depleted during conditions pertaining to cardiovascular disease and dysfunction (Lundberg et al., 2008). Both Type 1 & Type 2 diabetic (T1DM & T2DM) patients have been found to possess a reduced ability to generate NO from L-arginine. Apart from this, increased scavenging of NO by the formation of reactive oxygen species may also lead to NO deficiency (Omar et al., 2016; Omar and Webb, 2014; PACHER et al., 2007). This reduction in the bioavailability of NO plays a key role in the pathophysiology of metabolic dysfunction (d'El-Rei et al., 2016). NO has an essential role in endothelium-dependent vasodilation and hence regulation of vascular tone (Walker et al., 2019). Nevertheless, NO has also been associated with detrimental effects in the cells which can be particularly attributed to its oxidative product peroxynitrite ($ONOO^-$) interacting with proteins, lipids and DNA (PACHER et al., 2007). NO combines with superoxides leading to the production of $ONOO^-$ that react with tyrosine residues in specific proteins and consequently nitrating them, or nitrosylate proteins like Glutathione peroxidase, both rendering an altered activity of the targeted proteins (Kuzuya and Nishida, 2000; Landino, 2008; PACHER et al., 2007).

I.1. Background studies

In the mid 1990s, it was found that apart from the nitric oxide generated by the NO synthases (NOS), biological tissues can generate NO from other oxides of nitrogen, the nitrate and nitrite anions that circulate throughout the mammalian system (Benjamin et al., 1994; Lundberg et al., 1994; Zweier et al., 1995). This NO production was initially thought to be non-enzymatic and mediated through redox reactions under acidic and hypoxic conditions (Lundberg et al., 1994; Zweier et al., 1995), but later on several enzymes were found to be involved (Damacena-Angelis et al., 2017; Godber et al., 2000;

Hansen et al., 2016; Jansson et al., 2008; Li et al., 2003; Sparacino-Watkins et al., 2014; Webb et al., 2008). Since then, the inorganic form of nitrate and nitrite have been studied for their beneficial effects in varying aspects including cardiovascular health, exercise physiology, platelet aggregation and more lately, as an antioxidant (Apostoli et al., 2014; Bailey et al., 2014; Lundberg et al., 2011a; Menezes et al., 2019; Raubenheimer et al., 2017; Vanderpool Rebecca and Gladwin Mark T., 2015; Vanhatalo et al., 2010; Velmurugan et al., 2013; Velmurugan et al., 2015; Walker et al., 2019; Weitzberg et al., 2010). Exogenous application of nitrate or nitrite can significantly enhance the systemic NO availability and has been shown to contribute to cardioprotection in experimental studies (Lundberg et al., 2008; Lundberg et al., 2009; Lundberg et al., 2011a; Omar and Webb, 2014; Siervo et al., 2018). The role of nitrate or nitrite derived bioactive oxides of nitrogen becomes momentous when the NOSs are dysfunctional (Lundberg et al., 2011a). The classical pathway of NO synthesis, the L-arginine–NOS–NO pathway is complemented by non-classical nitrate–nitrite–NO pathway (Carlström et al., 2013; Lundberg et al., 2008; Lundberg et al., 2011a; Lundberg et al., 2011b). Inorganic nitrate supplementation increased tissue and plasma levels of bioactive nitrogen oxides and has been associated with a reduction in blood pressure and improvement in endothelial function (Walker et al., 2019). Nitrite has a half life of approximately 20 minutes in the circulation while the half-life for nitrate in plasma is relatively long, approximately 3.8 hours (Guillermo et al., 1995). The activity of oral commensal bacteria and gut flora converts the nitrate to nitrite, which then gets assimilated into circulation, concomitantly leading to an increased plasma nitrite level (Weitzberg *et al.*, 2010). Studies done by Gilchrist *et al.,* have implicated the therapeutic potential of nitrate and nitrite in blood pressure control (Gilchrist et al., 2011a; Gilchrist et al., 2013). Also in eNOS- deficient mice, dietary nitrate supplementation reversed several features of metabolic syndrome including lowering of serum triglycerides and improving the blood pressure (Carlström et al., 2010; d'El-Rei et al., 2016). The use of nitrite salt as a NO prodrug for the treatment of various pathophysiological conditions involving decreased NO bioavailability has ipso facto become increasingly attractive. A clinical trial (ClinicalTrials.gov Identifier: NCT01681810; Start date: October 2012) is being conducted absorbing overweight/obese adults with metabolic syndrome and high blood pressure to examine the effects of daily

inorganic nitrate and nitrite treatment on the cardiometabolic and hormonal disturbances observed in them. This is claimed to be the first human study to investigate the inorganic nitrate or nitrite effects (in any form) on insulin sensitivity in a patient population. Other studies incorporating nitrite and nitrate supplementations have revealed that the former ensures rapid acting effects upon absorption, whereas the latter would constantly provide a slow formation of nitrite over a prolonged period of time via the enterosalivary circulation pathway. In this scenario, elucidation of the biochemical, molecular and physiological activities of nitrite has caught the interest of a school of researchers exploring miscellaneous conditions in normal physiology and pathophysiology of the heart. Mitochondria a critical organelle comprising approximately one-third of the mass of the heart, form a vital component in cellular energy metabolism and regulation of intracellular signaling including apoptotic and non-apoptotic cell death (Camara et al., 2011; Tait and Green, 2012). Maintenance of mitochondrial homeostasis is vital for cardiac cell survival and dysfunction of mitochondria is central to several disorders affecting the heart such as diabetes and ischemic heart diseases (Camara et al., 2011; Carreira et al., 2011). Regulators of mitochondrial dynamics are being sought after as therapeutic targets with more causes and consequences of dysregulated mitochondrial dynamics being discovered each year (Frohman, 2015; Ong et al., 2015; Sharp, 2015; Sharp and Archer, 2015; Tait and Green, 2012). The preservation of mitochondrial structure and function hence remains the central objective in cardioprotection strategies (Ong et al., 2015).

I.2. Identification of the problem

In the setting of T2DM, a major manifestation is the fragmentation of the cardiac mitochondrial network, which is associated with a significant downregulation of mitochondrial fusion machinery. The effect of hyperglycemia *per se* has been studied in neonatal rat ventricular myocytes, where high glucose-mediated mitochondrial dysfunction was linked to dynamin-related protein (Drp1)-induced mitochondrial fission and activation of pro-apoptotic pathways (Frank et al., 2001; Yu et al., 2006). In another study with cardiomyocytes, prolonged exposure to high glucose elevates ROS levels,

derails the tubular network of mitochondria and subsequently induces mitochondrial permeability transition (MPT) pore opening (Yu et al., 2008). Consequently, there is a perturbed mitochondrial function and increased myocardial oxidative stress. Inorganic nitrite has been shown to modulate mitochondrial function in the cardiac and skeletal muscles thereby preventing the hypoxia-induced mitochondrial dysfunction (Horscroft et al., 2019). The nitrite anion has been earlier reported to modulate mitochondrial fission under normoxia too; nitrite preconditioning activates Protein kinase A (PKA), a pro-survival kinase and inactivates Drp1 thereby promoting mitochondrial fusion and renders cytoprotection on an ensuing simulated Ischemia/Reperfusion (Pride et al., 2014). There are reports that inorganic nitrite therapy may be involved in the regulation of glucose-insulin homeostasis and fatty acid metabolism in skeletal muscle (Ashmore et al., 2015; Gheibi et al., 2017; Jiang et al., 2014; O'Brien et al., 2019; Ohtake et al., 2015; Roberts et al., 2017; Wylie et al., 2019) though no studies have been done pertaining to organ-specific beneficial effects on cardiac muscle in the setting of hyperglycemia. Also, there is a paucity of studies pertaining to molecular changes introduced by inorganic nitrite/nitrate during hyperglycemia. The primary scope of this study can be delineated as to analyze beneficial/detrimental alterations in mitochondrial dynamics and function in cardiac and skeletal myoblasts inflicted by nitrite or NO donor supplementation under hyperglycemia.

I.3. Hypothesis

The nitrite/NO donor supplementation will result in an altered mitochondrial function and dynamics, and consequent metabolic and redox status from that induced by hyperglycemia in cardiac and skeletal myoblasts.

I.4. Broad objectives and sub-objectives of the study

A. To analyze the changes rendered by nitrite/NO donor supplementation under normal glucose (NG) and high glucose (HG) condition to myoblasts pertaining to mitochondrial redox status, function and dynamics.

Sub-objectives

I. To analyze the changes in intracellular and mitochondrial ROS production.
II. To examine the status of mitochondrial membrane potential.
III. To measure the changes in mitochondrial respiration.
IV. To investigate the alterations in proteome of myoblasts exposed to nitrite.

B. To investigate the role of Drp1 activity and the mechanisms of its regulation under high glucose conditions in the presence of inorganic nitrite.

Sub-objectives

I. To check status of Drp1 phosphorylation in myoblasts exposed to the HG with inorganic nitrite and to analyze the molecular pathways activated concomitantly
    a. Is nitrite modulating Drp-1 activation via Akt/GSK-3β or Akt/Pim1 axes?
II. To analyze the effect of HG/Nitrite after Drp1 silencing on mitochondrial respiration and dynamics and mitochondria mediated cellular processes

II. Review of Literature

II.1. Nitric Oxide- The signaling molecule

Nitric oxide (NO) is a gas that is both an endogenous vasodilator as well as a neurotransmitter. NO may diffuse into smooth muscle cells and bind to soluble guanylate cyclase (sGC) initiating confined vasodilation. In other cases, NO may be transported bound to the heme iron in red blood cells and released at vascular sites of deficient NO synthesis. Both Type 1 & Type 2 diabetic patients have been found to possess a reduced ability to generate NO from L-arginine. This reduction in bioavailability of NO is partly due to the quenching of NO molecules by superoxide anions (PACHER et al., 2007). In case of Type 2 Diabetes Mellitus (T2DM) particularly, the reduced NO production may be under the influence of associated insulin resistance, since the stimulation of NOS activity is one of the downstream effects of Akt activation rendered by insulin (Li et al., 2009; Symons et al., 2009). Moreover, the major role of insulin as a cardio-protective agent results from the phosphatidyl inositol 3'-kinase-protein kinase B-endothelial NOS (PI3K-Akt-eNOS)-dependent signaling mechanism which acts to phosphorylate eNOS and increase NO production (Dimmeler et al., 1999; Fulton et al., 1999). Prior to this comprehension, Steinberg et al. in 1994 had revealed insulin-mediated vasodilation of skeletal muscle vasculature to most likely occur via increasing endothelium-derived NO synthesis/release (Steinberg et al., 1994). In addition, studies have shown that reduced synthesis of nitric oxide (from L-arginine) in endothelial cells is a major factor contributing to the impaired action of insulin in the vasculature of diabetic subjects (Federici Massimo et al., 2002; Wu and Meininger, 2009). Supplementation of inorganic nitrite and nitrate as nitric oxide pro-drugs is therefore a potential therapeutic approach being employed in treatment regimens for coronary artery disease, ischemic syndrome, hypertension and other cardiovascular pathologies. Recently, nitrite supplementation has been shown restore the impaired NO-dependent nitrosation of GLUT4 which is necessary for its translocation to the plasma membrane and subsequent role in glucose uptake in rodent skeletal muscle. Thus, nitrite can improve insulin signaling through providing a backup for the NO-mediated effects in a scenario of abated NO bioavailability (Gheibi et al., 2017; Jiang et al., 2014). Thus, exogenous administration of nitrite has proved its

potential to become an important component in the prevention and treatment of metabolic disorders too.

II.2. Nitric Oxide and Nitrate/Nitrite in Physiology and Pathology

NO is a free radical that plays critical roles in the regulation of a multitude of cellular processes in both health and disease conditions. This has reinforced the pivotal position of the gas in various signaling pathways. On endothelial released of this gaseous hormone, it regulates normal blood flow delivery of nutrients to tissues. The endothelial NO synthase (eNOS) is the major contributor of NO under normal physiological conditions, but the bioavailable NO from this so-called classical pathway of NO synthesis (Martínez-Ruiz et al., 2011) is routinely depleted during conditions pertaining to cardiovascular disease and dysfunction. Under such situations of compromised NOS dependent NO generation as in physiological stress and in various risk factors of CVD like hypertension and metabolic syndrome, an alternative NO_3^-—NO_2^-—NO pathway has been proposed to act as a backing (Lundberg et al., 2008).

Nitrite and nitrate anions have a relatively longer half life than the NO radical (Zeballos et al., 1995) as discussed before, and act as a reservoir for NO through the assimilation into circulation (Lundberg et al., 2009; Lundberg et al., 2011b). Nitrite is also formed endogenously by the oxidation of NO mediated by the mitochondrial protein, cytochrome oxidase in cells and ceruloplasmin in blood (Bailey et al., 2014; Shiva et al., 2006). A study by Gilchrist et al., has pointed out the therapeutic potential of nitrate and nitrite for blood pressure control (Gilchrist et al., 2011b). The nitrite anion has evolved its status from an inert metabolic product of NO oxidation at its physiological levels to a storage reservoir of NO in the setting of low pH and hypoxic conditions (Bailey et al., 2014). Thus a metabolite which was considered to be the end point or waste products of NO metabolism is now believed to be a precursor of NO under pathological conditions (Calvert and Lefer, 2009). Nitrite reduction is found to occur primarily in somatic tissues unlike eNOS-mediated production of NO from arginine that occurs in the endothelium, NO production from nitrite occurs in the endothelium (Lundberg et al., 2009). The nitrite, in circulation exhibits dual reaction paths leading to different metabolites. It can either

form nitrate and methemoglobin (MetHb) by reaction with oxygen-bound hemoglobin or form NO, nitrosyl-hemoglobin, and other NO adducts by reaction with deoxyhemoglobin (Gladwin et al., 2009).

II.3. Landmarks in nitrite therapy pertaining to cardiovascular health

Formation of MetHb, which is incapable of transporting oxygen to the body's tissues and organs, is a major concern regarding the toxicology of nitrite (Mohler et al., 2014). Dose-dependent protective effects on cellular necrosis and apoptosis were observed by Duranski *et al.,* in the setting of hepatic ischemia-reperfusion injury in mice, when sodium nitrite solution was administered, with highly significant protective effects observed at near-physiological nitrite concentrations. In the same study, since nitrite intervention to myocardial I/R injury showed 67% reduction in infarct size, it was corroborated that such protection of liver and heart from ischemic injury was contributed by nitrite-derived NO (Duranski et al., 2005). A notable observation was that highly significant protective effects were observed at near-physiological nitrite concentrations and that it was independent of eNOS activity, the regular contributor of vascular NO formation. A placebo-controlled study has been done, which tested multiple doses of oral sodium nitrite in patients, most diabetics, suffering from peripheral artery disease. The study investigated the safety and tolerability over a period of 10 weeks considering endothelial flow-mediated dilatation (FMD) as the primary efficacy endpoint. The study results showed that FMD was significantly higher in diabetic patients who received a 80 mg dose of nitrite compared to controls (Mohler et al., 2014). Sodium nitrite administration provides protection against myocardial ischemia–reperfusion (I/R) injury in a pig regional ischemia model when compared to control and sodium nitrate treated pigs. Here, the beneficial effects included an increase in reactive oxygen species (ROS) scavenging enzymes like GPx, superoxide dismutase (SOD) and catalase with concomitant rise in NO_2^- /NO_3^- levels. There was also a decrease in the oxidative stress marker malondialdehyde (MDA) both in tissue and blood samples (Doganci et al., 2012). G. Johnson and associates investigated the effects of acidified sodium nitrite combined

with human SOD in a six hour model of myocardial ischemia (MI) with reperfusion in open-chest, anesthetized cats and found significant protection (Johnson et al., 1990).

Inorganic nitrate/nitrite supplementation increased tissue and plasma levels of bioactive nitrogen oxides (NO_X) and has been associated with a reduction in blood pressure and improvement in endothelial function. In this scenario, elucidation of the biochemical, molecular and physiological activities of nitrite has caught the interest of a school of researchers exploring miscellaneous conditions in normal physiology and pathophysiology of the heart. Despite the short half-life of NO, several NO-donor compounds have been in the market for decades, for instance, organic nitrates like nitroglycerin and nitroprusside, which provide a preconditioning effect and relief from angina crisis (Murrell, 1879). Contemporary research has focused on the beneficial effects of nitrite/nitrate supplementation in varied forms through different routes unlike earlier studies majority of which dealt with the negative consequences of the oxides of nitrogen inside the body. *In vivo* studies (mouse models) have been done where the animals are treated with nitrites/nitrates and the effect on blood pressure, myocardial ischemia reperfusion etc., has been analyzed. They have reported that dietary supplementation of nitrites/nitrates has beneficial effects in diseased conditions (Baliga et al., 2012; Bryan et al., 2007; Carlström et al., 2011). Even in physiological stress conditions as during aerobic exercise augmented NO availability improved muscle mitochondrial efficiency, indicated by reduced oxygen costs and ATP cost of muscle contractile force production (Layec et al., 2016; Shannon et al., 2017). Nevertheless, the administration of compounds those endow with bioavailable NO is delimited by several drawbacks: toxicity, tolerance, systemic hypotension (Parker and Gori, 2009; Thadani and Rodgers, 2006) (due to their inability of site-specific NO delivery) and aggravation of endothelial dysfunction. These negative effects are related to massive production of reactive species derived from oxygen or nitrogen, which trigger oxidative and nitrosative stress (PACHER et al., 2007; Patel et al., 1999). New NO donors are under development to overcome those disadvantages. In this hunt for prospective candidates, the prospects of nitrite and nitrate salts as NO pro-drugs for the treatment of various pathophysiological conditions involving decreased NO bioavailability is becoming increasingly attractive.

II.4. Prospects of nitrite therapy for metabolic syndrome

A horde of proteins has now been shown to be capable of producing NO via nitrite reductase activity under physiological conditions (Kim-Shapiro and Gladwin, 2014) (Omar and Webb, 2014). These include hemoglobin, myoglobin, xanthine oxidoreductase (XOR), aldehyde oxidase (AO), cytochrome P450, NOS enzymes and mitochondrial proteins like cytochrome oxidase. In the setting of hypoxia and acidosis, all of these proteins exhibit elevated activity. One or more of these enzymes take leading role in nitrite reduction in various organs for instance, myoglobin and XOR/AO are more active in the heart (Kim-Shapiro and Gladwin, 2014) (Omar and Webb, 2014). The former has been shown to be critical regulator of NO-mediated responses in the setting of cellular hypoxia and reoxygenation (Hendgen-Cotta et al., 2008) while the latter have been implicated in pro-angiogenic effects of nitrite salt supplementation during ischemic insult of diabetic mice (Jia and Sowers, 2014). The fact that the NOS enzymes are not the critical player in nitrite reductase activity during physiological stress points to an advantage of nitrite that its bioactivation can occur even in conditions typified by reduced eNOS activity. When the nitrite is taken orally, its intragastric conversion to NO contributes to vasodilation and the consequential anti-hypertensive effect (Pinheiro et al., 2012). Apart from this bioactivation pathway, nitrite-induced vasodilation may involve modes of actions through intermediates like S-nitrosothiols and nitro-fatty acids, both of which have cardioprotective effects during ischemia (Omar and Webb, 2014). The existence of eNOS/NO independent modes of nitrite action suggests a critical impact of exogenous nitrite in metabolic disorders (like diabetes mellitus), which are characterized by low NO bioavailability owing to eNOS uncoupling and generation of significantly high levels of ROS. Moreover, there are findings suggest that inorganic nitrite therapy may be involved in the regulation of glucose-insulin homeostasis (Jiang et al., 2014). These developments have attracted researchers towards the effects of nitrite therapy on cardiovascular health in the setting of metabolic disorders.

II.5. Apprehensions towards the Nitrite Therapy

In spite of all the above-mentioned promises, there are reports which bring into light the concerns that need to be addressed while administering nitrite/nitrate over a long duration. Supraphysiologically elevated NO levels can trigger inflammatory responses and the release of interleukin IL-1β which leads to dysfunction and damage β-cells of pancreatic islets (Shimabukuro et al., 1997). Prolonged ingestion of nitrite/nitrate may lead to the formation of carcinogenic N-nitrosamines (Hecht and Hoffmann, 1998; Tricker, 1997). There are reports disclosing the role of NO in the destruction of the pancreatic beta cells during development of type 1 diabetes mellitus (T1DM) in mice although with inadequate proofs (Cnop et al., 2005; Gurgul-Convey and Lenzen, 2015). Hence, there exists an admonitory need to consider the harmful effects of the same. Involvement of mitochondrial dysfunction in diabetic heart has been shown in many studies and the cause of this dysfunction has been always under dispute, although the role of oxidative stress (ROS/RNS) is proved by strong experimental data. Hence, while investigating the cardiovascular benefits in the setting of metabolic disorders, the monitoring of systemic effects of nitrite/nitrate therapy should be considered a mandate. The above findings support the notion that the inaccuracies in the positive results from animal and human studies pertaining to the diabetic heart, needs to be tackled. In this scenario, there is a need for delving deep into their molecular and biochemical targets and the changes effected by them (Ghasemi and Zahediasl, 2013). It is also imperative to investigate the signaling mechanisms influenced by nitrite, the regulation of its uptake into the cell and subsequent compartmentalization and ultimately obtaining the hitherto elusive leads to NO_X biology. The vast therapeutic implications being suggested for nitrite/nitrate therapy encompasses reduction of oxidative stress (Carlström et al., 2011) and mitochondrial uncoupling leading to improved systemic mitochondrial efficiency in humans (Larsen et al., 2011). Bringing cardiac tissue to attention, impairment in mitochondrial state 3 respiration and/or ATP synthesis rates and reduced expression of respiratory chain complexes in myocardium have been revealed in animal models of diabetes mellitus and transgenic models mimicking metabolic alterations of diabetic hearts (Bugger and Abel, 2010).

II.6. Mitochondria- the dynamic organelle

At the beginning of the 20th century, there were various studies done world-wide regarding the metabolic processes and pathways linked to mitochondria (Chandel, 2018). The mitochondrion is an essential organelle in the cell and is primarily important for its role in ATP synthesis required for various cellular processes (Tait and Green, 2012). Apart from energy production for the cell, mitochondria also regulate calcium buffering and apoptosis. Mitochondrial dynamics is a major determinant in maintaining the organelle's function, quality and homeostasis (Ashrafi and Schwarz, 2013; Chen and Chan, 2005; Zhu et al., 2018). Mitochondria undergo coordinated cycles of fission and fusion to maintain its shape, size, and distribution, with which mitochondria is known as the highly dynamic organelle of the cell. Any defects or mutations affecting mitochondrial dynamics are associated with various diseases in humans (Tilokani et al., 2018). Mitochondrial fission involves the division of single mitochondrion into two new ones, whereas the union of two mitochondria to form a single one is termed as mitochondrial fusion. Any imbalance in the mitochondrial dynamics will not only affect the mitochondrial function but also numerous other requirements of the cell or even activation of mitochondrial transition pore (Balog et al., 2016; Wai and Langer, 2016). There are two major types of fusion occurring in the mitochondria- the transient fusion and the complete fusion, where the former requires only the outer membrane of mitochondria and the latter involves the merging of both the inner as well as the outer membrane. Two homologous proteins Mfn1 and Mfn2 (Mitofusins) function together for merging the outer membranes of mitochondria (Ferree and Shirihai, 2012). Following the Mfn-mediated outer membrane fusion, Optic Atrophy type 1 (OPA1) mediates the inner membrane fusion (Lee et al., 2017). OPA1 is a dynamin-related guanosine triphosphatase that resides in the mitochondrial inner membrane and is essential for mitochondrial fusion and cellular health (MacVicar and Langer, 2016). It also helps in stabilization of the mitochondrial structure and elevates the mitochondrial respiratory efficiency (Varanita et al., 2015). Just like fusion mitochondria, its fission is also crucial for the preservation of the mitochondrial network and is mainly dependent on another GTPase protein called Dynamin-related protein1 or Drp1 (Bliek et al., 2013). A study in 2016 by Lee at al.

suggests that along with Drp1, another dynamin protein called DNM2 is also involved in the mitochondrial fission machinery (Lee et al., 2016). But contradictory to this, a recent study by Fonseca et al. shows that mitochondrial fission is completely depended on Drp1 and not on other dynamin proteins (Fonseca et al., 2019). However, the balance of all these fusion, as well as fission proteins is essential for the proper formation of healthy mitochondrial networks (Bliek et al., 2013). Any disturbance happening to the mitochondrial dynamics or balance is an indication of various stress conditions and diseases which leads to mitochondrial fragmentation and finally results in cell senescence (MacVicar and Langer, 2016) and in addition, fusion, as well as fission play an essential roles in disease-related processes like mitophagy and apoptosis (Bliek et al., 2013).

II.7. Role of Drp1 in mitochondrial dynamics and homeostasis

Even though Drp1 is basically known as a cytoplasmic protein, it is also found in the mitochondria (Lima et al., 2018). The translocation of Drp1 to mitochondria occurs when a stimulus like an uncoupling of mitochondrial membrane exists. Some of the proteins that are required for Drp1 recruitment includes mitochondrial fission factor (MFF), Fission 1 protein (FIS1), Endophilin-B1, Ganglioside-induced differentiation-associated protein 1 (GDAP1), and Mitochondria protein 18 kDa (MTP18) (da Silva et al., 2014). The mitochondrial morphology in yeast is regulated by the dynamin-related GTPase Dnm1 which controls the mitochondrial fission (Bleazard et al., 1999). In mammals, Drp1 activity inhibition leads to the formation of an elongated mitochondria (Lee et al., 2004). An illustration of the actions of Drp1 and other proteins involved inmitochondrial dynamics are shown in Fig. II.1.

Drp1 is a widely studied dynamin protein implicated in different pathological conditions. Inhibition of Drp1 results in an inhibition of BAX-BAK dependent release of cytochrome c (Cassidy-Stone et al., 2008), Drp1 helps in caspase-3 activation (Inoue-Yamauchi and Oda, 2012). It is reported in 2012, in lung cancer, Drp1 is required for cell proliferation and inhibition of Drp1 is associated with an increased apoptosis (Rehman et al., 2012), Drp1 phosphorylation on Ser-585 favors mitochondrial fission (Taguchi et al., 2007) and inhibition of Drp1 results in an increase oxidative capacity of

mitochondria (Zou et al., 2016). Drp1 also is the major protein that helps in tubule distribution which is crucial for the dynamic nature of mitochondria (Bereiter-Hahn and Vöth, 1994; Smirnova et al., 1998).

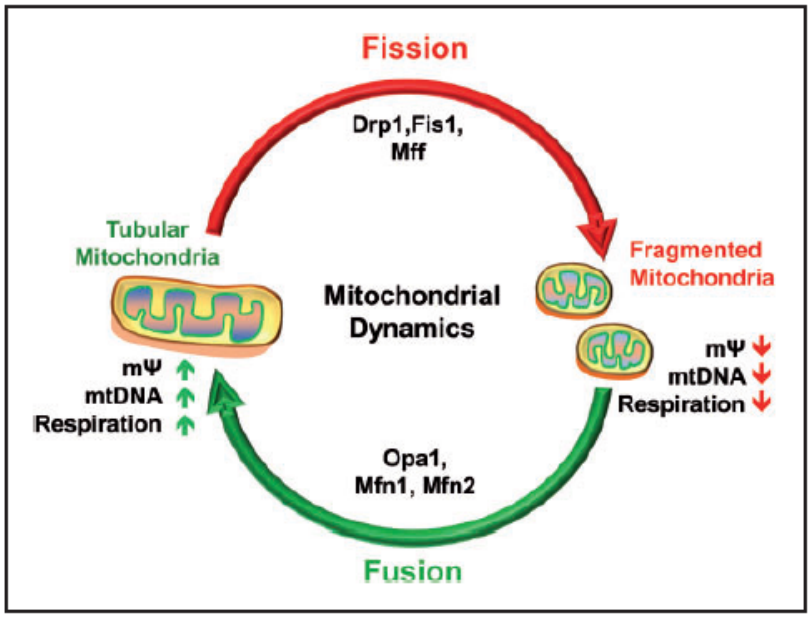

Fig. II.1. Mitochondrial homeostasis maintained by fission and fusion

(Balog et al., 2016)

II.8. Mitochondrial dynamics and cardiac function

Adult heart mitochondria have the ability to undergo both fission as well as fusion, which suggests that there is machinery to regulate the mitochondrial dynamics in adult heart. Most of the *in vitro* experiments done to study the role of mitochondrial dynamics in heart is carried out in H9c2 (cardiac embryonic myoblasts), HL-1 cells (transformed cardiac muscle cell line), VSMC (Vascular Smooth Muscle Cells), neonatal cardiomyocytes and so on. Since the mitochondria in adult cardiomyocyte are aligned closely, one in close contact with the other, they are relatively static. At the time of early cardiac differentiation, Drp1-mediated mitochondrial fission coincides with mitophagy (the removal of mitochondria) via p62. Also in the adult heart, Drp1 inhibition leads to impaired mitophagy, which later leads to cardiomyopathy. This shows that Drp1 is crucial for maintaining the mitochondrial network. Hence, from all these findings, it is

well corroborated that the inhibition of Drp1 for a long time period could be detrimental for the normal functioning of the heart (Ong et al., 2013). In addition to the above findings, there are reports from Kasahara et al. showing that Mfn1, Mfn2 and OPA1 plays a crucial role in the development of heart and also are essential for the proper functioning of heart (Kasahara et al., 2013).

II.9. Pro-survival kinases in the regulation of mitochondrial function

Phosphatidylinositol-3-kinase (PI3K) is a hydrophobic second messenger. It is a kinase that is essential for the Akt translocation to the plasma membrane where it gets activated by phosphoinositide-dependent kinases (PDKs). Activation of Akt, a Ser/Thr kinase plays a key role in cell proliferation and survival by phosphorylating various substrates (Osaki et al., 2004). Akt inhibits the apoptotic pathway by preventing the release of cytochrome c from mitochondria. By activating IκB kinase (IKK), Akt helps in the transcription of anti-apoptotic genes and thus called as a survival factor. (Whang et al., 2004) PI3K-PKB/Akt (phosphoinositide-3-kinase–protein kinase B/Akt) pathways is a well conserved pathway and its activation occurs through a multistep process (Hemmings and Restuccia, 2012).

The Pim kinases are the serine/threonine kinases consisting of three proteins Pim-1, Pim-2, and Pim-3 which belong to the CAMK (calmodulin-dependent protein kinase-related) group (Bullock et al., 2005). The enzyme is involved in regulating cell differentiation and proliferation and also reported to have a role in cell survival in myeloid and lymphoid cells (Wang et al., 2002). Pim-1 is an essential downstream molecule of Akt. Akt overexpression is found to increase Pim-1 expression in neonatal rat cardiomyocytes. It is also reported that PI3K-like kinases have dual effects on the regulation of Pim kinases (Fig. II.2.).

PI3K-like kinases can upregulate or downregulate Pim-1 expression. LY294002 (inhibitor of the PI3K-like kinases) increases Pim-1 expression (Liang and Li, 2014). In hematopoietic cells, Pim kinases act as an essential mediator of cytokine signaling pathways, and they also have roles in the progression of tumors including hematological

malignancies, prostate cancer and various other solid tumors (Brault et al., 2010). Many cytoplasmic and nuclear proteins are phosphorylated by the enzyme Pim kinase *in vitro* and these include transcriptional repressors (HP1), PAP1 (Pim-1 associated protein 1, activators (NFATc1 and c-Myb), and co-activators (p100), cell cycle regulators (p21WAF1/CIP1 (a cyclin-dependent kinase inhibitor), a phosphatase Cdc25A, and the kinase C-TAK1/MARK3/Par1A), TFAF2/SNX6 (membrane-associated protein) and nuclear mitotic apparatus protein (NuMA) (Bullock et al., 2005; Wang et al., 2002)

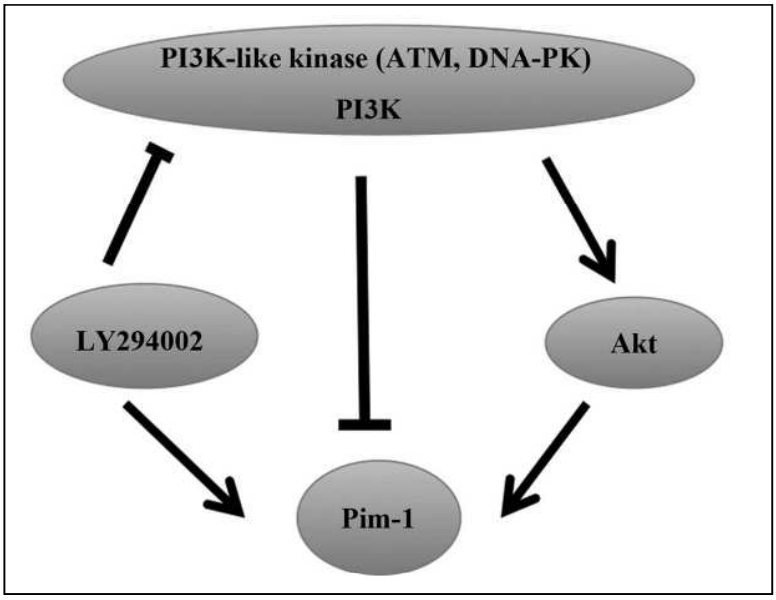

Fig.II.2. Pim-1 regulation by PI3K-like kinases

(Liang and Li, 2014)

Pim kinases are also found to phosphorylate BAD (the pro-apoptotic protein) and induce apoptotic resistance when there is a deprivation of growth factor (Fox et al., 2003). Likewise, cardiomyocytes overexpressing Pim-1 kinase show increased levels of Bcl-2 and Bcl-XL (anti-apoptotic markers) along with the inactivation of Bad. Pim-1 is an important mediator of cardioprotection and is downstream of JAK/STAT and Akt. The absence of Pim-1 in the myocardium results in the decreased levels of proteins involved in mitochondrial protection after myocardial infarction and hence increases fibrosis (Borillo Gwynngelle A. et al., 2010a; Muraski et al., 2007).

Din et al have shown that ischemic challenge promotes Drp1 translocation to the mitochondria in myocytes, which leads to the fragmented mitochondria, but Pim-1 kinase, the upstream molecule of Drp1 prevents those effects. Overexpression of Pim-1 is found to prevent the accumulation of Drp1 in the cardiac mitochondria and also decreases the total Drp1 levels. Drp1 translocation was found to be inhibited by Pim-1. Pim-1-Drp1 interaction occurs under basal as well as ischemic conditions. Pim-1 overexpression increases Drp1 phosphorylation at S637. Since Pim-1 has been shown to be involved in cardioprotective activity, Pim-1 could be a potential therapeutic agent against diseases characterized by cardiac cell death (Din et al., 2013).

Glycogen synthase kinase-3 (GSK-3) is another multi-functional serine/threonine kinase that is ubiquitously expressed and consists of two isoforms, alpha and beta and both exert similar functions (Zhai et al., 2007). GSK-3β is not present in the mitochondria, whereas a small amount of GSK-3α is present in the mitochondria. Usually, in normal myocardium, phosphor-Ser9-GSK-3β is present in the cytoplasm whereas, under conditions like ischemia/reperfusion, phosphor-Ser9-GSK-3β get translocated into mitochondria (Yang et al., 2017). GSK-3 isoforms have been associated with various pathological conditions like ischemic injury, heart failure, diabetes, Alzheimer's disease, myocardial aging, cardiomyocyte proliferation, myocardial fibrosis, inflammation, and cancer. It is one of the few protein kinases that can be inactivated by the addition of phosphate groups. GSK-3α and β are negatively regulated by phosphorylation of its serine residues at 21^{st} and 9^{th} positions respectively. The relationship between GSK-3α and heart is a widely studied subject and it is reported that GSK-3α regulates the proliferation of cardiomyocytes in the injured heart, and also in ischemic heart, the deletion of GSK-3α in cardiomyocyte is found to be protective (Lal et al., 2015). GSK-3β has been shown to regulate mitochondrial biogenesis, mitochondrial motility, mitochondrial bioenergetics, mitochondrial permeability and mitochondria-dependent apoptosis (Fig. II.3.) (Yang et al., 2017).

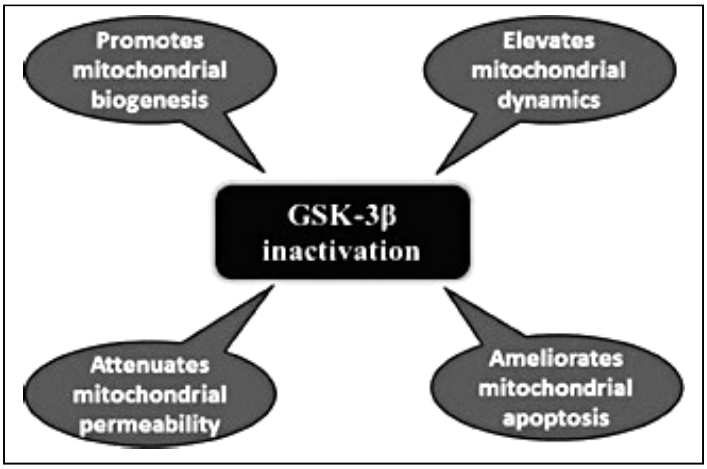

Fig.II.3. Major roles of GSK-3β in the Mitochondria

(Yang et al., 2017)

Both the GSK-3 proteins get activated upon dephosphorylation and it becomes inactivated upon phosphorylation by Akt. GSK-3β is found to be activated in diabetic condition and its phosphorylation or inactivation plays an important role in cardiac glucose metabolism (Wang et al., 2009). The ablation of either GSK-3α or GSK-3β in cardiac myocytes is reported to be protective after ischemia (Hall, 2014). GSK-3β deletion in the hearts of the embryos resulted in hypertrophic cardiomyopathy signifying the vital roles played by this kinase (Zhou et al., 2010).

II.10. Mitochondrial membrane potential and permeability transition pore

Mitochondrial permeability transition pore (mPTP) is present in the inner mitochondrial membrane and it consists of three main components- Adenine Nucleotide Translocase (ANT), cyclophilin D (CyP-D) and voltage-dependent anion channel (VDAC). mPTP is triggered and opened during stressful conditions such as oxidative stress and Ca2+ overload. The threshold for mPTP opening is positively correlated to the phosphor-Ser9-GSK-3β levels indicating that alterations in the phosphorylation of GSK-3β might contribute to the dysregulation of mPTP directly or indirectly. GSK-3β is reported to modulate respiratory chain activity (Yang et al., 2017).

Just like the inner mitochondrial membrane, the outer membrane of mitochondria too possesses various channels for the influx and efflux of metabolites**.** VDAC, otherwise called as mitochondrial porin, thus regulates the cross-talk between mitochondria and other cellular components. VDAC plays multiple functions in the mitochondria which includes the regulation of mitochondrial metabolism and energetics, mitochondria-mediated apoptosis and is also a crucial element for various cell survival and death signals by interacting with other proteins and ligands (Shoshan-Barmatz et al., 2010)**.**

Adenine nucleotide translocase or translocator (ANT) is a protein complex in the family of integral membrane transport molecules, which consists of two subunits and is located in the IMM. It helps in the exchange of cytosolic ADP and mitochondrial ATP (Sharer, 2005). There are four different isforms of ANT proteins in humans. They are: ANT1, a predominantly expressed isoform in the mitochondria of heart, brain and skeletal muscle tissue, ANT2 is commonly seen in the liver and in those cells with high proliferation capacity, and is sparse in differentiated cells. ANT3 is ubiquitously expressed. ANT4 is specific for testis, liver, and undifferentiated embryonic stem cells (Chevrollier et al., 2011; Dolce et al., 2005). ANT plays several important roles including the constant supply of ADP required for the maintenance of the oxidative phosphorylation. ATP/ADP exchange by ANT plays an essential role for the maintenance of ATP synthase activity and mitochondrial membrane potential. Impaired ANT activity of reduces the intra mitochondrial ADP and ATP production which increases the mitochondrial membrane potential (Fiore et al., 1998; Vander Heiden et al., 1999). It is the only carrier for ADP and ATP present in the mitochondria, helping in the energy production in mitochondria and energy consumption in the cytosol (Nebigil Canan G. et al., 2003). In case of impaired ATP/ADP exchange, ANT plays an essential role in ROS production and apoptosis apart from this, ANT also involved in fatty acid mediated uncoupling of mitochondria (Kim et al., 2010).

When electron transport is not used to drive ATP synthesis or any other useful work, the process is termed as “mitochondrial uncoupling” (Mookerjee et al., 2010). Mitochondrial uncoupling is mainly mediated by proteins like UCPs, ANT, and mitochondrial thioesterase I (MTE-1) (Boudina et al., 2007). Uncoupling proteins (UCPs) are anion

carrier proteins that reside in the IMM that are capable of inducing proton leak and dissipate the proton gradient, thereby affecting the efficiency of energy metabolism. Several isoforms of UCPs are associated with diabetes and obesity which includes UCP-1, 2 and 3. Out of these, UCP3 is found to regulate fatty acid metabolism especially in the skeletal muscle. Also it is upregulated in response to oxidative stress and prevents ROS generation and ROS mediated DNA damage (Busiello et al., 2015; Cadenas, 2018). UCP3 plays a critical role in cytoprotection in the setting of type 2 diabetes (T2DM) in skeletal muscle and cardioprotection during I/R and also in adaptive responses to acute exercise and starvation (Busiello et al., 2015; Cadenas, 2018; Ozcan et al., 2013). UCP3 is expressed mainly in skeletal muscle, heart and brown adipose tissue, and is linked with energy metabolism in whole body (Busiello et al., 2015; Schrauwen, 2002). As mentioned above, it also protects the heart from I/R injury, mainly through preventing myocardial necrosis, contractile dysfunction, and arrhythmias and hence is a major determinant of infarct size and post-ischemic cardiac remodeling (Cadenas, 2018; Ozcan et al., 2013). All these evidence suggests that UCPs are one of the important potential therapeutic targets for IR injury and also, cardiovascular risk factors like obesity, T2DM and atherosclerosis (Cadenas, 2018).

II.11. Mitochondria and oxidative stress

Mitochondrial oxidative stress occurs due to the overproduction of reactive oxygen species (ROS), which can cause mtDNA mutations, can damage mitochondrial respiratory chain, alter the membrane permeability of mitochondria, and influence mitochondrial defense systems (Guo et al., 2013). Superoxide free radicals and their product, hydrogen peroxide (H_2O_2) are referred as ROS (He et al., 2016). Oxidative stress has been proved to have roles in various pathological conditions including I/R injury (Halestrap et al., 1998). Mitochondria are usually protected from oxidative damage with the action of anti-oxidant systems present in the mitochondria like superoxide dismutase (SOD), glutathione peroxidase (GPx), catalase and glutathione reductase (Green et al., 2004; Wei et al., 2001). When the balance between ROS and these antioxidants gets

disrupted due to the excess free radicals, it results in the damage of DNA, protein as well as lipid degradation (Guo et al., 2013)**.**

SOD2/ MnSOD (a Manganese-dependent enzyme) is the mitochondrial isoform of SOD and is localized within the mitochondrial matrix, which is the major free radical production site (from electron transport chain) (Flynn and Melov, 2013). Inside the mitochondrial matrix, SOD2 helps in converting superoxide to H_2O_2, which further gets metabolized by Gpx1 and peroxiredoxin (PrxIII). SOD2 overexpression diminishes mitochondrial ROS production, protects mitochondrial respiratory function and prevents apoptosis. Gpx4, otherwise known as phospholipid hydroperoxide glutathione peroxidase is a membrane-associated anti-oxidant enzyme with a small fraction localized in the mitochondria. Gpx4 helps in reducing the hydroperoxide groups on lipoproteins, phospholipids and cholesteryl esters (Ott et al., 2007). GPx1, another important isoform of GPx mainly resides in the cytosol, but a small fraction is also present within the mitochondrial matrix (Pushpa-Rekha et al., 1995). Diabetes is characterized by metabolic events leading to oxidative stress which in turn induces overproduction of mitochondrial superoxide (Giacco and Brownlee, 2010; Pieme et al., 2017). Overexpression of SOD2 can reverse diabetes induced disruption of cardiac morphology and impaired contractility, whereas it has no effects on non-diabetic hearts. It also improved the abnormal mitochondrial function and mass associated with diabetes (Shen et al., 2006). Reduced levels and the activities of the antioxidant enzymes, GPx, SOD, and catalase observed in patients with T2DM in comparison with normal subjects also indicate the impact of enhanced oxidative stress in the manifestations of diabetes (Ansley and Wang, 2013).

Aconitase is an enzyme that catalyses citrate to isocitrate and it exists in two different forms- cytosolic aconitase (aconitase 1) and mitochondrial aconitase (aconitase 2). The enzyme possesses an iron-sulfur cluster which is sensitive to oxidation and it helps in the regulating cell metabolism. One of the major factors that regulate aconitase function is ROS. The enzyme undergoes modification and inactivation in aging and some of the oxidative stress-related disorders. Aconitase2, the mitochondrial isoform helps in the conversion of citrate to isocitrate and is involved in the Krebs cycle (Lushchak et al.,

2014a). It was proved that when exposed to NO donors, certain cell shows a loss of aconitase 2 activity. Exposure of aconitase at higher concentrations for longer period can inactivate the enzyme (Tórtora et al., 2007). Lin et al. have suggested that aconitase phosphorylation may impair the Krebs cycle function, which could lead to the dysfunction of mitochondria in the diabetic heart. Aconitase phosphorylation may be a common mechanism of aconitase activity regulation in the heart in both type 1 as well as type 2 diabetes. It was found that under the conditions of high oxidative stress, aconitase 2 activity was unchanged or increased in skeletal muscle subjected to exercise (Lin et al., 2009).

II.12. Mitochondrial transcription factor A (TFAM)- A regulator of mitochondrial copy number

Mitochondrial transcription factor A (TFAM) is a protein that belongs to the high-mobility-group (HMG). It performs various functions for mitochondrial DNA (mtDNA). Some of them are: mtDNA maintenance, mtDNA transcription, mtDNA replication, packaging of mtDNA into nucleoids and mtDNA repair. The interaction between TFAM and mtDNA also helps in the regulation of mitochondrial biogenesis. Its interaction with mtDNA helps in reducing ROS production and calcium mishandling (Kunkel et al., 2016; W. R. Lee et al., 2017; Picca and Lezza, 2015; Suarez et al., 2008). Since TFAM is essential for mtDNA, mitochondrial function is impaired in hyperglycemic conditions with reduced TFAM expression or activity (Choi et al., 2001; Kanazawa et al., 2002; Nishio et al., 2004; Palmeira et al., 2007). TFAM disruption in cardiomyocytes leads to deletion of mtDNA and hence results in dilated cardiomyopathy. Therefore, TFAM can be considered as a therapeutic target for mitochondrial dysfunction (Suarez et al., 2008).

II.13. Drp1 and mitophagic regulators

Mitophagy is a form of autophagy that removes dysfunctional or damaged mitochondria (Li et al., 2015). Some of the important molecules involved in mitophagy are PTEN-induced kinase 1 (PINK1) and Parkin and the mitophagic mechanism can be either PINK1/Parkin-independent or PINK1/Parkin-dependent mechanism. The latter is the

most well documented mechanism of mitophagy (Yoshii et al., 2011; Youle and Narendra, 2011). Park et al. have shown that inhibition of Drp1 reduced the expression of Parkin, PINK, and LC3II (an autophagic marker). This finding thus suggests that Drp1 is involved in the regulation of PINK1/Parkin mediated mitophagy pathway. Drp1 knockdown using siRNA in SHSY5Y cells increased the level of PINK1 in the cytosol by blocking its translocation into mitochondria (Park et al., 2018). All these suggest that Drp1-dependent fission can coordinate with Parkin and PINK1 to trigger mitophagy.

II.14. Apoptosis and mitochondrial dynamics

Activation of Drp1 leads to structural and functional abnormalities in the mitochondrial, which in turn inhibits the ATP generation, and results in the activation of pro-apoptotic signaling cascades (Frank et al., 2001; Reddy et al., 2011). OPA1 overexpression blocks mitochondrial fission and protects cells from apoptosis occurring through the intrinsic/mitochondrial pathway (Frezza et al., 2006). When the fission proteins like Fis1 or Drp1 gets downregulated, it leads to the inhibition of mitochondrial fission and thus reduces apoptosis (Lee et al., 2004).

II.15. Rationale of the study

From the literature discussed above, it is unknown whether the nitrite/nitrate derived NO or the anions themselves could render changes in mitochondrial function and metabolic status of myocytes in the setting of hyperglycemia. So, the present study focuses on the effects of sodium nitrite supplementation on myoblasts under hyperglycemic conditions as compared to under normoglycemic conditions. Also, to check the acute effects of NO under the above glycemic levels, an NO donor was used. The changes pertaining to mitochondrial dynamics, respiration, ROS generation and the mitochondrial fission regulator, dynamin-related protein1 was focused.

II.16. Hypothesis

The nitrite/NO donor supplementation will result in an altered mitochondrial number and function, and consequent metabolic and redox status from that induced by hyperglycemia in cardiac and skeletal myoblasts

III. Materials and Methods

III.1. Reagents, antibodies, drugs and Instruments used

III.1.A. Reagents, antibodies and drugs

The inhibitors and FCCP for respirometric studies and most chemicals needed for other experiments, including S-Nitroso-N-acetyl penicillamine (SNAP), sodium nitrite, Nγ-Nitro-L-arginine Methyl Ester (L-NAME) and carboxy-phenyl-tetramethylimidazoline-1-oxyl-3oxide (cPTIO) were purchased from Sigma Aldrich (St. Louis, MO, USA). Acrylamide-Bis-acrylamide solution, West Pico Chemiluminescence Detection Kit, BCA protein assay kit, West femto Enhanced Chemiluminescent reagents, RIPA buffer, Protease and Phosphatase Inhibitor cocktails were from Pierce Biotechnology (MA, USA). OptiBlot ECL from Abcam (Cambridge, UK) and ClarityMax ECL Kit from Bio-Rad Laboratories (Hercules, CA, USA) were also used. TaqMan gene expression assay master mix and TaqMan probes were from Applied Biosystems (Beverly, MA, USA). Pure link RNA mini kit was from Invitrogen Corporation (Carlsbad, CA, USA). Antibodies against Vinculin, α-Tubulin, p-Akt1, Akt, p-GSK3β, GSK3β, p-eNOS, eNOS, p-Drp1, Drp1, OPA1, cleaved Caspase 7 and 3, cleaved PARP, Bcl2 and Aco2, Horse Radish Peroxidase (HRP)-conjugated secondary antibodies and the chemical LY294002 were purchased from Cell Signaling Technology (Danvers, MA, USA). Anti β-actin antibody was from Sigma. PVDF membrane, syringe filters and filter membranes for media filtration were from Millipore (MA, USA). Antibodies against PGC1α/β, ANT1, UCP3, MnSOD, GPx4, Pink1, Parkin and VDAC were from Abcam (Cambridge, UK) and Pim1 from ImmunoTag (St. Louis, MO, USA). Rapigest SF was from Waters (Milford, MA, USA), siRNA from Eurogentec (Seraing, Belgium) and Transfection reagent from Polyplus Transfection SA (Illkirch-Graffenstaden, France). Consumables/plasticwares were purchased from Tarsons (Kolkata, India) and Axygen Scientific (Union City, CA, USA). Culturewares were procured from Nunc (Thermofisher Scientific, MA, USA) and Becton Dickinson (Franklin Lakes, NJ, USA).

III.1.B. Instruments

PCR Thermal Cycler (Bio-Rad Laboratories, Hercules, CA, USA), ELISA plate reader (Bio-Tek Instruments, Winooski, Vermont, USA), Oroboros O2K Oxygraph (Innsbruck, Austria), Mini-PROTEAN Tetra Cell Electrophoresis Unit, Powerpac universal, Semi Dry Blot Apparatus and Wet-transfer Apparatus (Bio-Rad Laboratories, Hercules, CA, USA), UV-visible spectrophotometer (Shimadzu, Kyoto, Japan), Water bath (Julabo, Seelbach, Germany), Weighing balance (Sartorius, Gottingen, Germany), pH meter (Eutech, Singapore), Magnetic Stirrer (Schott, Mainz, Germany), Micro-Pipettes (Eppendorf, Hamburg, Germany), -20^{o}C Freezer (Vest frost, Falkevej, Denmark), -80^{o}C Freezer (New Brunswick Scientific, Sayreville, NJ, USA), Cooling centrifuge (Eppendorf, Hamburg, Germany), Centrifuge (REMI, Mumbai, India), MultiTherm shaker (Benchmark Scientific Inc., Edison, NJ, USA), CO_2 incubator (Sanyo, Osaka, Japan), Laminar Air Flow Hood (MicroFilt, Pune, India), BD FACS Jazz Cell Sorter (Becton and Dickinson, Franklin Lakes, NJ, USA), Phase Contrast Microscope with fluorescence filters (Olympus, Shinjuku, Tokyo, Japan), Gel Documentation System (Bio-Rad Laboratories, Hercules, CA, USA), 7500 Real-Time PCR System (Applied Biosystems, Foster City, CA, USA).

III.2 Cell culture and maintenance

III.2.A Procedure

Embryonic rat cardiac myoblasts- H9c2 and mouse skeletal myocytes- C2C12 were obtained from National Centre for Cell Science (NCCS), Pune, India. The cells were grown in monolayer culture in DMEM containing 10% FBS and antibiotic-antimycotic cocktail (Sigma, MO, USA) in a humidified atmosphere of 5% CO_2 at 37°C. For all treatments during experiments, DMEM containing 1 % FBS (H9c2)/2% FBS (C2C12) were used or else specified.

For culture maintenance, media were changed every 2-3 days, depending on rate of growth of cell lines, H9c2 being a slow multiplier than C2C12. Cultures were split at confluency to 1:3 ratios. The cells were removed from the dish/flask by using Trypsin-

Phosphate-Versene-Glucose (TPVG). The cells were centrifuged and the supernatant was removed. Then the cells were resuspended in 1.0 ml of freezing medium (50% FBS and 5% DMSO in Low Glucose DMEM) and stored at -80 °C freezer.

III.2.B. Reagents Used

III.2.B.1. DMEM preparation (1 litre) (pH 7.4)

Low Glucose DMEM powder (16g), 2g $NaHCO_3$ (Sodium bicarbonate), 10 mL Antibiotic-antimycotic cocktail (100x) mixed in sterile distilled water, filtered and stored in autoclaved bottles.

III.2.B.2. Phosphate-buffered saline (PBS) (pH 7.4)

Sodium chloride- 137 mM, potassium chloride- 2.7 mM, disodium hydrogen phosphate- 10.14 mM, potassium dihydrogen phosphate- 1.76 mM in sterile deionised water.

III.2.B.3. TPVG solution (pH 7.4)

0.1% trypsin, 0.2% EDTA and 0.05% glucose in PBS.

III.2.C. High glucose treatment

High-glucose medium containing 30 mmol/L glucose and 2% FBS H9c2 cells were used to incubate with H9c2 cells for 24 h and 48 h after achieving 70% confluence. The D-glucose (Sigma) was dissolved in normal medium to prepare a medium with 30 mmol/L glucose.

III.2.D. Other reagents used

III.2.D.1. LY294002 stock (50 mM)

1.5 mg in 98 µL DMSO

III.2.D.2. DCFDA stock (10 mM)

5 mg in 1.026 mL DMSO

III.2.D.3. DAF-FM DA stock (10mM)

50 µg (one pack) in 10 µL DMSO

III.2.D.4. MitoSOX Red Stock (5 mM)

50 µg (one pack) in 13 µL DMSO

III.3. Cell viability assays

III.3.A. MTT assay procedure

Cell growth assays were carried out by MTT assay as described elsewhere with slight modifications (Babykutty et al., 2012). This is a colorimetric assay that measures the reduction of yellow 3-(4,5-dimethythiazol-2-yl)-2,5-diphenyl tetrazolium bromide (MTT) by dehydrogenase present in the viable cells. The MTT enters the cells and passes into the cell where it is reduced to an insoluble, coloured (dark purple) formazan crystals.

To analyse NO/nitrite induced cell death, cells were grown in 96-well microtitre plates (1 x 10^4 cells/well) and incubated with or without different concentrations of SNAP (200-25 µM), sodium nitrite (1000-1 µM), or DMSO/HBSS vehicle in DMEM medium with 1 % foetal bovine serum. After incubation periods, the medium was removed; fresh medium was added and MTT (1 mg/mL) in HBSS was added to each well. The plates were incubated for another 3 h, the formazan crystals formed by metabolically viable cells were solubilized with 150 µl of acidic isopropanol. The color developed was quantified (Measuring wave length: 570 nm, Reference wave length: 630 nm) with a 96 well Microplate Reader (BioTek instruments, Winooski, VT, USA). The cell viability was expressed as percentage over the control by using the formula (T/C) x 100 where T= test sample and C= control.

III. 3.B. Hoechst –PI staining procedure

Cell death analysis was performed using Hoechst/PI double staining method. After various treatments, the cells were incubated with 1µg/ml Hoechst (Sigma-Aldrich, St. Louis, MO, USA) at room temperature for 15 min and then 1mg/ml PI (Propidium

Iodide, Sigma-Aldrich, St. Louis, MO, USA) for 5 min. The cell death percentage was then calculated using the formula; $[(PI/H)_{Test} / (PI/H)_{Control}]x100$, where PI= No. of PI stained nuclei and H= No. of Hoechst stained nuclei.

III. 3.C. Reagents Used

III.3.C.1. SNAP stock (100 mM)

25 mg in 500 µl DMSO

III.3.C.2. Sodium Nitrite stock (100 mM)

69 mg in 10 mL PBS

III.3.C.3. MTT stock

MTT salt 5 mg in 1 ml PBS. (Freshly prepared)

III.3.C.4. LY294002 stock (50 mM)

1.5 mg in 98 µL DMSO

III.3.C.5. Hoechst 33342 stock (10 mM)

2 mg in 1 mL DMSO

III.3.C.6. Propidium iodide stock (10 mg/mL)

5 mg in 500 µL DMSO

III.4. Measuring the levels of intracellular and mitochondrial ROS

III.4.A. Intracellular ROS measurement by H_2DCFDA staining

For fluorescent microscopic studies, the cells were seeded in 24-well plates and after treatments were incubated with 10 µM DCFH-DA at 37 °C in the dark for 30 min. Cells treated with H_2O_2 were used as a positive control. Cells were then washed twice with HBSS and counterstained with nuclear stain, Hoechst 33342 (Sigma-Aldrich). Fluorescence was measured over the entire field of vision by using a fluorescence microscope (IX50, Olympus, Tokyo, Japan) connected to a color camera linked with the Image processing software, Progres Capture. The MFI (Mean Fluorescence Intensity)

from five random fields was measured using Image J 1.49a software, and the MFI was used as an index of the quantity of ROS.

For fluorimetry, cells were cultured in a black 96-well plate with DMEM medium. After the different treatments, the wells were washed two times with HBSS and H_2DCF-DA incubation was done as above. The wells were washed twice with HBSS, and the DCF fluorescence was measured from the wells using Fluorimeter (BioTek instruments, Winooski, VT, USA).

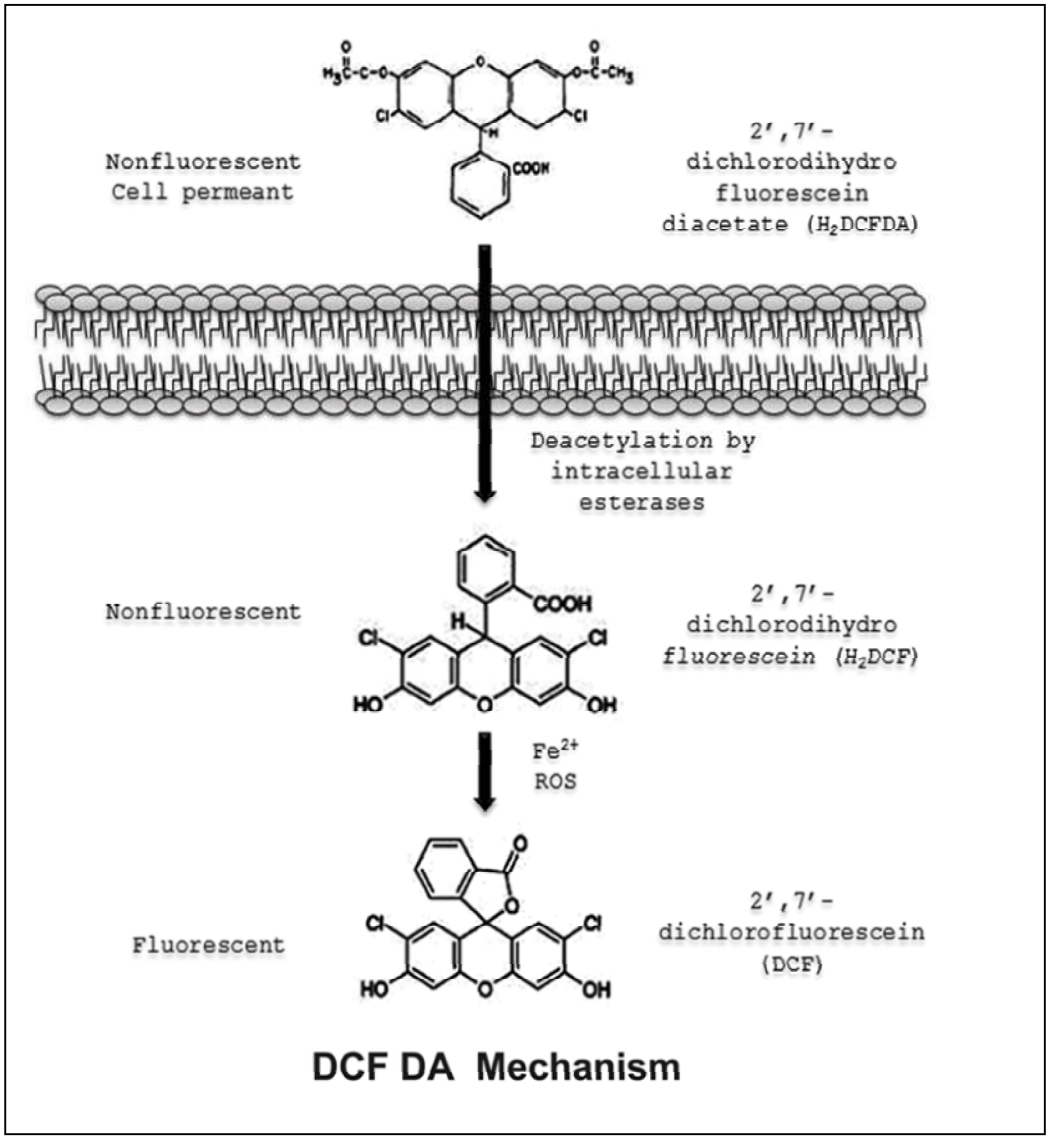

Fig. III.1. Mechanism of DCFDA processing inside a cell yielding the fluorescent DCF moiety

Caption on next page

H_2DCFDA on entering the cell is acted upon by cellular esterases to release the reduced form of DCF which is non-fluorescent. Depending on the level of ROS present inside the cell, H_2DCF gets oxidized to the fluorescent DCF moiety.

Flow Cytometric analysis was done with cells cultured in 60 mm dishes and given the treatments. The cells were harvested and resuspended in HBSS. After a single wash, the cells (1 x 10^6) were transferred to Falcon round-bottom polystyrene tubes and incubated with DCFH-DA as above. The cells were then centrifuged at 150 g for 5 min, washed with pre-warmed HBSS and then directly subjected to flow cytometry (BD FACS Jazz, BD Biosciences, San Jose, CA, USA). Forward and Side scatter gating was established to exclude cell aggregates and debris from analysis. DCF fluorescence was analyzed at Ex/Em = 488/535 nm.

III.4.B. Mitochondrial ROS measurement by MitoSOX Red staining

Mitochondrial ROS generation was determined by the mitochondria-targeted probe MitoSOX Red (Molecular Probes [Invitrogen] Eugene, OR, USA). The fluorogenic probe is selectively targeted to the mitochondria where it is oxidized by superoxide and becomes fluorescent on binding to nucleic acids. MitoSOX Red stock was prepared by dissolving 50 µg of probe in 13 µL anhydrous DMSO and the working solution was prepared in warm HBSS (with Ca^{2+}).

Overnight starved cells in 96-well plates were given the treatments for 24 h, washed and were incubated with 5 µM of MitoSOX Red probe for 10 min at 37 °C. After two washes with warm HBSS, the cells were counterstained with Hoechst 33342. Fluorescent (Ex-500nm/Em-590nm) emission was imaged using an Olympus fluorescence microscope (IX 51; Olympus Corporation, Tokyo, Japan), images analyzed using Image J 1.49a and relative fluorescence intensity was calculated as percentage fluorescence normalized to control.

III.5. Measuring the levels of intracellular NO_X production

An essentially non-fluorescent cell permeable reagent, 4-Amino-5-Methylamino-2',7'-difluorofluorescein Diacetate (DAF-FM DA) (Molecular Probes [Invitrogen] Eugene, OR, USA) can measure low concentrations of NO in live cells by conversion into a

benzotriazole derivative on combining with NO as shown in Fig. III.3. (Kojima et al., 1998a; Kojima et al., 1998b)(Kojima et al., 1998).

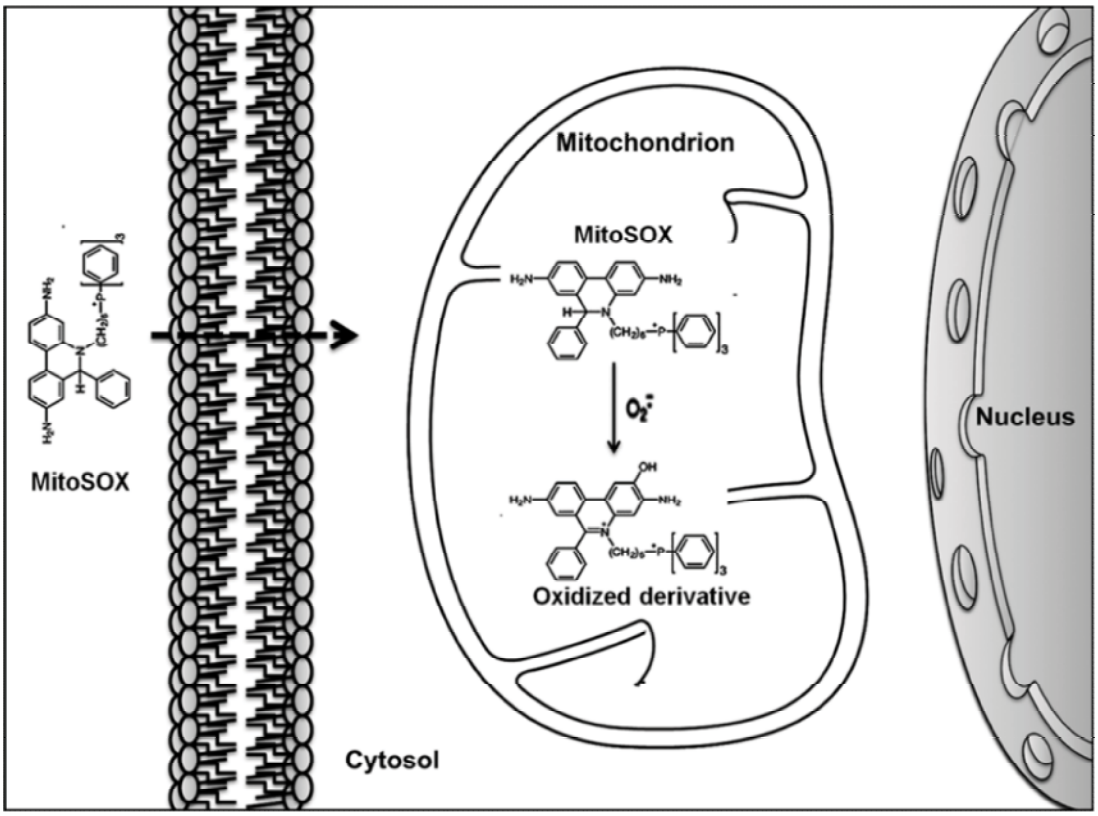

Fig. III.2. Mechanism of MitoSOX Red entry specifically to mitochondria and its oxidation

MitoSOX on entering the cell is directed specifically to the mitochondria where the superoxide anions oxidize it to form a red fluorescence emitting moiety.

Analysis of NO_X production by fluorimetry was performed with cells seeded in 96 well black culture plates at a seeding density 5 x 10^3 cells/well. The cells on completion of treatments were washed in HBSS and then DAF-FM DA was added to a final concentration 10 µM to the cells and incubated for 30 min at 37 °C. Finally, the excess dye was washed off and the DAF-FM fluorescence at Ex-490nm/Em-515nm was measured with a Fluorimeter (BioTek instruments, Winooski, VT, USA).

Cells were seeded in 24-well plates at a density of 1 x 10^4 cells/well for fluorescent imaging, and after different treatments, were incubated with DAF-FM DA as above. Cells were then washed twice with HBSS and counterstained with the nuclear stain,

Hoechst 33342 (Sigma-Aldrich). Fluorescence was measured over the entire field of vision by using a fluorescence microscope (IX50, Olympus, Tokyo, Japan) connected to a color camera with linked Image processing software, Progres Capture. The MFI (Mean Fluorescence Intensity) from five random fields was measured using Image J 1.49a software, and the MFI was used as an index of the quantity of NO_X.

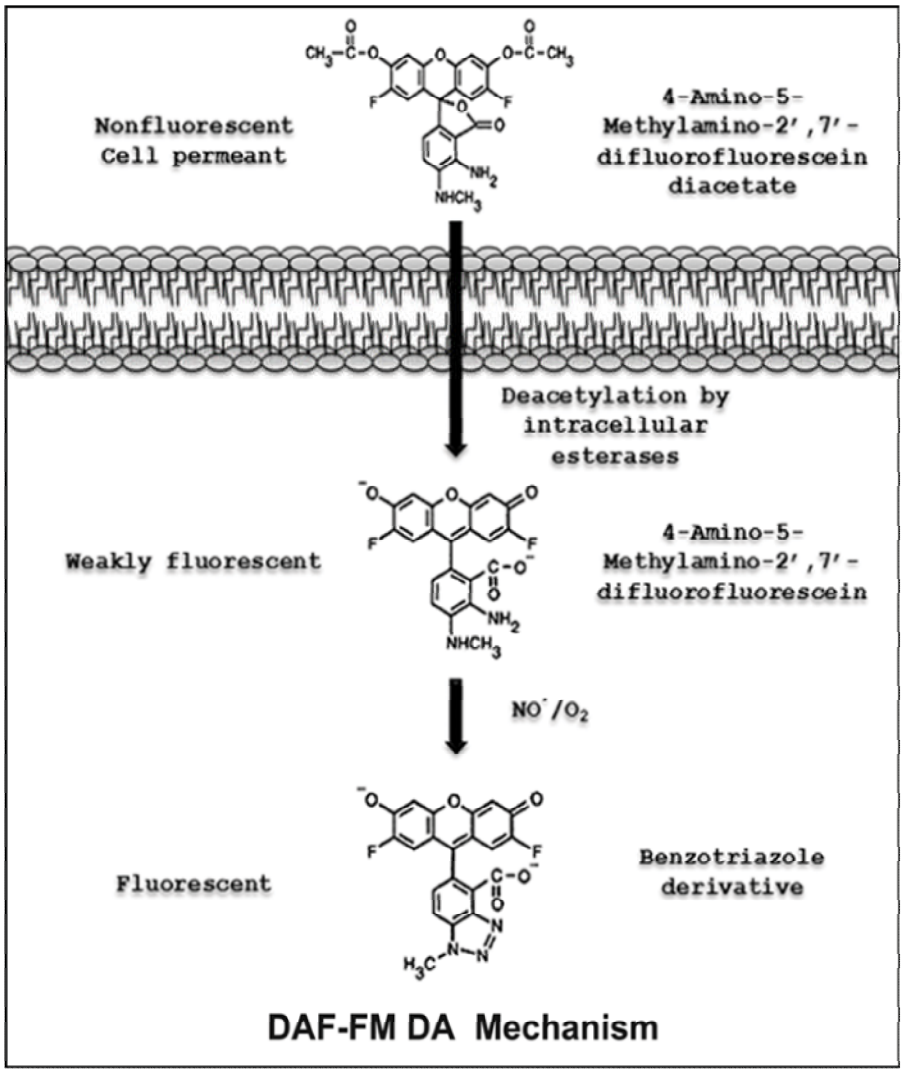

Fig. III.3. Mechanism of DAF-FM DA processing inside a cell yielding a fluorescent derivative

DAF-FM DA on entering the cell is acted upon by cellular esterases to release the weakly fluorescent form of DAF-FM. Depending on the level of NO_X present inside the cell, DAF-FM gets converted to the fluorescent benzotriazole derivative.

III.6. Measuring the mitochondrial membrane potential, morphology and mass

The cells were cultured on 24 well plates. After nitrite treatment under hyperglycemia for 24 h along with respective controls, the media were changed to HBSS (with Ca^{2+} or Mg^{2+}; Himedia Labs, India) with a cyanine dye, JC1 (Molecular Probes, Eugene, OR, USA), which gets localized to the mitochondria to form either aggregates or remain as monomers (Perelman et al., 2012; Reers et al., 1991; Smiley et al., 1991). The fluorescent probe was added at a final concentration 5 μM. The cells were incubated at 37°C for 20 minutes and the distribution of fluorescent intracellular JC1 was observed under a fluorescence microscope (IX 51; Olympus Corporation, Tokyo, Japan) for green and red fluorescence emissions. The relative fluorescence intensity was calculated as ratio of green to red fluorescence measurements using ImageJ 1.49a and normalized to control. For estimating the morphological parameters, the images of red fluorescence were background corrected using a Gaussian filter, binarized and threshold adjusted for resolving the individual mitochondria. This was then subjected to particle analysis in ImageJ ('Analyze Particles' command) to get the morphological measurements that can be used to calculate the parameters- Aspect Ratio (Major axis/minor axis) and Form Factor ($Perimeter^2/4\pi*Area$)(Dagda et al., 2009; Krebiehl et al., 2010; Wiemerslage and Lee, 2016). Images of 20 individual cells were assessed for each treatment group and control. The percentages of mitochondria (Particles) having Form Factor < 2 and Aspect Ratio < 3 were estimated as a measure of decline in mitochondrial elongation or reticulate property. For analysis of mitochondrial mass, the treated cells were incubated with 100 nM MitoTracker Deep Red FM (Invitrogen, Carlsbad, CA, USA) for 20 min at 37 °C and washed with HBSS for 5 min twice. MitoTracker Deep Red fluoresces on entering mitochondria regardless of membrane potential. For counterstaining, Hoechst stain (360 nm/450 nm) was used to fluorescently label the nuclei. The fluorescent images were obtained at 590 nm excitation / 650 nm emission wavelengths. The images were binarized and threshold adjusted using ImageJ and the mean fluorescent area was calculated after normalizing with the nuclei count.

III.7. Western blot

III.7.A. Cell lysate preparation

The culture plates having either H9c2 or C2C12 were decanted off the media and washed twice thoroughly with ice-cold PBS to remove all traces of media and other chemicals. After decanting off the PBS, the cells were incubated for 5 min in ice-cold Radio Immunoprecipitation Assay (RIPA) buffer containing protease/phosphatase inhibitor cocktail. The cells were scrapped using a cell scrapper to collect the suspension of lysed cells into a microcentrifuge tube. The lysates were vortexed in a Multitherm shaker at 4°C for 30 min. The cell lysates were centrifuged at 16,000 rcf for 20 min and the supernatants were stored at -80°C.

III.7.B. Protein quantification

RIPA soluble cell proteins were quantified using Bicinchoninic acid assay method (Smith et al., 1985) as per kit instructions (Pierce Biotechnology, MA, USA). For microplate assay, the cell lysates diluted 10-times and BSA protein standards containing a range of 125 to 2000 µg/mL protein were added to the wells. A 50:1 mix of Pierce BCA Reagent 'A' and BCA Reagent 'B' was prepared and 200 µL added to each well. The plate was incubated for half an hour in dark at 50°C and absorbance was measured at 562 nm after the plate cooled to room temperature. A standard curve of absorbance vs. micrograms protein of standard was plotted to get a linear equation using which the concentration of protein in µg/µL in the lysates were determined.

III.7.C. Electrophoresis and Blotting

The protein lysates (30-60 µg) were mixed with 6x Laemmli buffer containing 2-mercaptoethanol (2-ME), heat denatured for 5 min at 95°C and resolved on 5-12% polyacrylamide gels using Tris-Glycine-SDS buffer. The gels after the Sodium Dodecyl Sulphate- Poly Acrylamide Gel Electrophoresis (SDS-PAGE) at 100V were equilibrated with transfer buffer and excess SDS was removed. The resolved proteins in the gel were electrophoretically transferred (Burnette, 1981) using a Trans Semi Dry Blot apparatus (Bio-Rad Laboratories, Hercules, CA, USA), on to a PVDF membrane (pre-wetted with

100% methanol) at 10V for 30-40 min. The membrane was blocked for 1 h at room temperature using either 5% skimmed milk (for non-phosphoprotein detection) or 1% Bovine Serum Albumin (BSA) solutions in TBST (Refer III.F.5.11.). The membrane was then probed with antibodies (prepared in 3% BSA-TBST) specific to target proteins at 4°C overnight. Secondary antibodies conjugated to Horse Radish Peroxidase (HRP); anti rabbit IgG; 1:5000-1:8000, anti mouse IgG; 1:10000-1:20000 (Cell Signaling Technology, Danvers, MA, USA) were used to probe the primary antibodies by incubation for 1 h at room temperature.

III.7.D. Chemiluminescent detection

Protein bands were visualized using Enhanced Chemiluminescence detection. Equal volumes of luminol and peroxide solutions were mixed and added on to the membranes. Light emitting bands were captured on an X-ray film and developed and then documented in Gel Doc™ XR Imaging System (Bio-Rad Laboratories, Hercules, CA, USA) and quantified using Quantity One 1 D Analysis Software.

III.7.E. Reagents Used

III.7.E.1. Acrylamide 40%

Acrylamide- 38.67 % (w/v) and N, N'-methylene bisacrylamide- 1.33% (w/v) in 100 ml in deionized water.

III.7.E.2. Blocking solution

Skim milk- 5% (w/v) in 1X TBST (For detecting Non-phospho proteins)

BSA- 1% (w/v) in 1X TBST

III.7.E.3. 10 X TGS buffer (Running Buffer, pH-8.3)

Trizma base – 25 mM, Glycine –192 mM, SDS –1% in deionised water.

III.7.E.4. Ponceau S stain

1% Ponceau in 5% glacial acetic acid.

III.7.E.5. 8 X Resolving gel buffer (pH - 8.8)

SDS - 0.2%, Tris – 3 M in deionized water.

III.7.E.6. RIPA (Radio Immuno Precipitation Assay) Buffer pH – 8.0

25 mM Tris HCl (p^H-7.6), Sodium chloride – 150 mM, Nonidet-P-40 (NP-40) – 1.0%, Sodium deoxycholate – 0.5%, SDS – 0.1% in deionized water.

Protease and Phosphatase Inhibitors (Cocktails) added as required

III.7.E.7. SDS gel loading buffer (6X) pH – 6.8

SDS – 12%, 2- mercaptoethanol – 12.5% (Add fresh), Glycerol – 60%, Bromophenol blue – 0.012%, Tris-, HCl - 0.375 M (p^H-6.8) in deionized water.

III.7.E.8. 4 X Stacking gel buffer (pH– 6.8)

SDS – 0.1%, Trizma base 0.5 M in deionised water.

III.7.E.9. 10 X Towbin's buffer (Transfer buffer, pH-8.3)

Trizma base – 25 mM, Glycine –192 mM, 20% methanol in deionised water.

III.7.E.10. Tris-buffered saline (10 X, pH-7.6)

Tris base- 24.2 g, sodium chloride- 80 g in 1L deionized water.

III.7.E.11. Tris-buffered saline with Tween-20 (TBST) [1 X]

1X TBS containing 0.5% Tween-20.

III.7.E.12. To prepare 10% resolving gel (~10 mL)

40% acrylamide: bis-acrylamide (29:1)	- 2.5 mL
8X resolving gel buffer	- 1.25 mL
TEMED	- 10 μL

20% APS - 20 µL

Deionised water - 6 mL

III.7.E.13. To prepare 5% stacking gel (~5 ml)

40% Acrylamide- bis acrylamide gel (29:1) - 0.625 ml

Stacking gel buffer - 1.25 ml

TEMED - 5 µl

20% APS - 10 µl

Deionised water - 3.125 ml

III.8. Gene Expression Assays

III.8.A. Reagents for Agarose Gel electrophoresis

III.8.A.1.TBE Buffer (5X)

1.1M Tris, 900 mM Borate & 25 mM EDTA, pH 8.3.

III.8.A.2. 1% agarose gel

Low EEO Agarose (1%) molten in 1X TBE and casted in a gel cast

III.8.A.3. Ethidium bromide (EtBr)

EtBr dissolved at 3% concentration in distilled water.

III.8.B. RNA extraction and cDNA synthesis

Cells after treatments were washed with HBSS; lysed and total RNA was extracted using PureLink RNA Mini Kit (Invitrogen, Carlsbad, CA, USA) as per the kit instructions provided. Briefly, cells were added lysis buffer and homogenized by passing through 21G needle 8-10 times. The lysate was centrifuged at 16000 rcf and the supernatant was added with one volume of 70% ethanol and mixed well. The mixture was transferred in to spin cartridges, centrifuged and the flow-through was discarded. The columns were then washed with wash buffer I and wash buffer II. The RNA bound to the spin columns were eluted in 40 µL RNase free water. The concentration and purity of the extracted RNA

was checked using BioPhotometer Plus (Eppendorf AG, Hamburg, Germany) by measuring A260, A260/A230 and A260/A280 absorbance. Intactness of RNA was ascertained by 1% agarose gel electrophoresis by observation of intact 28S and 18S rRNA bands. The RNA samples were aliquoted and stored at -80^{o}C till use. Repeated freeze-thaw was avoided to minimize RNA degradation. Using 1 µg RNA for each sample, first strand cDNA was synthesized in a Thermocycler- iCycler (Bio-Rad, Hercules, CA, USA), as per manufacturer's protocol, using the Reverse Transcriptase Core Kit (Eurogentec, Seraing, Belgium). Briefly, the reaction mix was prepared as per Table (III.1.) keeping all reagents on ice.

Component	Volume (µL)	Final concentration
10x reaction buffer	**1**	**1x**
25 mM $MgCl_2$	**2**	**5 mM (or as required)**
2.5 mM dNTP	**2**	**500 µM each dNTP**
Random nonamer	**0.5**	**2.5 µM**
RNAse Inhibitor	**0.2**	**0.4 U/µL**
EuroScript RT	**0.25**	**1.25 U/µL**
RNase free water	**3.05**	**-**
Template	**1**	**1µg - 2µg Total RNA**
Total Mix	**10 µL**	

Table III.1. Reaction mix for reverse transcription PCR

To PCR tubes containing equal quantities of the reaction mix, the templates were added. A negative control was kept by adding water instead of template. The PCR tubes were kept on the thermal cycler and the program was set as below.

Initial step	→	10 minutes at 25°C
Reverse Transcriptase step	→	30 minutes at 48°C
Inactivation of the RT enzyme	→	5 minutes at 95°C

III.8.C. Quantitative PCR for TFAM

The cDNA was used for qPCR analysis of TFAM mRNA expression using Applied Biosystems TaqMan Gene Expression Assays. The assay primers/probes used were: Rat TFAM- Rn00580051_m1 and Rat β-actin- Rn00667869_m1. The pre-optimized protocol for comparative Ct method of TaqMan qPCR assays was performed in the Applied Biosystems 7500 Real-Time PCR System (Applied Biosystems, Carlsbad, CA) using TaqMan Gene Expression Master Mix. Briefly, 2 min hold at 50 °C for Uracil DNA Glycosylase (UDG) activity followed by 10 min hold at 95 °C for activation of the Taq Polymerase and then 40 cycles of Denaturation: 15 sec at 95 °C and Annealing/Extension: 1 min at 60 °C. The Ct values obtained for each reaction were used to calculate the ΔCt values by taking the difference between the Ct values of TFAM and the Ct values of β-actin as a reference gene. The average ΔCt of each treatment group was subtracted by the average ΔCt of the control to obtain the ΔΔCt value and then the normalized expression level of the target gene TFAM was calculated as $2^{-\Delta\Delta Ct}$ (Livak and Schmittgen, 2001). Values are expressed as fold of the control.

- $\Delta Ct = Ct_{target} - Ct_{reference\ gene}$
- $\Delta\Delta Ct = (Avg\ \Delta Ct)_{treatment} - (Avg\ \Delta Ct)_{control}$
- Relative fold of target mRNA levels of treated with respect to control = $2^{-\Delta\Delta Ct}$

III.9. Mass Spectrometric Analysis

III.9.A. Protein extraction with Rapigest SF

III.9.A.1 Reagent Preparation

Rapigest Extraction buffer

Preparation of the Rapigest-50mM NH_4HCO_3/DNAse/Protease inhibitor, further referred to as Rapigest Extraction Buffer

- Prepare 1mL 50 mM NH_4HCO_3 buffer using analytical-grade (mili-Q) water:
    - MW of NH_4HCO_3 = 79.06 ; Dissolve 3.95 mg NH_4HCO_3 in 1 mL H2O.

- Add 5µL of Phenyl methane sulfonyl fluoride (PMSF) [Protease inhibitor] from 100mM Stock solution dissolved in isopropanol.
- Add DNAse II, at concentration of 2 µg/mL. Use the normal bovine DNAse II Boehringer (DRC stock solution 0.4 mg/mL, use at final 5 µL/mL = 1/200)
- To a tube containing 1 mg Rapigest detergent, add 50 µL of 50 mM NH_4HCO_3/DNAse/Protease inhibitor buffer and re-suspend vigorously.

III.9.A.2. Extraction of protein using sonication/freeze-thaw/detergent

The cells at a density of 1.5 x 10^6 per mL were used for processing after washing twice with ice cold PBS. After the second wash, the pellet was dispersed in 300 µL PBS in a 1.5 mL safe-lock tube and spin down vigorously. The supernatant is removed from the pellet through aspiration and 50 µL Rapigest Extraction Buffer is added and resuspended vigorously. The suspension is then sonicated for 10 minutes in a water bath without ice, at room temperature to allow DNAse to be active. If slimy threads are persisting on pipetting, sonication was repeated for another 10 minutes. The lysate was then centrifuged at 16000 rcf for 10 minutes and the supernatant was collected leaving the debris in the tube. The clear supernatant was stored at -80°C freezer as aliquots after quantifying the protein using BCA assay. Each aliquot would have 100 µg of protein which is the optimal concentration for proteomic analysis.

III.9.B. Proteomic profiling

The RapiGest-extracted proteins were subjected to in-solution trypsin digestion to get a solution of digested peptides. This solution is then centrifuged at 16000 rcf for 15 minutes, and the supernatants were subjected to Liquid Chromatography-tandem mass spectrometry (LC/MS/MS) based proteomics analysis. Three technical replicates runs were performed for each sample. A nano ACQUITY UPLC® chromatography system (Waters, Milford, MA, USA) coupled to a Quadrupole-Time of Flight (Q/TOF) mass spectrometer (SYNAPT-G2, Waters, Milford, MA, USA) controlled by MassLynx4.1 SCN781 software (Waters, Milford, MA, USA) was used for the proteomics analysis. Proteins were identified and quantified using Progenesis QI for Proteomics (Non-linear Dynamics, Newcastle upon Tyne, UK). The UniProt IDs for the peptides from *Rattus*

norwegicus protein database were converted into gene symbols, and their relative quantities were determined as fold change over control. The fold increase or decrease was considered significant only when the 'q' values (False discovery rate) were ≤ 0.05.

The fold increase or decrease was considered significant only when the 'q' values (p values corrected for false discovery rate set at 1%) were ≤0.05.

III.10. High Resolution Respirometry

Cell cultured in 100 mm dishes were given different treatments for 24 h and 48 h, trypsinized, washed and resuspended in serum free DMEM at a cell density of $1x10^6$/mL, to be loaded into the 2 mL chambers of O2k Oxygraph (Oroboros, Innsbruck, Austria) for high resolution respirometry. The respiratory measurements were acquired at an oxygen concentration of 185 nmol O_2/mL medium, on air saturation at 100 kPa barometric pressure. Oxygen consumption by the suspended cells stirred at 750 rpm was measured at 37 °C and recorded as oxygen flux per million live cells. The oxygen flux is derived as the negative slope of the oxygen concentration vs. time using the DatLab6 Analysis Software (Oroboros, Innsbruck, Austria). State 4 respiration (Leak) was determined by addition of oligomycin (2.5 μM). Uncoupled state of respiration (ETS) which represent the maximal mitochondrial respiratory capacity was determined in presence uncoupler FCCP (1-2 μM). Complex I was inhibited by rotenone (0.05 μM) and finally, antimycin-A (2.5 μM) was added to inhibit complex III- mediated respiration for the measurement of non-mitochondrial respiration.

Data acquisition and analysis of oxygen consumption rate (OCR) were performed with DatLab6 software. Uncoupler and inhibitors (Table III.2.) for respiratory experiments were added to the serum free medium containing cells in a step-by-step manner with the use of micro syringes.

The measurements obtained from the plot of oxygen consumption/flux JO_2 were:

Basal (Routine) respiration (R): "Respiration used to meet the endogenous ATP demand of the cell and drive proton leak pathways."

Leak Respiration (L): “Protons can leak across the inner mitochondrial membrane independently of ATP synthase (oligomycin insensitive).”
Maximal Respiration (E): “The maximum rate of respiration induced by a protonophore that dissipates the proton gradient.”
Residual oxygen consumption (ROX): “The oxygen consumption mainly due to the activities of non-mitochondrial oxidases such as NAD(P)H oxidases and due to the instrumental background.”

Chemical	FW	Stock solution Conc. (mM)	Stock solution Amount added to 2 mL chamber	Final concentration in 2 mL
Antimycin A	**540**	**5**	**1 µL**	**2.5 µM**
Carbonyl cyanide p-(trifluoro-methoxy) phenyl-hydrazone (FCCP)	**254.21**	**1**	**1 µL titrations**	**0.5 µM per addition**
Oligomycin	**800**	**5**	**1 µL**	**2.5 µM**
Rotenone	**394.4**	**1**	**1 µL**	**0.5 µM**

Table. III.2. Stock preparation and working concentrations of chemicals for Oxygraph

All oxygen consumption values (JO_2) were measured as slope in ‘dat’ files which are the output files of Oroboros O2K Oxygraph and the mean values were extracted from appropriately marked time points on the dat files. The first three respiratory measurements are corrected for the ROX value and used for calculating the coupling efficiency of the intact cell mitochondria.

Coupling Efficiency is the percentage of mitochondrial oxygen consumption linked to ATP synthesis at a given membrane potential. Mathematically,

Coupling Efficiency = 100 x (R-L)/R

OR **100*(ATP linked respiration/Basal respiration)**

The fraction of routine respiration and leak respiration to the ETS capacity (E) was represented as Flux Control Ratios. The routine control ratio will be R/E and the leak control ratio is computed as L/E. The L/E ratio also represents the reciprocal of intact cell respiratory control ratio, which is another measure of mitochondrial efficiency. All these measurements are fractions and hence exclude the need for normalizing the data with cell number, protein content or citrate synthase activity.

III.11. RNA silencing

The H9c2 cells cultured in 35 mm dishes were grown till 60% confluence. For 50 nM concentration, 110 pmoles of Drp1 siRNA was mixed with 200 µL of jetPRIME® buffer and mixed well by inversion. To this, 4 µL jetPRIME® reagent was added and the mixture was then vortexed for 2 seconds, spun down and incubated at room temperature for 10-15 minutes. The transfection mix was added to 2 mL of serum-free culture medium for each dish. After addition of the medium containing the transfection mix, the culture dishes were gently rocked back and forth and from side to side and then incubated in CO_2 incubator at 37°C. After 4 h, the media was changed to 2% DMEM to avoid the toxicity of transfection reagent. The transfection was analyzed after 48 h of incubation at 37°C.

III.12. Statistical Analysis

All values are given as means ± Standard Error of Mean (SEM). A p- value of less than 0.05 was considered as significant for all statistical evaluations. Comparisons between more than two groups were performed using one-way ANOVA followed by Tukey's post

hoc multiple comparison tests, if not mentioned otherwise. Some of the data were analyzed by two-way ANOVA with Dunnett's post hoc tests. {In the associated publication, most data were analyzed by two-way ANOVA with Tukey's post hoc tests to differentiate between independent main effects and interactions between nitrite treatment and hyperglycemia effects. Also the variations in the data were depicted by Standard Deviation (SD) instead of SEM. Further, the numbers of replicates in most data were increased to ≥ 4 instead of 3}. Statistical evaluations and graph preparation were done using Graph pad Prism 6.

IV. Results

IV.1. Assessment of Cell Viability

The culture media used for the NO pro-drugs was having varying glucose concentrations and so a viability test was conducted to determine the time-dependent effect of glucose exposures on cell viability before determining the NO pro-drug concentrations to be utilized. The viability of the cells after exposure to high glucose (HG), SNAP and nitrite ($NaNO_2$) was determined by MTT and Hoechst/Propidium iodide (PI) assays. DMEM containing 30 mM glucose was considered as HG and DMEM containing normal glucose concentration of 5.5 mM (NG) along with mannitol (24.5 mM) was taken as osmotic control (Man) to account for hyperosmolarity of the medium (He et al., 2013; Xie et al., 2008). The effect of HG on the metabolic activity (indirect measure of viability) of H9c2 cardiac myoblasts for different time durations- 3, 6, 12 and 24 h was first checked using MTT assay. It was observed that a significant decrease in metabolic activity occurred at 24 h for H9c2 (Fig. IV.1. A). Further, a Hoechst-PI staining of the cells after 6, 12, 18, 24 and 48 h of HG exposure showed that the percent of PI stained nuclei (non-viable) over Hoechst stained (total) nuclei increased from 18 h onwards but significantly in 24 h and 48 h time points (Fig. IV.1. B and C). HG exposure for 24 h, where initiation of a significant cell death occurred was used for all subsequent experiments but for respirometric studies 48 h time point was also studied to account for any functional alterations in mitochondria. Such a selection of time point was in order to exclude the drastic changes in cellular signaling happening on initiation of apoptotic pathways.

For determining the appropriate concentrations of SNAP and nitrite for ensuing experiments, MTT assays were performed under both NG and HG. Serial dilutions of SNAP with concentrations from 200 to 25 µM and sodium nitrite concentrations from 1000 to 1 µM were used from stocks prepared as discussed in methods. H9c2 cells exposed for 24h to NG and HG and nitrite was supplemented throughout the 24 h while SNAP was added 4 h prior to the end of the treatment. Thus, nitrite treatment represented a chronic supplementation of an NO pro-drug while SNAP addition corresponds to an acute exposure. The percent viability of cells was unaltered by SNAP concentrations up to 50 µM compared to their respective controls under NG and HG.

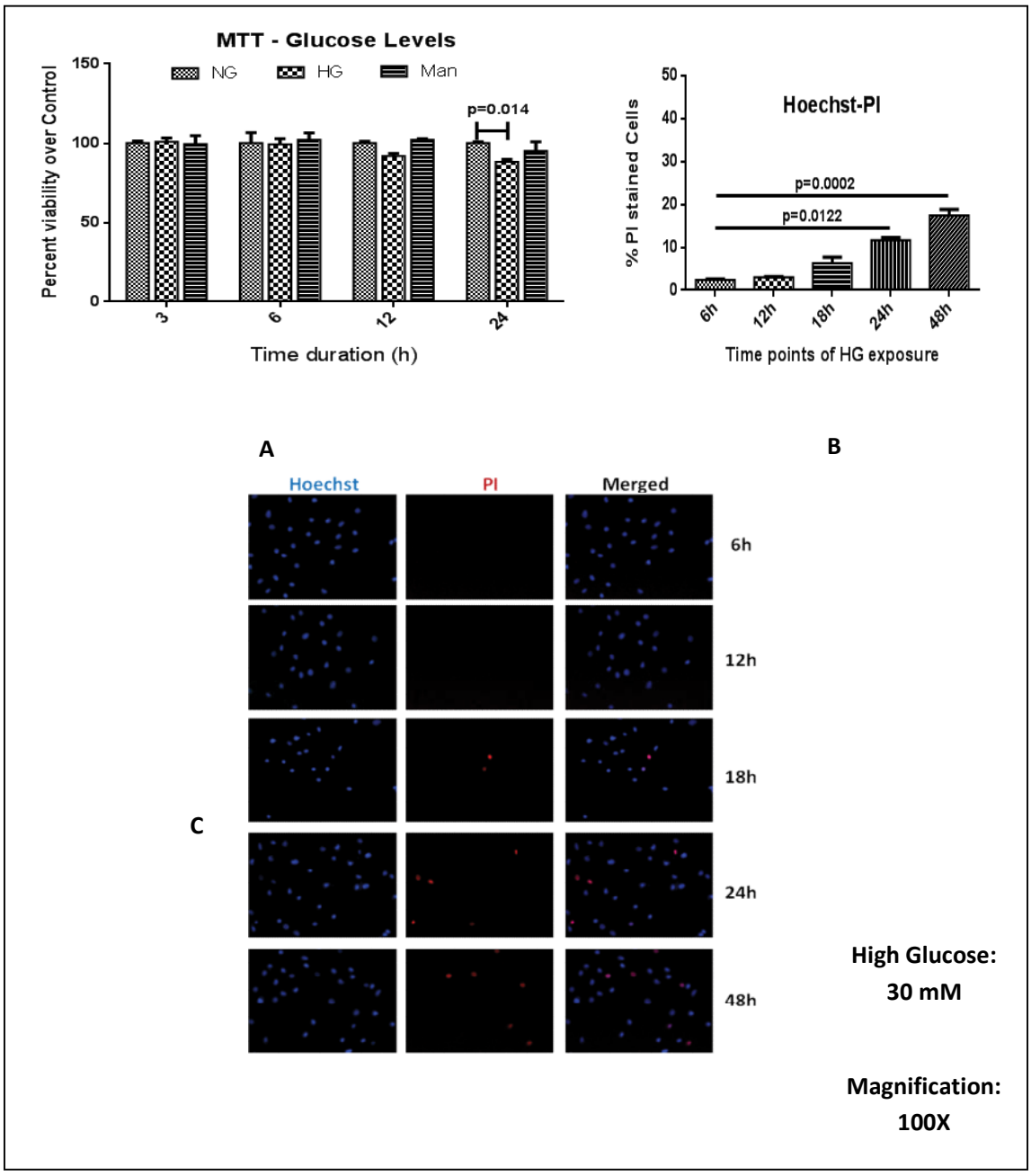

Fig. IV.1. Time dependent effect of high glucose (HG) on H9c2 cell viability

Sub confluent cultures of H9c2 were exposed to 30 mM glucose for different time durations and analyzed by MTT and Hoechst-PI assays as discussed above. For MTT, the absorbance by the formazan formed are calculated as percent over control and represented as mean ± SEM, n=5. Two-way ANOVA followed by Tukey's post hoc test was performed to analyze the data (A). For Hoechst-PI staining, the percentages of PI to Hoechst ratio are represented as means ± SEM, n=3. Data analysis was done using one-way ANOVA followed by Dunnett's multiple comparisons test (B, C).

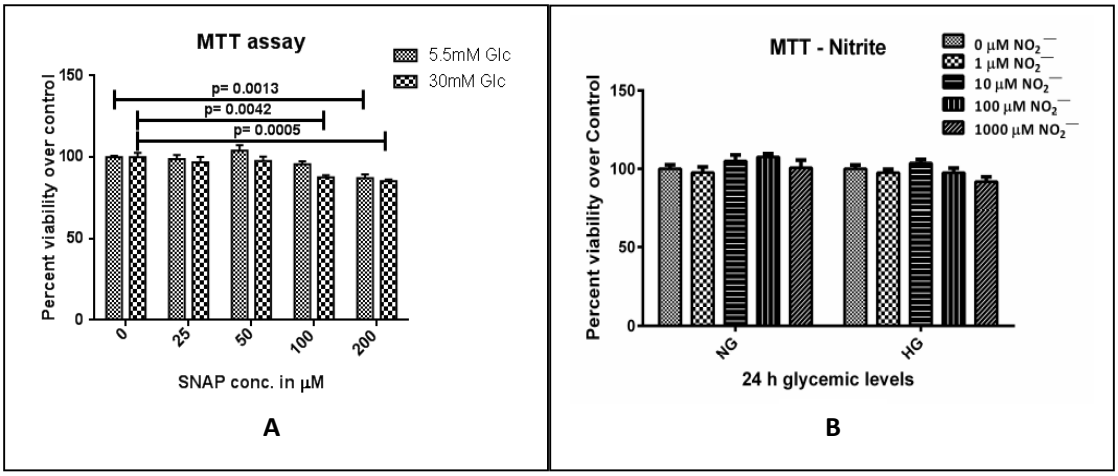

Fig. IV.2. Effect of different SNAP (4 h) and nitrite (24 h) concentrations on H9c2 cell viability under NG and HG conditions

H9c2 cells were exposed for 24h to NG and HG along with either SNAP (A) or nitrite (B) treatments. The percent viability over respective controls are shown as bar graphs of mean values and error bars represent the SEM., n=4. Data were analyzed using one-way ANOVA followed by Dunnett's post hoc test.

Nevertheless, the viability declined significantly on 100 µM and 200 µM SNAP exposures under HG while under NG significant drop was observed at 200 µM exposure (Fig. IV.2. A). After nitrite treatments at different concentrations, there was no significant difference among the groups under both NG and HG conditions (Fig. IV.2. B). Hence, 50 µM SNAP and 500 µM nitrite was chosen for subsequent experiments. Nitrite concentration of 500 µM was used by Roberts and associates (Roberts et al., 2017) with C2C12 cells and they had also reported a plasma concentration of 500 µM nitrate corresponding to metabolically improved phenotypes in mice on dietary nitrate supplementation.

From the MTT results it was apparent that nitrite *per se* is not altering the viability of H9c2 cells. In order to confirm this, a Hoechst-PI staining was performed with H9c2 in 96- well plates exposed to 500 µM nitrite under NG and HG and the percent of PI stained cells to Hoechst stained cells was found to be decreased similarly in both HG and HG with nitrite (HGN) when compared to NG and NG with nitrite (NGN) (Fig. IV.3 A & B).

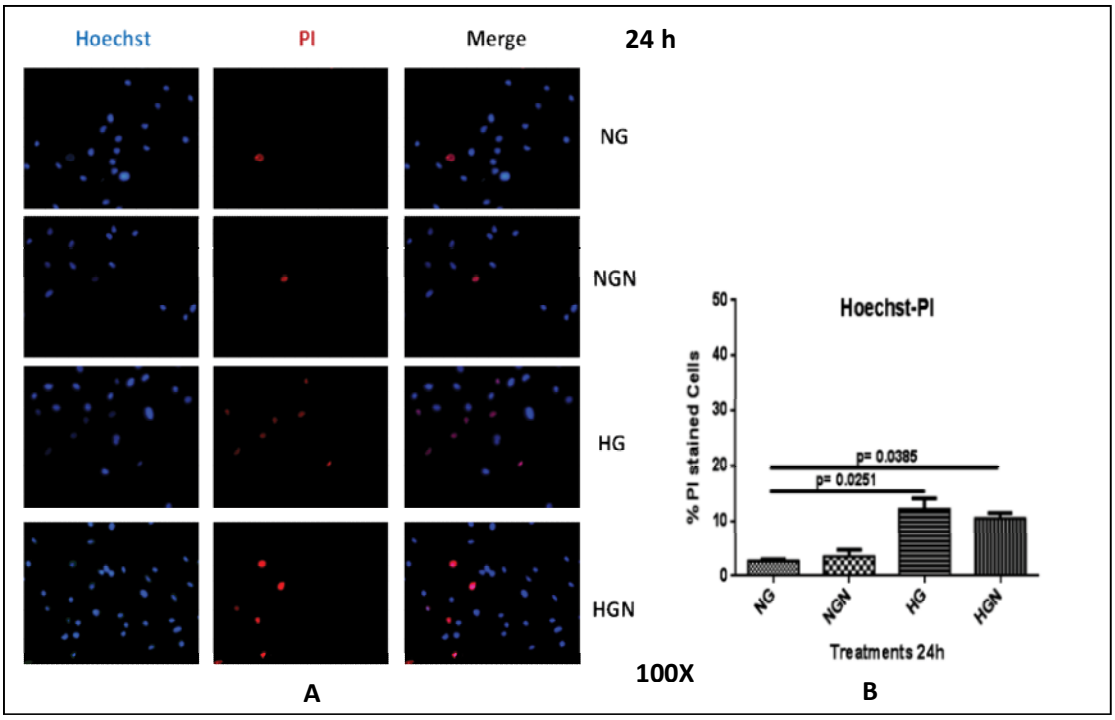

Fig. IV.3. Hoechst-PI staining showing that HG induced cell death is unaltered on nitrite treatment

H9c2 cells were exposed for 24h to NG and HG with and without nitrite (500 µM) treatments and stained with Hoechst and PI (A). The percentages of PI to Hoechst ratio on counting atleast 200 cells per well are represented as means ± SEM, n=3 (B). One-way ANOVA followed by Tukey's post hoc test was performed to analyze statistical significance of differences between the means.

IV.2. Intracellular NO_X production on nitrite treatment

In order to check whether nitrite supplementation augments the NO_X generation in H9c2 cells, the NO sensitive fluorescence probe DAF-FM diacetate was used. Nitrite (500 µM) treatment for 24 h increased the DAF fluorescence while it was abrogated by 1 h pre-treatment followed by co-treatment with a pan nitric oxide synthase (NOS) inhibitor, L-NAME (5 mM) or the NO scavenger, carboxy-PTIO (50 µM). The concentrations of the antagonists of NO levels in the cell used were as mentioned in previous literatures (Roberts et al., 2017; Villa-Abrille et al., 2008). The control group of cells was added with DMSO at a final concentration 0.1% in cell medium and the pharmacological compounds dissolved in DMSO were added such that final DMSO concentration was ≤0.1% which wielded no discernible effect on the myocytes (Butler et al., 2015; Li et al.,

2019; Truitt et al., 2018). The fluorescence micrographs revealed that nitrite treatment is augmenting the NO levels inside the H9c2 cells (Fig. IV.4.).

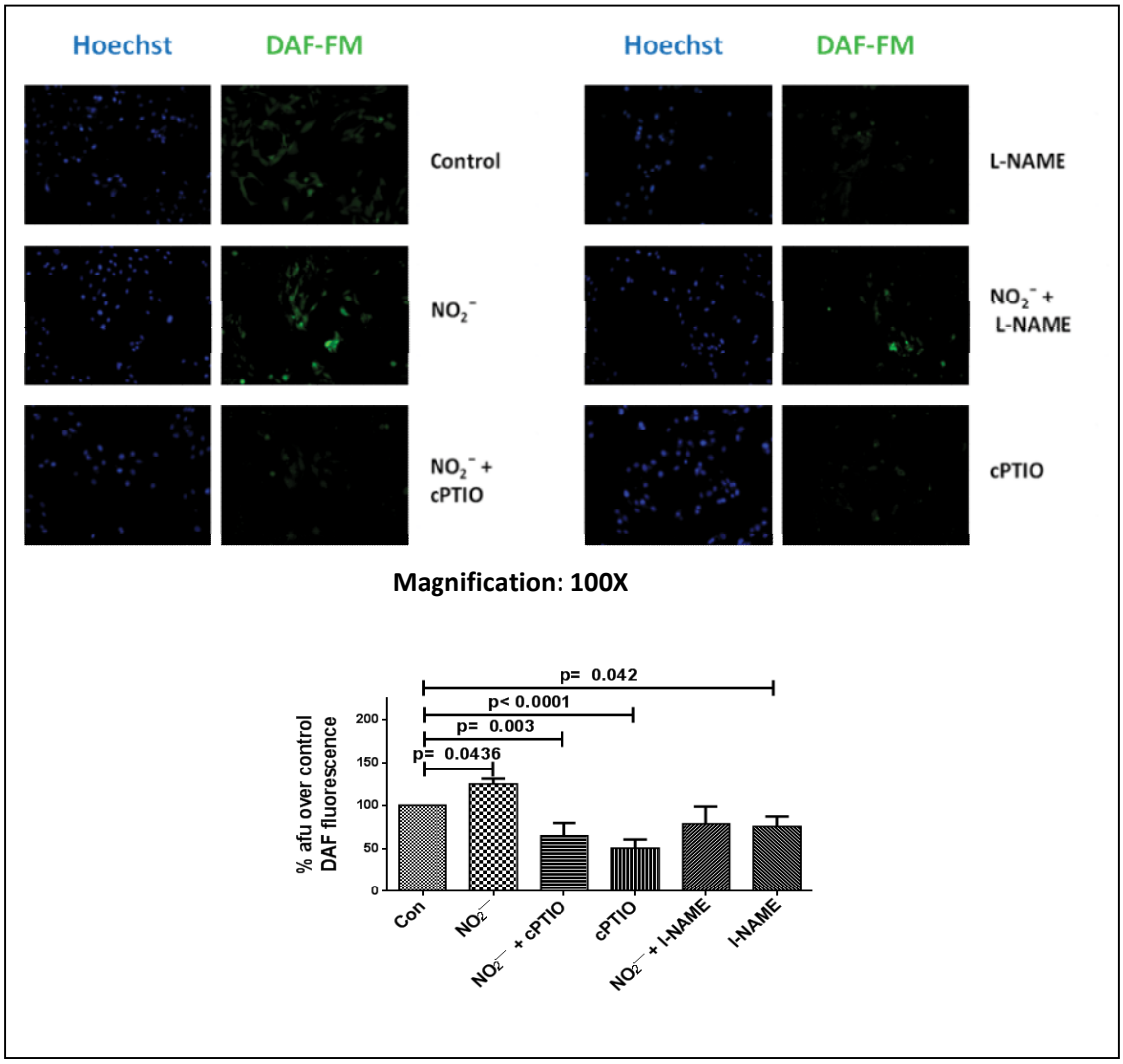

Fig. IV.4. DAF-FM staining confirming that intracellular NO_X levels increase on nitrite treatment

H9c2 cells were exposed for 24h to NG with and without nitrite (500 µM) treatments and stained with the NO detection probe, DAF-FM diacetate and Hoechst 33342 counterstain for capturing fluorescent images. H9c2 cells treated with L-NAME or cPTIO alone served as negative controls. The percent fluorescence intensities are represented as mean ± SEM (n=3).

IV.3. Unaltered endothelial nitric oxide synthase activity by nitrite

Dietary supplementation of inorganic nitrite has been reported to reduce the endothelial nitric oxide synthase (eNOS) activity in mice aorta (Carlström et al., 2013). In order to

verify if nitrite has similar effect *in vitro* on myoblasts cultured under NG and HG, lysates of nitrite treated H9c2 and respective controls were examined for inhibitory (Thr495) and activation (Ser1177) phosphorylations of eNOS. It was found that nitrite under NG did not exert any significant effect on either of the phosphorylations. However under HG irrespective of nitrite treatment, H9c2 cells showed enhanced Thr495 phosphorylation and a reduced Ser1177 phosphorylation of eNOS implying a reduced activity. Hence, nitrite *per se* is not affecting the eNOS activity under both NG as well as HG (Fig. IV.5.).

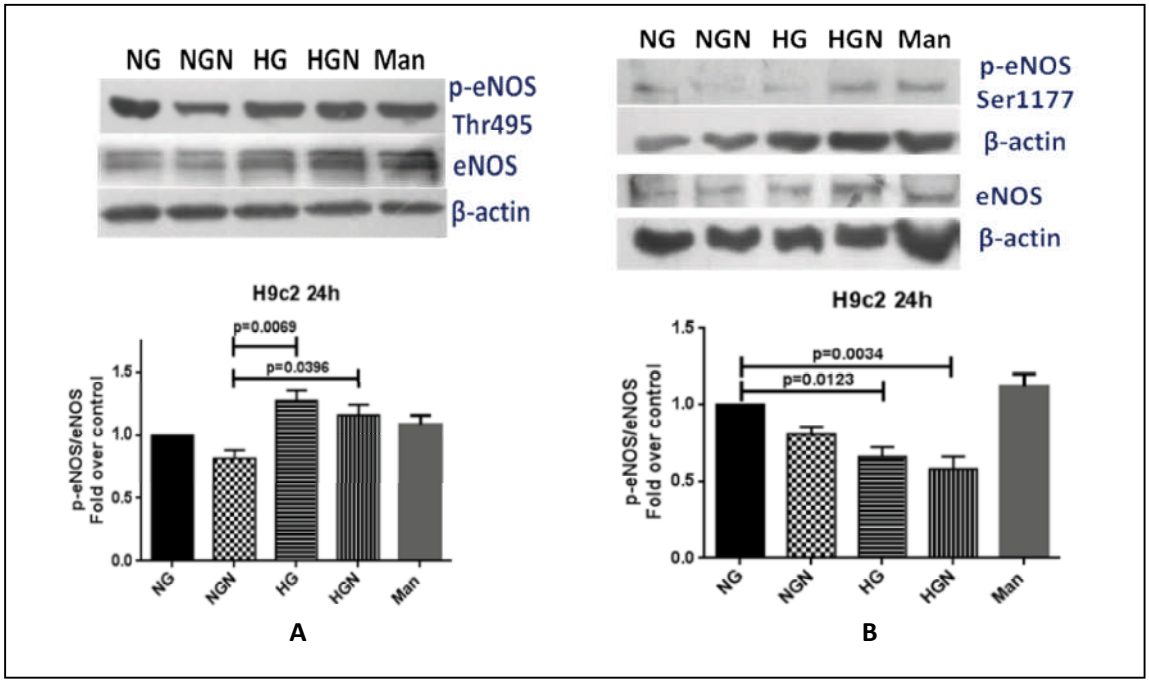

Fig. IV.5. Reduced activity of eNOS under HG with or without nitrite treatment

H9c2 cells lysates after treatment with NG and HG with and without nitrite (500 µM) were probed using antibodies specific for eNOS phosphorylations at Thr495 (A) and Ser1177 (B). Their relative expressions with total eNOS were quantified and represented as mean values of fold over control (NG). Mannitol treated cells acted as osmotic control. Error bars refer to SEM, n=3.

IV.4. Altered intracellular ROS production on HG/Nitrite treatment

As Pride and associates have shown that nitrite preconditioning enhances mitochondrial fusion and consequent mitochondrial ROS generation in cardiomyocytes (Pride et al., 2014), it was imperative to verify the effect of nitrite on ROS production under high

glucose (HG) condition. With this intention, the H9c2 cells treated with nitrite under NG and HG were labeled with H_2DCFDA probe and analyzed with a flow cytometer.

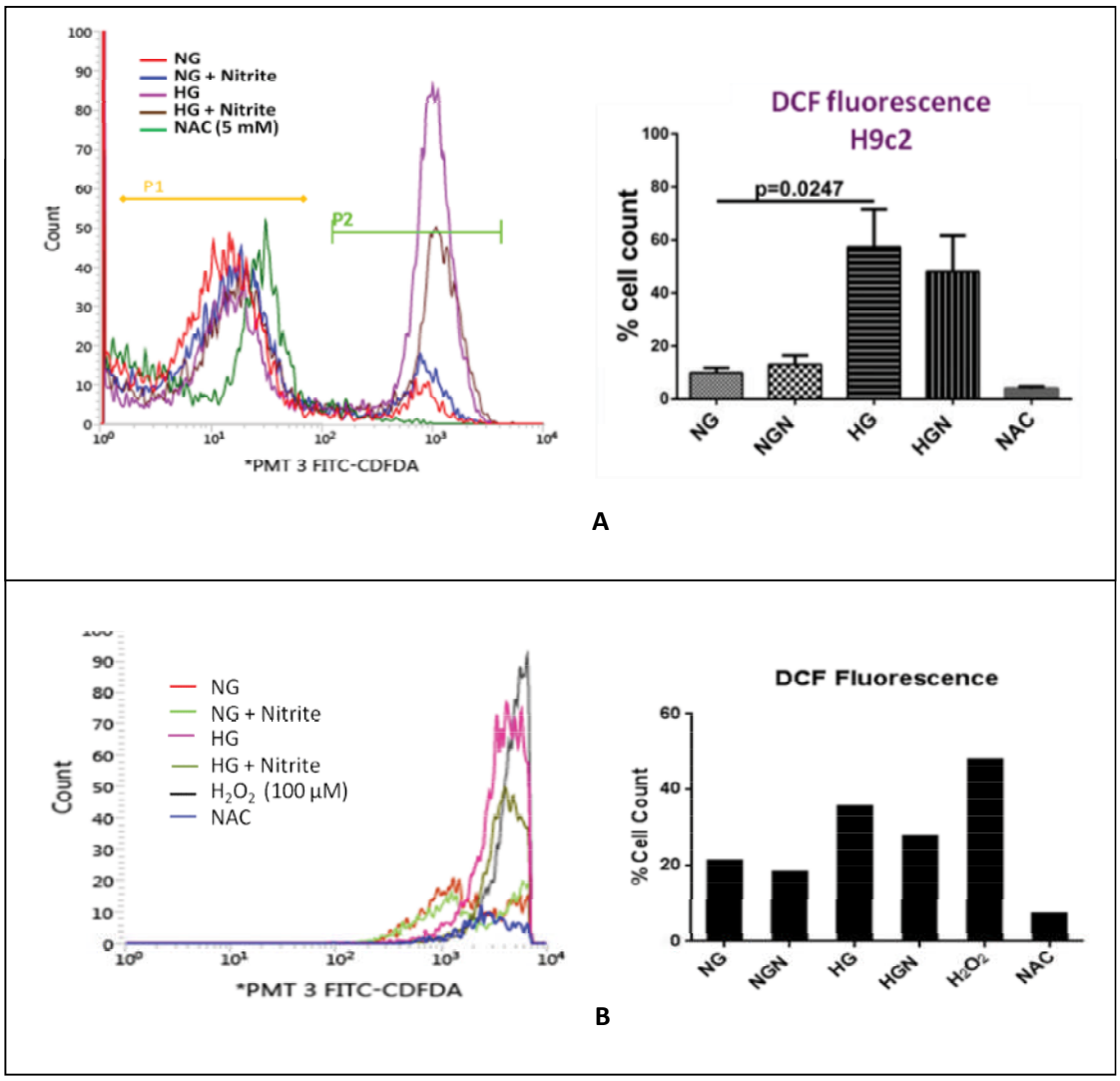

Fig. IV.6. FACS analysis for ROS measurements in H9c2 and C2C12

H9c2 cells after HG treatment with or without nitrite along with respective controls were analyzed for ROS induced DCF fluorescence. The percent count of cells with DCF fluorescence greater than or equal to 1 x 10^2 arbitrary fluorescence units are shown as bar graphs for H9c2 (A),n=3 and C2C12 (B) cells, n=2.

Cells in NG, pre-treated for 2 h with 5 mM N-acetyl cysteine (NAC) which abrogates ROS levels, were used as the negative control (Rouschop et al., 2013; Valdivieso et al., 2018; Wang et al., 2019). Similarly, a set of FACS analysis was performed with C2C12

myoblasts along with a positive control of cells (NG) treated with 100 µM H_2O_2 one hour prior to harvesting for H_2DCFDA labeling.

Interestingly, inorganic nitrite treatment for 24 h reduces the intracellular ROS levels insignificantly under HG, in both cell lines (Fig. IV.6). In order to confirm this observation a similar set of treatments was done with H9c2 cells followed by H_2DCFDA labeling for fluorimetric analysis. Here, two sets of the nitrite treated cells under NG and HG were used, one set with a NAC pretreatment and the other without it.

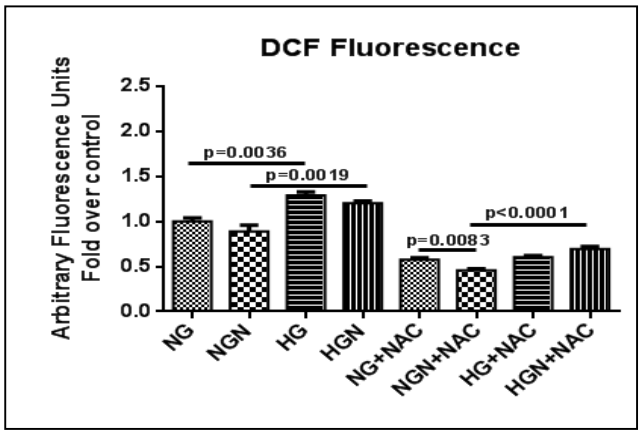

Fig. IV.7. Fluorimetric analysis with H_2DCFDA probe for ROS measurements on nitrite supplementation in H9c2 after depletion of basal ROS

H9c2 cells were treated similar to previous experiment with and without a 2 h NAC pre-treatment and DCFDA assay was performed using fluorimetry. DCF fluorescence measured from fluorimeter was represented as bar graph of mean values with arbitrary fluorescence units, and SEM denoted by error bars.

From the fluorimetric measurements, it was observed that DCF fluorescence was high in both the HG treated groups, while the 24 h nitrite treatments tends to decrease the fluorescence levels insignificantly under both NG and HG. This is in contrast to the preconditioning effect of nitrite on H9c2 cells where it transiently enhances ROS generation (Pride et al., 2014). A remarkable observation that came across was the effect of nitrite on cells depleted of basal ROS levels by NAC pretreatment. In the NG conditions, nitrite significantly reduced the ROS generated in the cells after NAC pretreatment. Meanwhile under HG, ROS production was found to be enhanced by nitrite in comparison with the former group (Fig. IV.7.). These observations point to the

differential effects of nitrite on cellular redox status based on the ROS environment already prevailing in the cells.

IV.5. Altered mitochondrial ROS production on HG/Nitrite treatment

Apart from the total intracellular ROS, the mitochondrial specific superoxide generation was analyzed in H9c2 cells after the nitrite treatments under NG and HG. For this, the mitochondrial superoxide specific probe, MitoSOX was used and the fluorescent micrographs revealed higher fluorescence intensity in both the high glucose treated groups. However, compared to HG group the intensity was significantly lower in HGN group indicating lesser mitochondria generated ROS. This observation is in concordance with the FACS data where the total intracellular ROS was inclined to decrease in cells given nitrite under HG (Fig. IV.8.). The superoxide generated from the mitochondrial complexes during oxidative phosphorylation, especially complexes I and III are the major source of intracellular ROS in myocytes having a high mitochondrial content (Bleier and Dröse, 2013; Brand, 2010; Wong et al., 2017; Zhao et al., 2019).

IV.6. Altered expressions of antioxidant enzymes and the ROS sensitive Aconitase 2 enzyme by HG, nitrite and SNAP treatment

As there is an elevated ROS under HG conditions, the effects on the antioxidant enzymes, Glutathione Peroxidase4 (GPx4) and mitochondrial superoxide dismutase (SOD2) expressions were examined. The former increased in HG treated cells while on SNAP treatments under NG and HG, no significant change was observed. In the case of SOD2, SNAP treatment under NG elevated the protein levels two-fold while HG also increased its expression. Meanwhile on addition of SNAP under HG, the SOD2 levels were significantly lower than the expression in NGS group (Fig. IV.9.). This indicates the differential effect of SNAP in the normal and hyperglycemic levels on mitochondrial antioxidant levels, but its implications are ambiguous as the activity of the SOD2 enzyme might also be altered. A similar set of experiments where nitrite was given instead of SNAP indicated a rise in both GPx4 and SOD2 levels after HG treatment, while nitrite

non-significantly reduced the levels of MnSOD which is in concordance with the MitoSOX results (Fig. IV.10.).

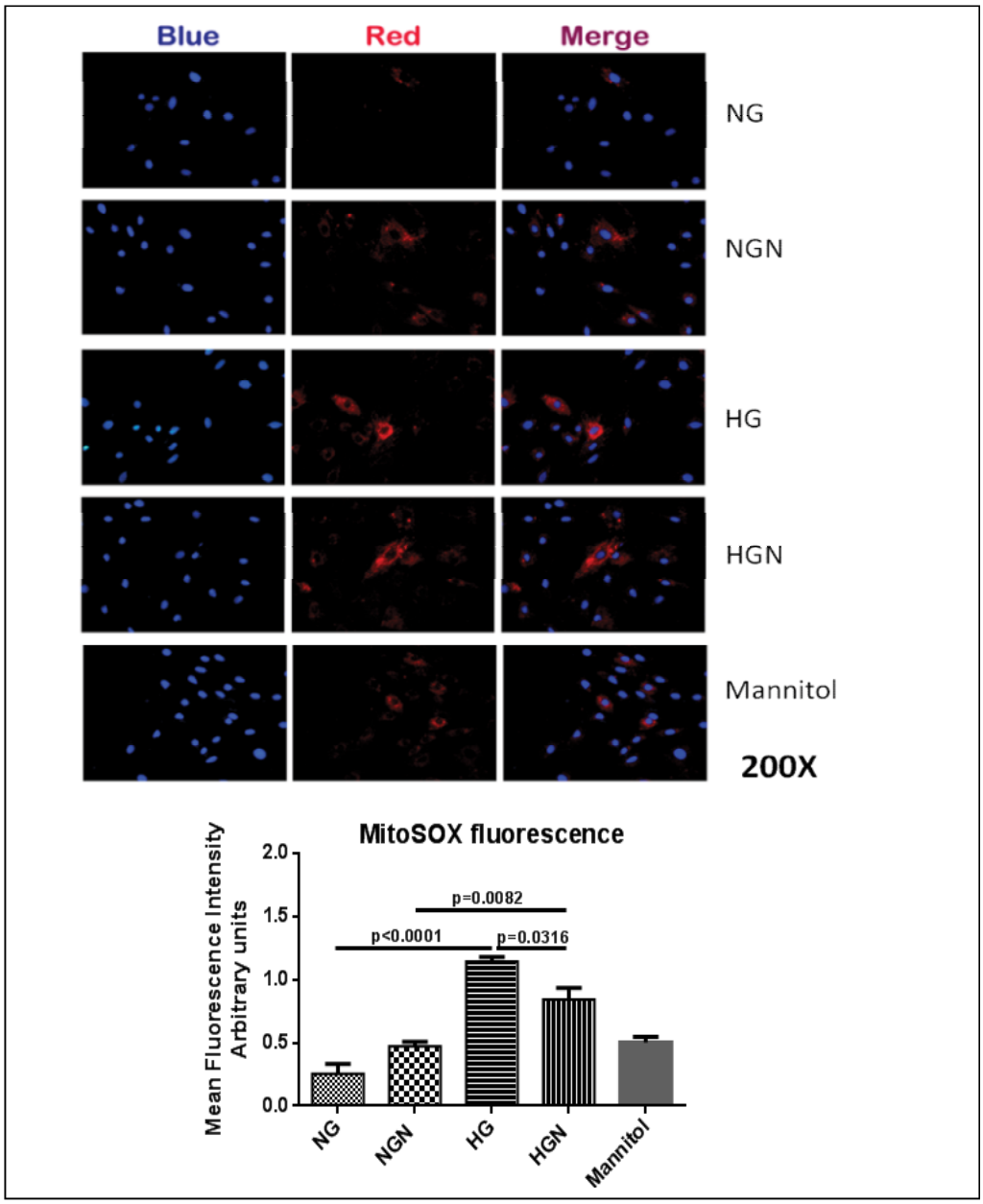

Fig. IV.8. Elevated mitochondrial ROS labeled by MitoSOX staining in HG and HGN groups

H9c2 cells were exposed for 24h to NG with and without nitrite (500 µM) treatments and stained with the mitochondrial ROS detection probe, MitoSOX Red and nuclear stain Hoechst. The fluorescence intensity of oxidized MitoSOX was high in both the HG treated groups but the intensity was significantly lower in the

nitrite treated group as indicated by the bar graph denoting mean ± SEM. Representative images of one field per group are shown, n=3.

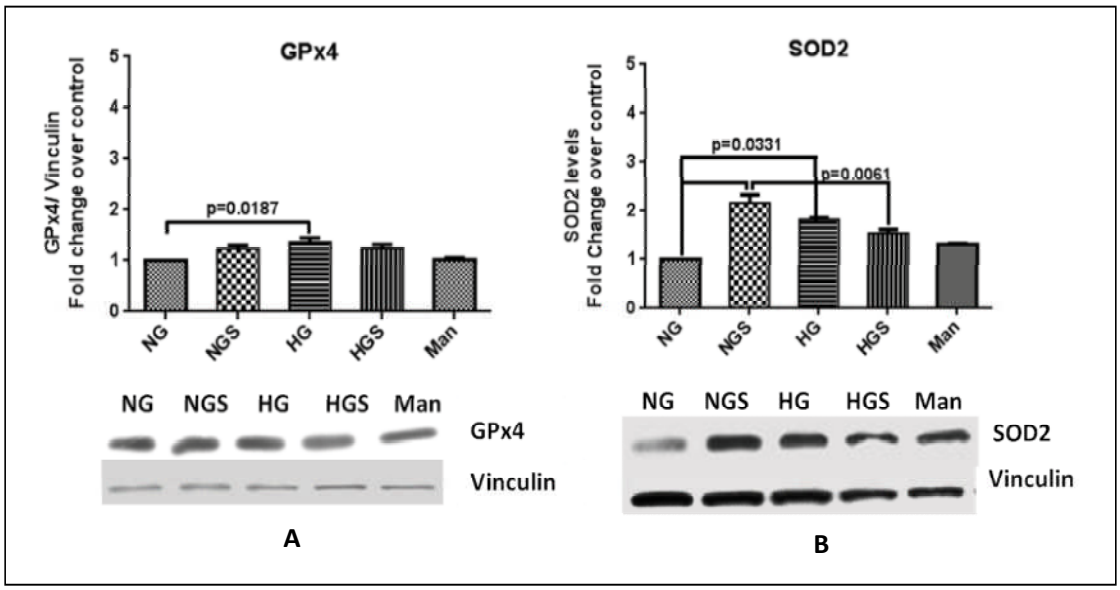

Fig. IV.9. Equivocal expression of GPx4 and SOD2 after HG and SNAP treatments

Lysates of H9c2 cells prepared after treatment with SNAP under NG and HG were probed by immunoblotting for GPx4 (A) and SOD2 (B). Their relative expressions with vinculin were quantified and represented as mean values of fold over control (NG). Error bars denote the SEM, n=3.

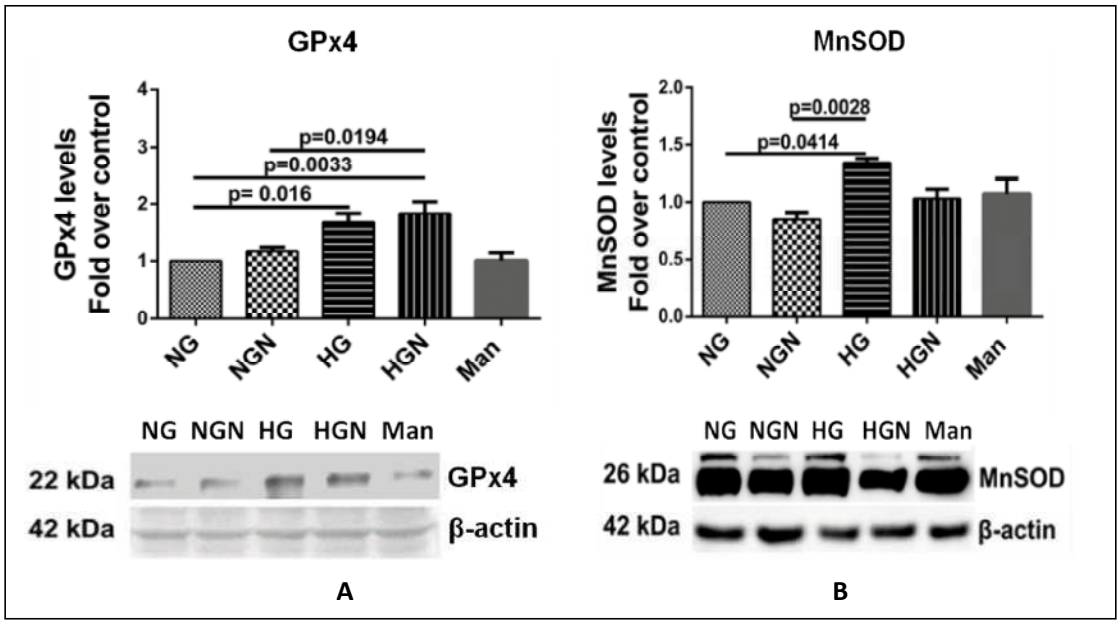

Fig. IV.10. Altered expression of GPx4 and SOD2 after HG and nitrite treatments

The H9c2 cell lysates were immunoblotted using GPx4 and SOD2 antibodies to know the effect of nitrite treatment on antioxidant levels under NG and HG. The representative blots from four independent experiments are shown and bar graphs represent the mean values with SEM.

Further, by examining the expression of the mitochondrial enzyme Aconitase2 under both of the above conditions, the effect of SNAP and nitrite on a ROS sensitive enzyme was studied (Lushchak et al., 2014b; Scandroglio et al., 2014). Also, Aco2 has been reported in astrocytes to generate ROS when it gets inactivated by exogenous peroxide, thereby exacerbating neurotoxicity (Cantu et al., 2009). The expression of Aconitase 2 in H9c2 cells showed no alterations after nitrite or HG treatments (Fig. IV.11. A) while SNAP treatment imparted a downregulation under HG as opposed to when given under NG (Fig. IV.11. B).

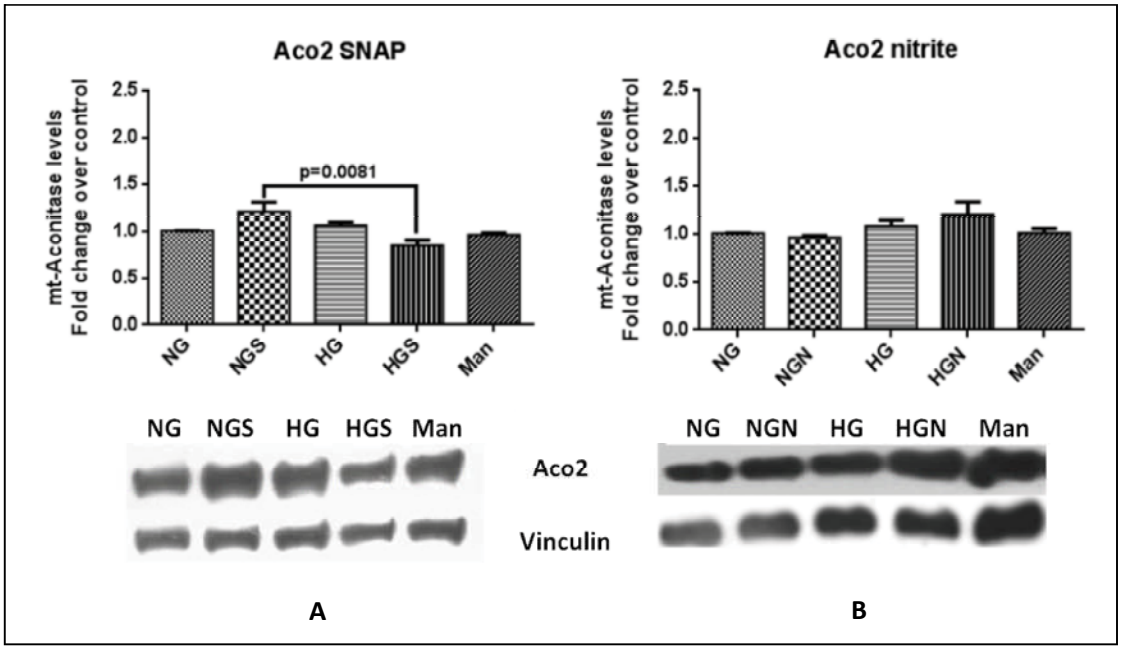

Fig. IV.11. Mitochondrial Aconitase expression on HG, SNAP and nitrite treatments

The aconitase 2 expressions in H9c2 cells are represented as mean ± SEM of fold change over control. The bands were normalized with those of Vinculin as loading control, n=3. Bar graphs of SNAP/HG treatments (A) and Nitrite/HG treatments are also shown (B).

IV.7. Decreased mitochondrial membrane potential in H9c2 cells on HG, nitrite and SNAP treatment

As observed in Fig. IV.8. nitrite treatment reduced formation of superoxide in the mitochondria under HG. The superoxide generation is closely linked to the membrane permeability of the mitochondria and also the rate of ROS production from mitochondrial complexes is dependent on the membrane potential (Düssmann et al., 2003; Suski et al., 2012; Suski et al., 2018). So, a mitochondria specific dye, JC1 which is sensitive to transient membrane potential changes induced by ADP or inhibition of oxidative phosphorylation was used (Sivandzade et al., 2019; Smiley et al., 1991).

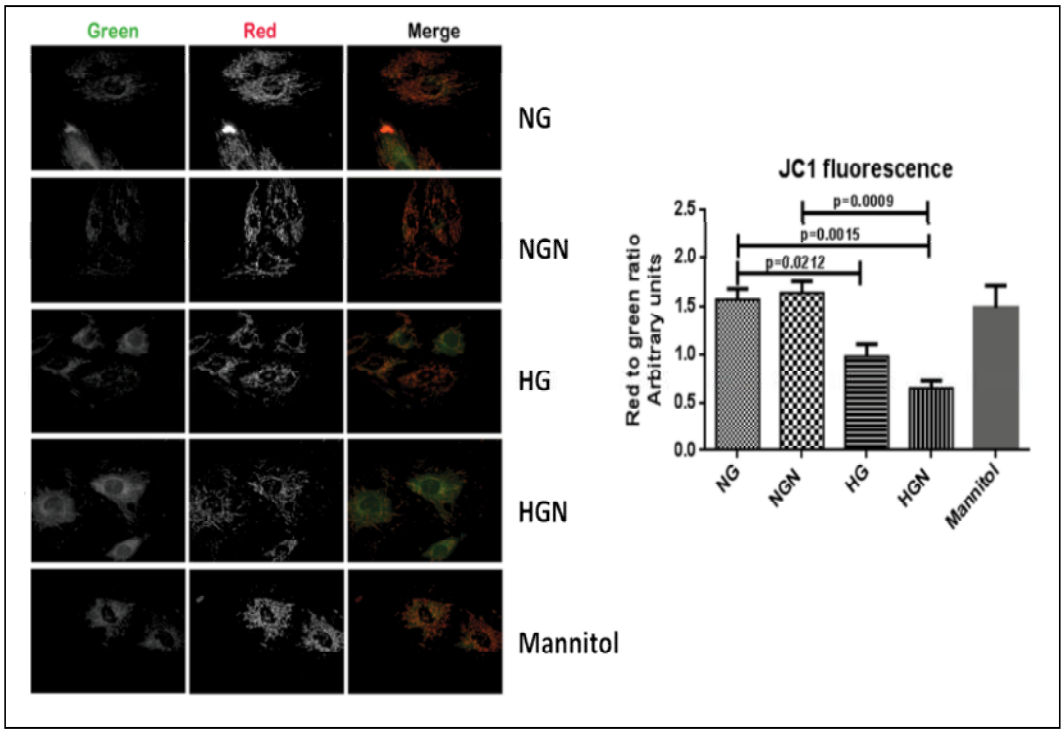

Fig. IV.12. Dwindling of mitochondrial membrane potential in H9c2 on HG treatments

The decline in red to green ratio of JC1 fluorescence in H9c2 cells on HG treatments with or without nitrite compared to respective controls depicted in micrographs from epifluorescence microscope. The bar graphs represent the mean values of ratio between red and green fluorescence intensities obtained simultaneously from random fields. Three independent experiments were done and error bars represent SEM. Magnification- 400X

JC1 forms aggregates or exists as monomers emitting red and green fluorescence respectively and thereby differentiates mitochondria with high membrane potential from that with a low membrane potential (Garner and Thomas, 1999; Reers et al., 1991). JC-1 does not detect mitochondrial impairment as such, but simply indicates the cell's health status. However, JC-1 could be utilized as an alternative to the ATP assay for indirectly determining membrane capacity to convert electrochemical gradient to ATP and should be conducted at the 24 h time point only (Rana et al., 2011).

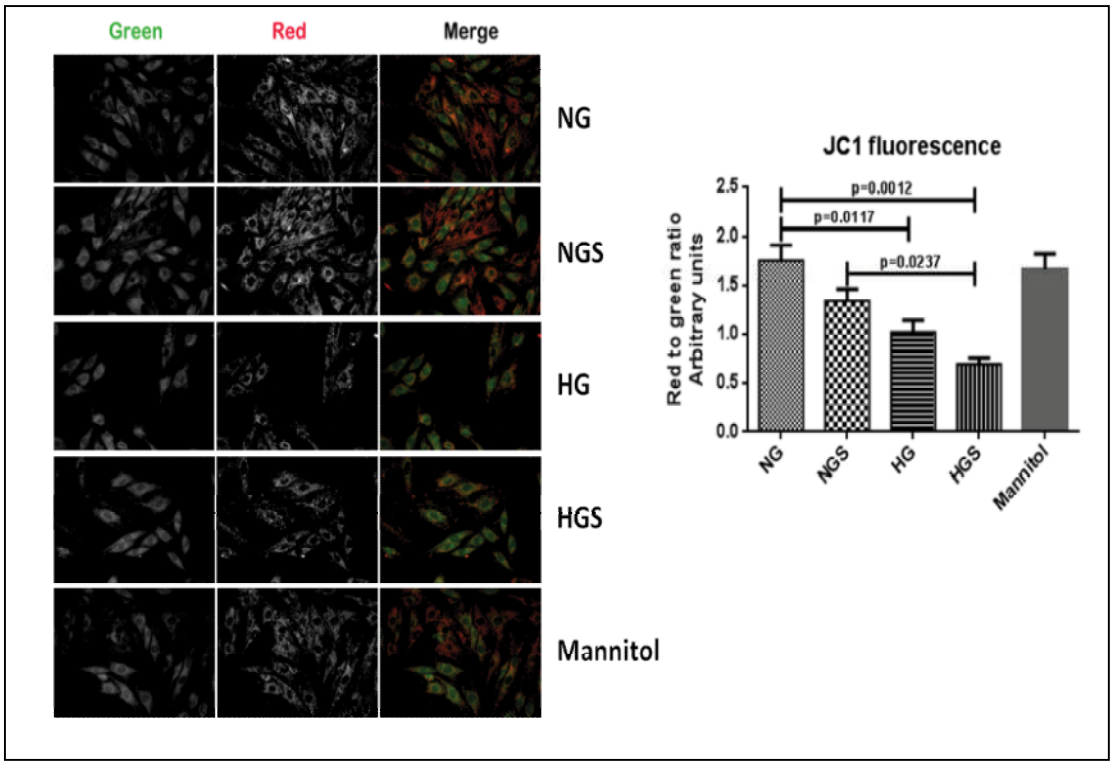

Fig. IV.13. Decreased mitochondrial membrane potential in H9c2 on HG/SNAP treatments

The ratio of red fluorescence to green fluorescence decreased on HG treatments indicating a decline in mitochondrial membrane potential. The micrographs are representative of one field per experimental group. The ratio of mean fluorescence intensities are represented by bar graphs in arbitrary units as means ± SEM. Magnification- 200X

For the JC1 staining experiments, H9c2 cells treated with SNAP and nitrite under NG and HG were incubated with the dye as discussed in methods section. The red to green fluorescence ratio decreased significantly in HG treated cells in comparison with control,

irrespective of SNAP or nitrite additions. Further, a non-significant decrease in the red/green ratio was observed in both SNAP and nitrite treated cells under hyperglycemia when compared to their respective HG groups (Fig. IV.12 and Fig. IV.13). This indicates that there is a concomitant decline in mitochondrial membrane potential under hyperglycemic conditions along with increased superoxide production. The reduction in mitochondrial superoxide generation on nitrite treatment under HG might be linked to the minor reduction in membrane potential as it is reported that there is more superoxide production and retention in mitochondria at high membrane potential and a reduction in the mitochondrial potential usually inhibited the ROS production (Korshunov et al., 1997; Skulachev, 1996; Suski et al., 2012; Suski et al., 2018).

Further on evaluating the morphological parameters of the mitochondrial population, the aspect ratios and form factors were found to be affected by SNAP treatment under HG. The Aspect Ratios (AR) estimated from the red fluorescence images of JC1 staining showed that there is an increase in the population of mitochondria with AR < 3 in the HGS and HGN groups as well as both the HG groups compared to their respective controls (Fig. IV.14. A & C). The Form Factor (FF) derived from the area and perimeters of individual mitochondrial networks were showing a trend similar to the Aspect Ratios. The percent of mitochondria with FF < 2 were relatively higher in the HG and HGN groups albeit non-significant, than the control (Fig. IV.14. B).

However, there was a significant increase in the population of mitochondria with AR < 3 in the HGS group compared to control (Fig. IV.14. D). Higher ARs depict the elliptical nature and elongation of the mitochondrion, meanwhile higher FFs indicate longer, more branched mitochondria.

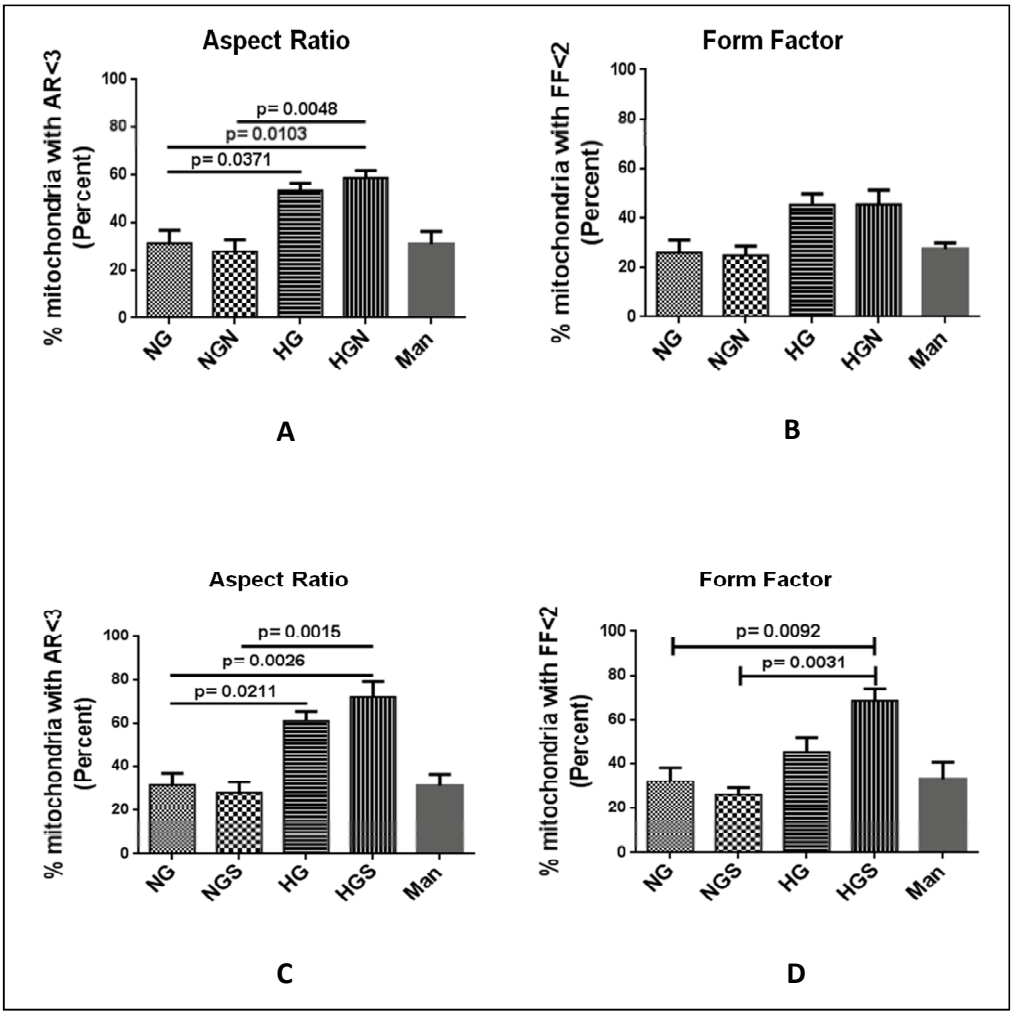

Fig. IV.14. Assessment of mitochondrial morphological parameters in H9c2 cells

The fluoromicrographs of JC1 staining were analyzed for mitochondrial dimensions and the Aspect ratios and form factors of each individual mitochondrion were measured. The percent of mitochondria having aspect ratios < 3 and form factors < 2 are represented as mean ± SEM for nitrite/HG treatments (A,B) and SNAP/HG treatments (C,D).

The mitochondrial membrane proteins adenine nucleotide translocase (ANT1) and the uncoupling protein, UCP3 are important determinants of the mitochondrial membrane potential (MMP). Overexpression of ANT1 has been related to complete loss of MMP and its upregulation during aging correlates to decrease in MMP (Heger et al., 2018; Jang

et al., 2008; Skárka et al., 2003) whereas UCP3, when overexpressed led to decreased MMP without a decrease in ATP content in human primary myocytes (García-Martinez et al., 2001). Taking this into account, the expressions of UCP3 and ANT1 were analyzed in H9c2 on nitrite and SNAP treated cells under NG and HG by immunoblotting.

IV.8. Altered expression of ANT1 and UCP3 in H9c2 cells on HG, nitrite and SNAP treatments

The ANT1 expression was increased in the HG-nitrite treated cells over control while UCP3 increased significantly only in the HG group (Fig. IV.15. A and Fig. IV.15. B). This is in line with the reduced MMP observed above in the two HG treated groups during JC1 assays. When SNAP treatments were given, the H9c2 cells showed increased ANT1 expression under both NG and HG conditions (Fig. IV.16. A). This might be contributing to the non-significant decrease of MMP in NGS vs. NG group and HGS vs. HG group. Also the significantly increased expressions of UCP3 in both the HG treated groups correlate with the decreased MMP observed in those groups with respect to controls (Fig. IV.16. B).

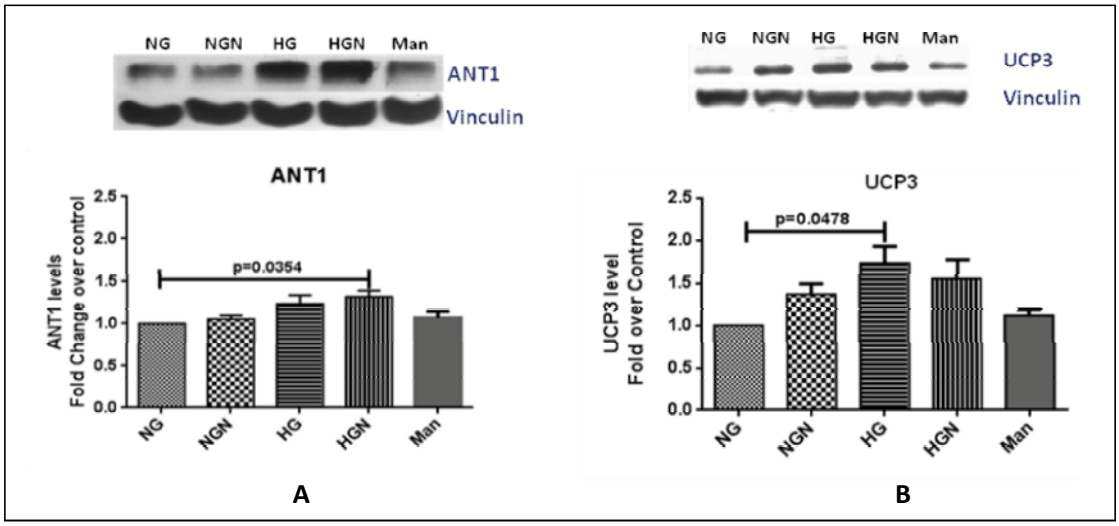

Fig. IV.15. Augmented ANT1 and UCP3 expression in H9c2 on HG/nitrite treatments

The H9c2 cell lysates were analyzed for ANT1 and UCP3 protein levels to know the effect of nitrite treatment under NG and HG. The ANT1 levels were upregulated in HGN (A) whereas UCP3 was upregulated in HG group (B). Mean values and SEM are shown as bar graphs with error bars.

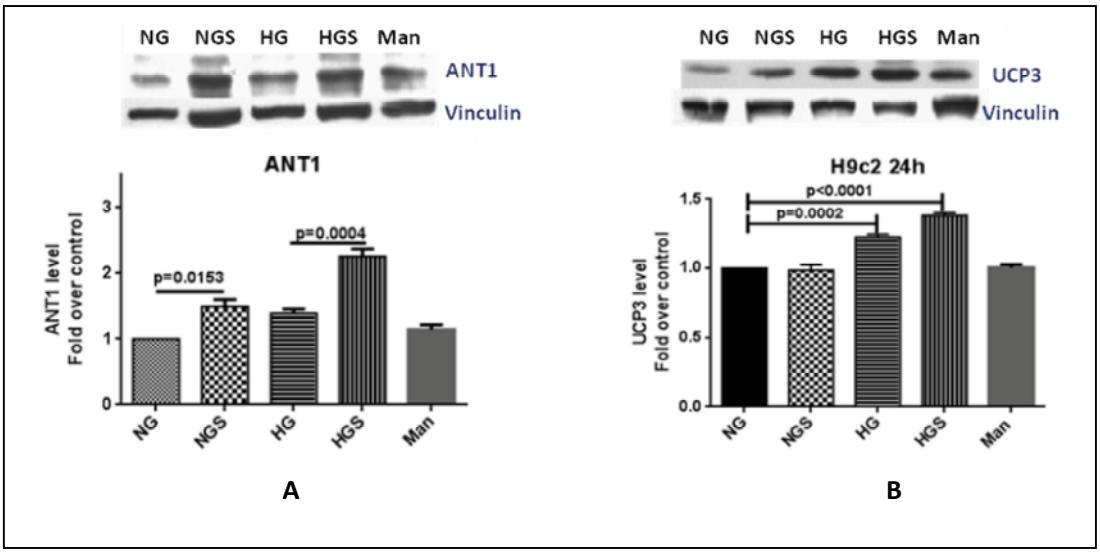

Fig. IV.16. Augmented ANT1 and UCP3 expression in H9c2 on HG/SNAP treatments

Immunoblots showing ANT1 and UCP3 protein levels on SNAP treatment under NG and HG. The ANT1 levels were upregulated by SNAP under both glycemic conditions (A) whereas UCP3 was upregulated by HG with or without SNAP (B). Mean values and SEM are shown as bar graphs with error bars.

IV.9. Unaltered mitochondrial coupling efficiency in H9c2 myoblasts on SNAP or nitrite treatments under NG and HG

Assessment of mitochondrial function through measuring the respiration or oxygen consumption reflects the effect of any treatment or intervention on the intracellular energy metabolism (Kuznetsov et al., 1998; Kuznetsov et al., 2008; Saks et al., 2004). For this a polarographic oxygen sensing technique known as high resolution respirometry was utilized. The respirometric experiments were conducted with intact H9c2 cells after different treatments as discussed in methods section. The Basal (Routine) respiration (R), Leak Respiration (L), Maximal Respiration (E) and Residual oxygen consumption (ROX) were measured and the mean values were extracted from the 'dat' files. The ROX corrected values of R and L were used for determining the changes in mitochondrial coupling efficiency of the intact cell mitochondria after different treatments. Coupling Efficiency is the percentage of mitochondrial oxygen consumption linked to ATP synthesis at a given membrane potential. The Coupling efficiency decreased slightly in SNAP treated cells under normal glucose whereas nitrite treatment does not alter the

intact cell mitochondrial coupling efficiencies under either glycemic condition (Fig. IV.17.).

IV.10. Estimating the RNA expression of the mitochondrial Transcription Factor A (TFAM) and the overall mitochondrial mass

The absence of any consequences of HG/Nitrite treatments in the mitochondrial coupling efficiency despite lowering of mitochondrial membrane potential might be due to a compensatory change in mitochondrial biogenesis. In order to verify whether such a manifestation is occurring, the gene expression of mitochondrial Transcription Factor A (TFAM) was quantified using real time PCR. Confluent cultures of H9c2 given the HG/nitrite treatments for 24 h along with respective controls were lysed with a lysis buffer containing guanidinium isothiocyanate provided with the RNA isolation kit as discussed in the Methods. The total RNA was isolated as per kit instructions and then was run on a 1% agarose gel to confirm the integrity of the RNA (Fig. IV.18. A). First strand cDNA synthesis was done from 2 µg RNA using a mix of oligo-dT primer and random hexamers and M-MLV reverse transcriptase. The cDNA was co-amplified for 40 cycles with TaqMan assay probe specific for rat TFAM and β-actin (internal control) using Real-time qPCR analysis.

The TFAM gene expression in response to nitrite treatment for 6 h in NG conditions remained at comparable levels with the control. Meanwhile the fold change of TFAM mRNA over control significantly enhanced on HG treatment at 6 h time-point. Interestingly, such a significant elevation was not observed in HG-Nitrite group when compared to NG-nitrite group (Fig. IV.18. B). However at 24 h, the TFAM mRNA levels dropped in HG group albeit non-significantly in respect of control and both the nitrite treated groups were showing a trend towards an increase compared to their respective controls (Fig. IV.18. C). The only significant difference observed among the groups was the higher TFAM RNA in NGN with respect to HG. The initial increase in TFAM mRNA on HG exposure might be the first response to the substrate excess and then subsides afterward due to the high ROS generated (Palmeira et al., 2007).

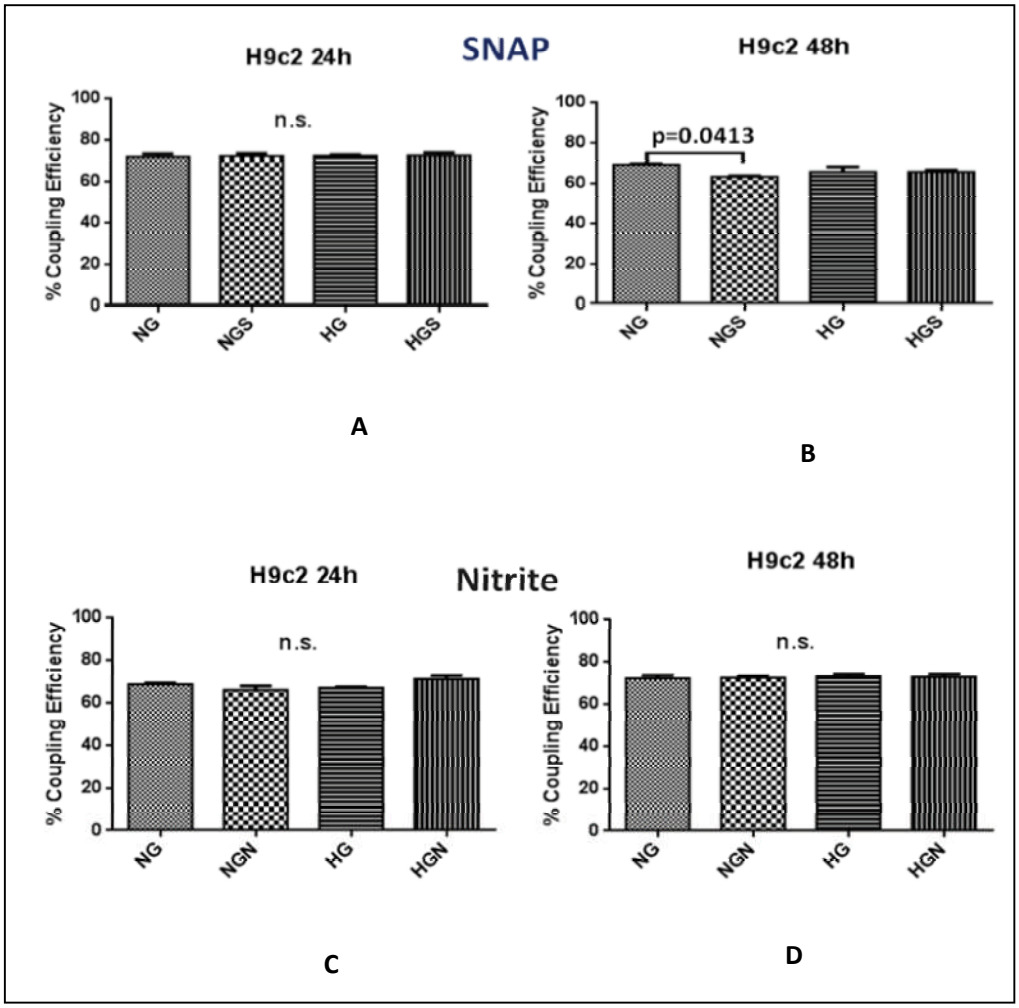

Fig. IV.17. Unchanged mitochondrial coupling efficiency in HG/SNAP and HG/Nitrite treated cells

The coupling efficiency of the mitochondria in intact H9c2 cells was not changed by HG/SNAP treatments at both 24 h (A) and 48 h (B) or by HG/Nitrite treatments at 24 h (C) and 48 h (D) time-points. The data are represented as mean values of percent coupling efficiency without normalizing to the values of control group and error bars represent the SEM.

Further, on evaluating the effect of nitrite and/or hyperglycemia on mitochondrial mass by MitoTracker staining, and it was observed that none of the treatment groups were significantly different from each other and compared to control (Fig. IV.19.)

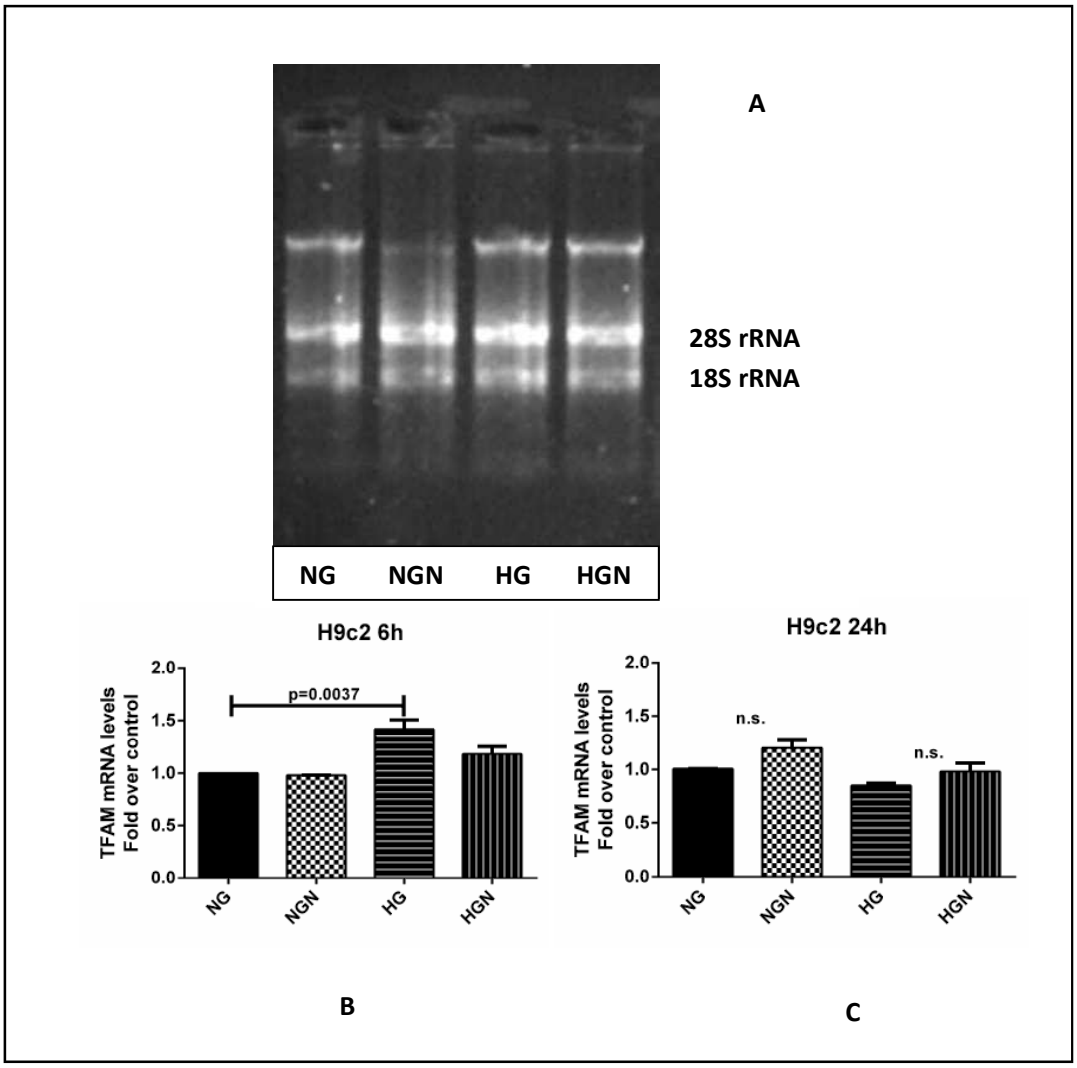

Fig. IV.18. Agarose gel electrophoresis of total RNA isolated from H9c2 cells and Real time PCR for mRNA expression of TFAM in H9c2 cells on HG/Nitrite treatments

The H9c2 cells given treatments same as previous experiment for 6 h and 24 h were lysed and the total RNA was extracted. The RNA was subjected to 1% agarose gel electrophoresis. The presence of intact 28S and 18S bands was documented using Bio-Rad Gel Documenting System (A). After cDNA preparation, the TFAM expression was quantified using TaqMan Gene Expression assays. At 6 h time-point HG group was showing significantly elevated TFAM gene expression in comparison with the NG groups but at 24 h, HG vs. NG had no significant difference.

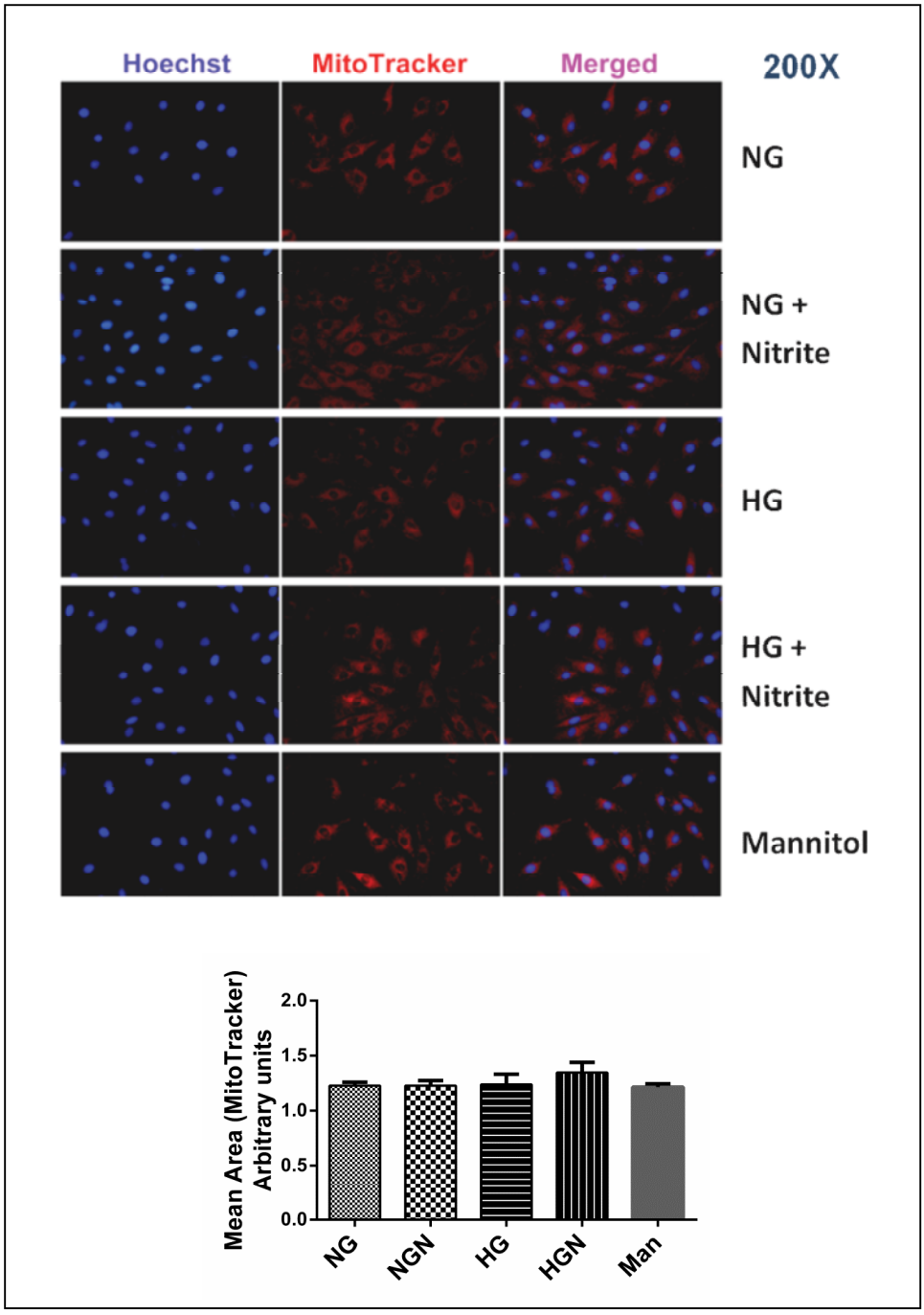

Fig. IV.19. Estimation of the overall mitochondrial mass in H9c2 cells

Fluoromicrographs representing the MitoTracker Deep Red staining of H9c2 cells and the representative graph depicting the mean area of mitochondrial mass from three independent experiments (mean ± SEM). Magnification: 200X

IV.11. Alterations in proteome of H9c2 myoblasts exposed to Nitrite

To determine the effects of nitrite supplementation on the total proteome of the H9c2 myoblasts, protein digests of cells exposed to nitrite for 24 h were subjected to Liquid Chromatography-tandem mass spectrometric (LC/MS/MS) analysis and the peptides identified and quantified using Progenesis QI (Waters Corporation, MA, USA) for Proteomics. The UniProt IDs from Rat protein database were converted into gene symbol and their relative quantities were determined as fold change over control. The fold increase or decrease was considered significant only when the 'q' values (p values corrected for false discovery rate).

The significantly upregulated proteins were subjected to string analysis (www.string-db.org) for interactions and cellular function related to organelles especially mitochondria. Due to the small number of upregulated proteins which had reported interactions among them, the only biological interpretation that can be reported is an enrichment of proteins involved in organelle organization. The proteins were identified as the cytoskeletal components, Tubulin alpha-4A chain (Tuba4a), Septin2 (Sept2) and Phosphatidylinositol-binding clathrin assembly protein (Picalm) of which only Septin2 has a reported role related to mitochondria, the fission process. Septin2 can localize to mitochondria, interact with Drp1 and thus regulate mitochondrial fission (Pagliuso et al., 2016). The only mitochondrial protein found to be upregulated in the interactome was the mitochondrial Aldehyde dehydrogenase1 (Aldhb1) enzyme that has association with the cytosolic enzyme Acyl-CoA thioesterase-12 (Acot12) (Fig. IV.20.).

The mass spectrometry data gives leads about the group of interacting proteins that gets altered relatively to a control and needs to be validated by further analysis like western blotting.

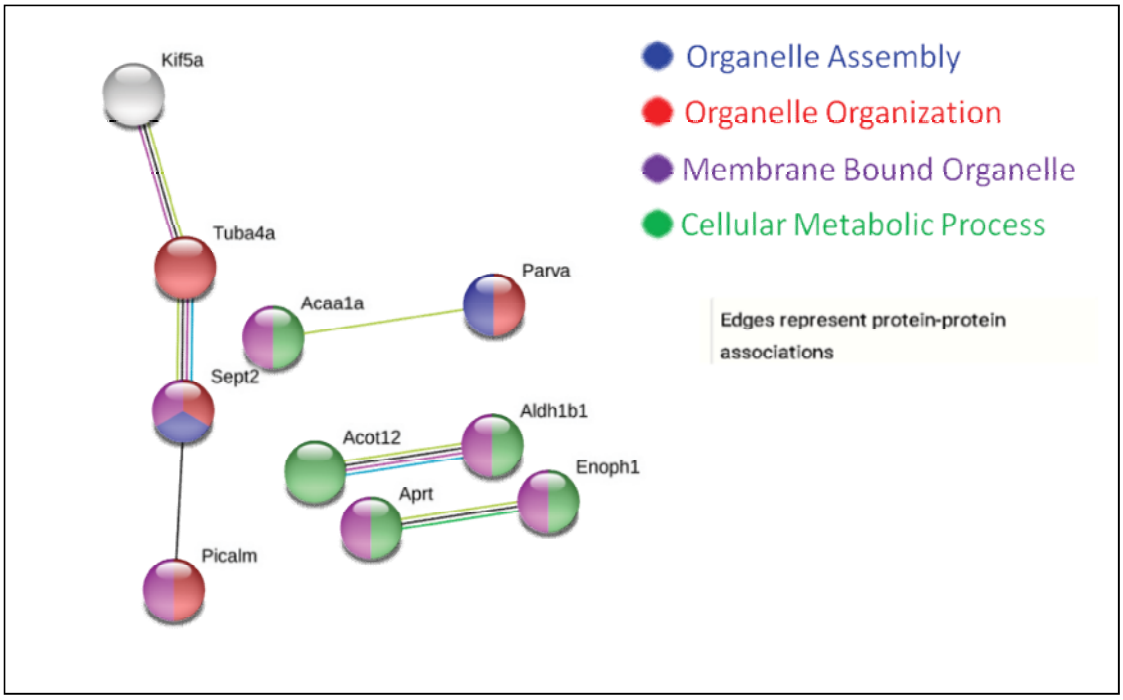

Fig. IV.20. Retrieval of interacting proteins using string analysis of the upregulated proteins in H9c2 cells after nitrite treatment under normal glucose conditions

The H9c2 cells treated with nitrite for 24 h under high glucose were processed for mass spectrometry and the list of upregulated proteins was subjected to string analysis. The proteins represented are: Kif5a- Kinesin heavy chain isoform 5A, Tuba4a- Tubulin alpha 4a chain, Sept2- Septin2, Picalm- Phosphatidylinositol-binding clathrin assembly protein, Acaa1a- 3-ketoacyl-CoA thiolase_ peroxisomal, Parva- Alpha-parvin, Acot12- Acyl-CoA thioesterase-12, Aldh1b1- Aldehyde dehydrogenase X_ mitochondrial, Aprt- Adenine phosphoribosyltransferase, and Enoph1- Enolase-phosphatase E1.

IV.A. Key findings (Broad Objective A)

- Nitrite has differential effects on cellular redox status of myocytes based on the ROS environment already prevailing in the cells.
- Both SNAP & Nitrite treatments decrease mitochondrial membrane potential of H9c2 myoblasts under high glucose conditions.
- UCP3 & ANT1 levels are increased under HG conditions and by SNAP correlating to the decreased mitochondrial membrane potential.
- Mitochondrial coupling efficiency is unchanged under HG on SNAP or nitrite treatments.

IV.12. Alteration of Drp1 activity by nitrite/SNAP under HG

As indicated from above results, nitrite and SNAP treatments under hyperglycemia leads to reduction in the mitochondrial membrane potential without any alteration of its coupling efficiency in H9c2. Now, for examining the effects of the above treatments on mitochondrial dynamics, the focus was laid on the mitochondrial outer membrane fission protein Drp1 and the inner membrane fusion protein OPA1.

Firstly, to check whether the above alterations in mitochondrial membrane potential and superoxide generation is associated with molecules regulating in the mitochondrial fission processes, changes in Drp1 activity were studied. H9c2 cells cultured under NG and HG were given nitrite and SNAP were lysed and probed with pDrp1-Ser637 and Drp1 specific antibodies after SDS-PAGE as discussed in Methods.

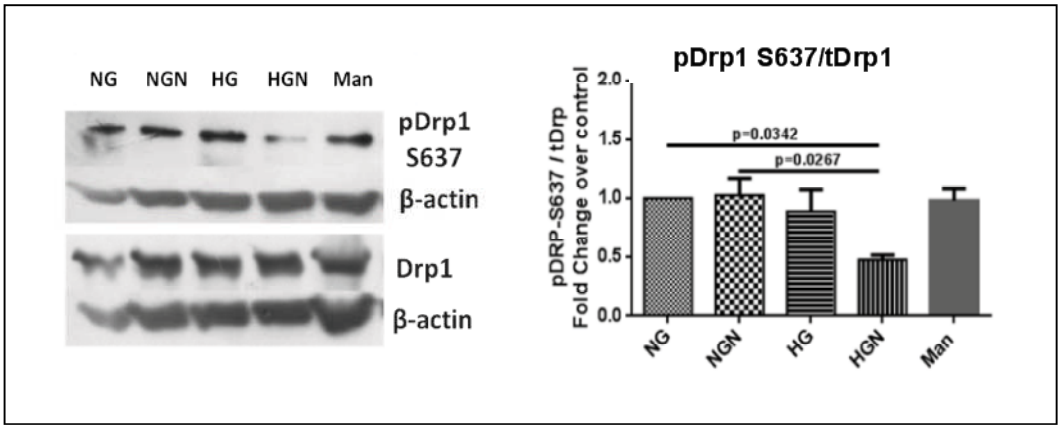

Fig. IV.21. Downregulation of Drp1 phosphorylation at Ser637 on nitrite treatment under HG

H9c2 lysates probed for pDrp1-Ser637 and Drp1 along with β-actin as loading control showed a decreased ratio of pDrp1-Ser637 to Drp1 in the HGN group in comparison with NG and NGN groups. The fold changes over NG group are represented in the bar graph as mean ± SEM from 4 independent experiments.

Dephosphorylation of Drp1 at Ser637 might lead to increased Drp1-mediated fission since studies have reported that repression of the dephosphorylation process in myocytes leading to consequent suppression of mitochondrial fission (Kim et al., 2013; Marsboom Glenn et al., 2012; Okada et al., 2016). The H9c2 cells after HG/nitrite treatments and controls were analyzed for Drp1 phosphorylation and under hyperglycemia; nitrite reduces phospho-Drp1 Ser637 levels (Fig. IV.21.). This might signal the translocation of

Drp1 to mitochondria and leading to its activation. The activity of Drp1 is a key determinant of mitochondrial membrane potential as cells expressing mutant Drp1 has been found to exhibit high MMP (Tomer et al., 2018). The decrease in inhibitory phosphorylation of Drp1 is possibly leading to its increased activity and hence can contribute to lowering of MMP.

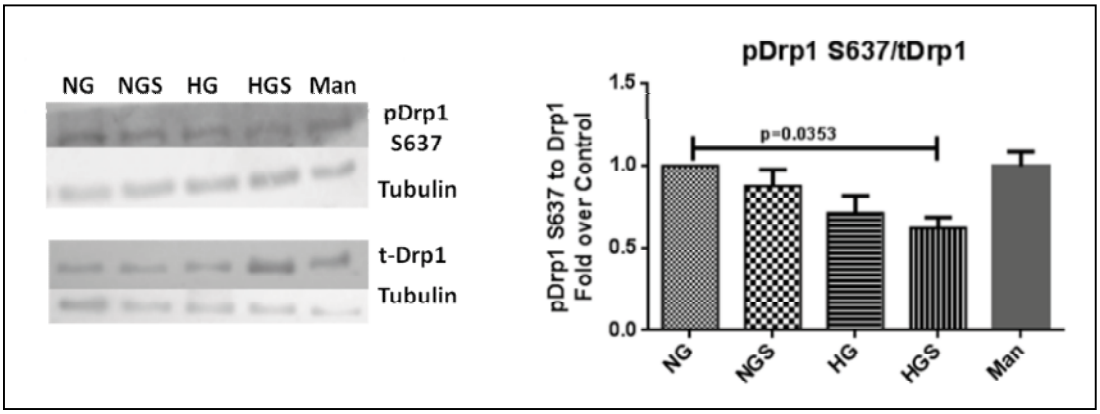

Fig. IV.22. Ratio of pDrp1-Ser637 to total Drp1 decreased on SNAP treatment under HG

H9c2 lysates probed for pDrp1-Ser637 and Drp1 along with Tubulin as loading control showed a decreased ratio of pDrp1-Ser637 to Drp1 in the HGS group in comparison with NG and NGN groups. The fold changes over NG group are represented in the bar graph as mean ± SEM from 3 independent experiments.

A similar set of experiments when done with SNAP treatments, comparable levels of p-Derp1 Ser637 was observed. Here as well, the inhibitory phosphorylation was significantly lowered in the HG-SNAP treated cells compared to NG control (Fig. IV.22.). This probably gives an indication that inorganic nitrite is acting through a mechanism similar to or mediated through NO signaling.

To delve further into the possible mechanism of nitrite/SNAP action under hyperglycemia, activity of some of the cellular kinases already reported to regulate Drp1 phosphorylation directly or indirectly was analyzed.

IV.13. Akt1 activity inhibition by nitrite/SNAP under HG

The Drp1 protein is under the regulation of several cellular kinases and since its reduced activity is also related to mitochondria mediated cytoprotection (Cho et al., 2013; Ong et

al., 2015), it was reasonable to examine whether the enhanced activity of Drp1 is associated with a concomitant change in activity of a pro-survival kinases like Akt1. Protein kinase B or Akt1 is a kinase upstream of two of the recognized modulators of Drp1, the GSK3β and Pim1 kinase. The Immunoblot analysis with H9c2 lysates showed that Ser-473 phosphorylation (an activation phosphorylation) was found to be decreased in the HGN and HGS groups similar to Drp1 phosphorylation (Fig. IV.23.). The activation phosphorylation at Ser 473 residue of Akt1 reduced significantly in the nitrite treated groups under HG but not in HG alone group indicating a combined effect of nitrite and HG rather than standalone effects.

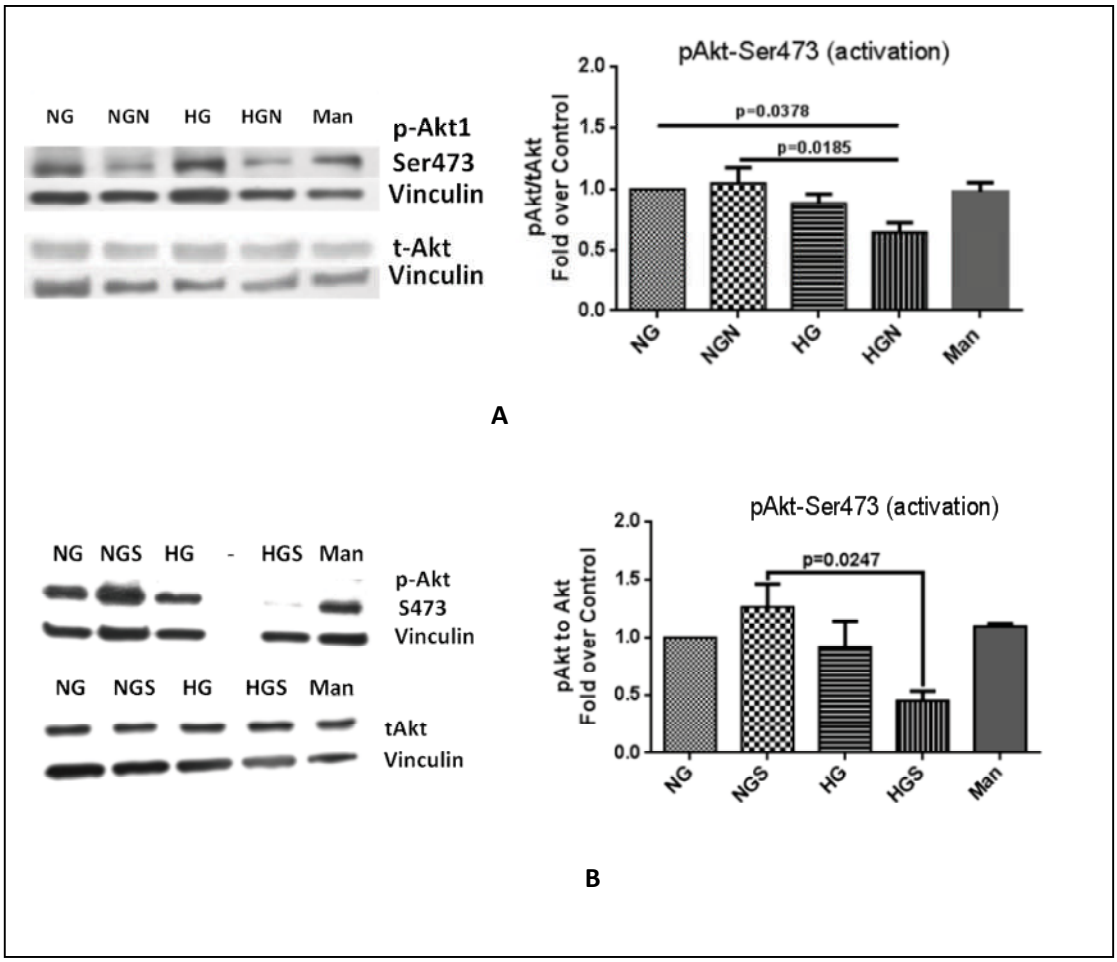

Fig. IV.23. Ratio of pAkt1-Ser473 to total Akt decreased on nitrite/SNAP treatment under HG

H9c2 lysates probed for pAkt1-Ser473 and t-Akt along with Vinculin as loading control showed a significantly decreased pAkt1-Ser473 to t-Akt ratio in the HGN group in comparison with NG and NGN

groups (A) and in the HGS group when compared to NGS group (B). The fold changes over NG group are represented in the bar graphs as mean ± SEM from 4 independent experiments.

IV.14. Pharmacological inhibition upstream of Akt1 in the presence of nitrite has no additional downstream effects

The Phosphatidyl Inositol 3-Kinase inhibitor, LY294002 reduces the activation phosphorylation on Akt1 and also subsequently leads to reduced regulatory phosphorylation of GSK3β at Ser9 residue (Cross et al., 1995; Li et al., 2019; Moe et al., 2013). To check whether nitrite and LY294002 have synergistic effects on the phosphorylation status of Akt1 and its downstream effectors, H9c2 cells were exposed to LY294002 with or without nitrite for 4 h and lysates probed with phospho-specific antibodies. The levels of pAkt-Ser473, pGSK3β-Ser9, pDrp1-Ser637 and pDrp1-Ser616 were analyzed. The LY294002 treated cells were showing significantly reduced phosphorylation levels of Akt1 but non-significant decrease in p-GSK3β Ser9 levels. Also, a concomitant decrease in Ser637 phosphorylation and an increase in Ser616 phosphorylation was observed in the PI3-K inhibitor treated cells without any additional effects by nitrite. Nitrite *per se* had no effect on any of the above phosphorylation levels (Fig. IV.24).

The absence of significant effect of LY294002 on p-GSK3β Ser9 levels may be due to the short time-point which was however sufficient for decline in Akt1 activity and simultaneous Drp1 activation. Another reason might be the presence of other kinases which can phosphorylate either the GSK3β and/or Drp1.

IV.15. Effects on GSK-3β and Pim1 kinase concomitant with the modulation of Drp-1 and Akt1 activities

The reduced activation of Akt1 might lead to alteration of the downstream kinases like GSK3β and Pim1 kinase. To examine this, the phosphorylation levels of GSK3β at Ser9 which is an inhibitory phosphorylation introduced by an activated Akt1 and the protein levels of Pim1 kinase which has a constitutive kinase activity were analyzed. In the case of the Ser-9 phosphorylation of GSK3β, there was a non-significant reduction in HG-

nitrite group compared to control, which again might be due to the action of other kinases on GSK3β as observed in LY294002 treatments (Fig. IV.25. A).

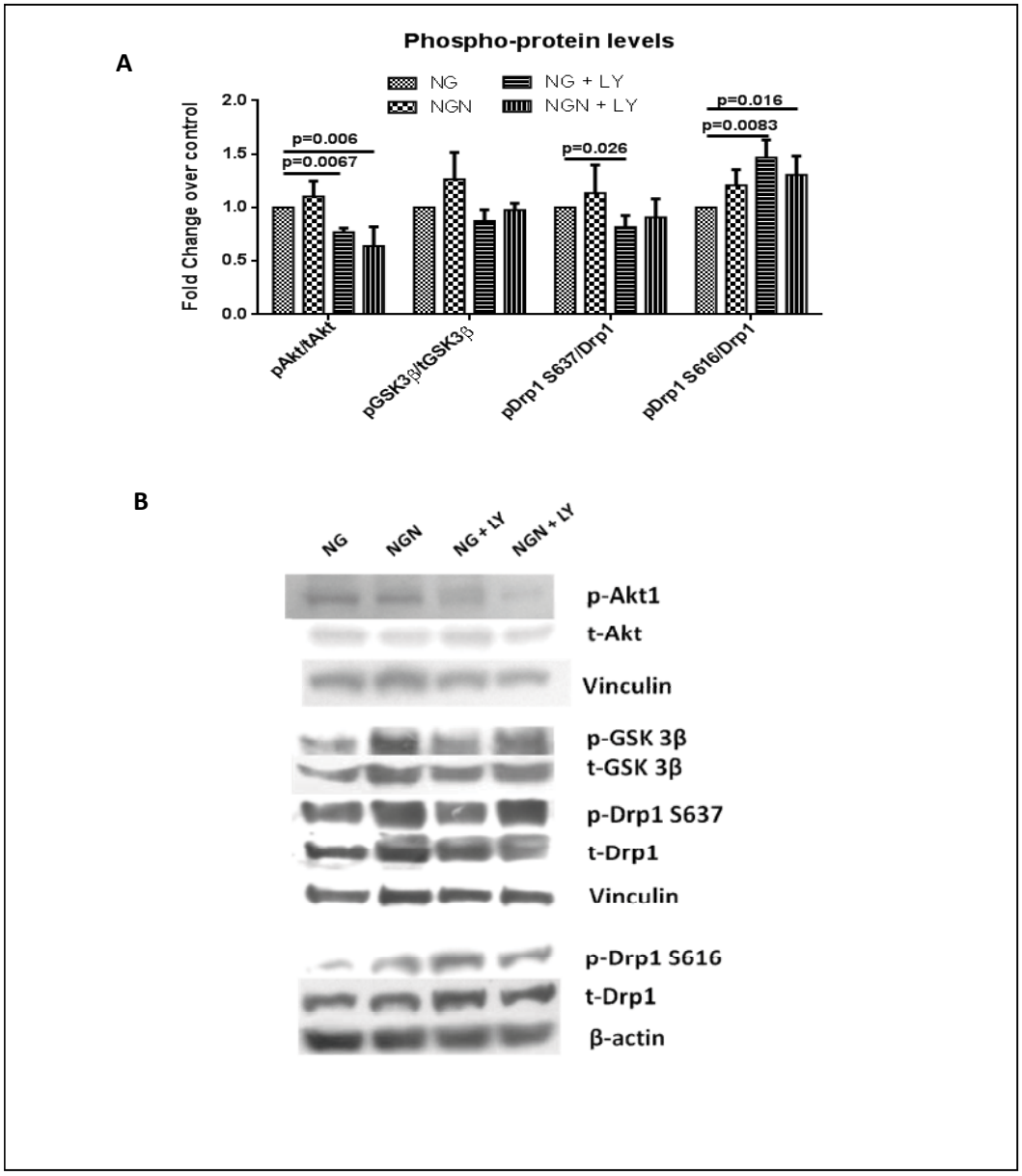

Fig. IV.24. Levels of phosphorylated Akt1, GSK3β and Drp1 at activation and/or inhibitory Ser residues in H9c2 lysates treated with LY294002 and nitrite under NG

The H9c2 cell lysates after 4 h of LY294002 and nitrite treatments alone and in combination under NG conditions were immunoblotted for phospho-antibodies. The bar graphs represent the mean ± SEM from 4 independent experiments (A).The representative bands from a single experiment are shown (B).

Pim1, a pro-survival kinase known to inhibit Drp1 by phosphorylating it at Ser637 (Borillo Gwynngelle A. et al., 2010b) was less expressed in the HG-nitrite group of H9c2 cells in comparison with both the NG treated groups (Fig. IV.25. B). These observations point toward the possible link of Drp1 activation with the Akt1/Pim1 axis rather than the Akt1/GSK3β axis when nitrite is supplemented under HG. Nevertheless, this is just a preliminary observation and needs further corroboration and elucidation of the mechanisms involved using techniques to analyze protein-protein interactions.

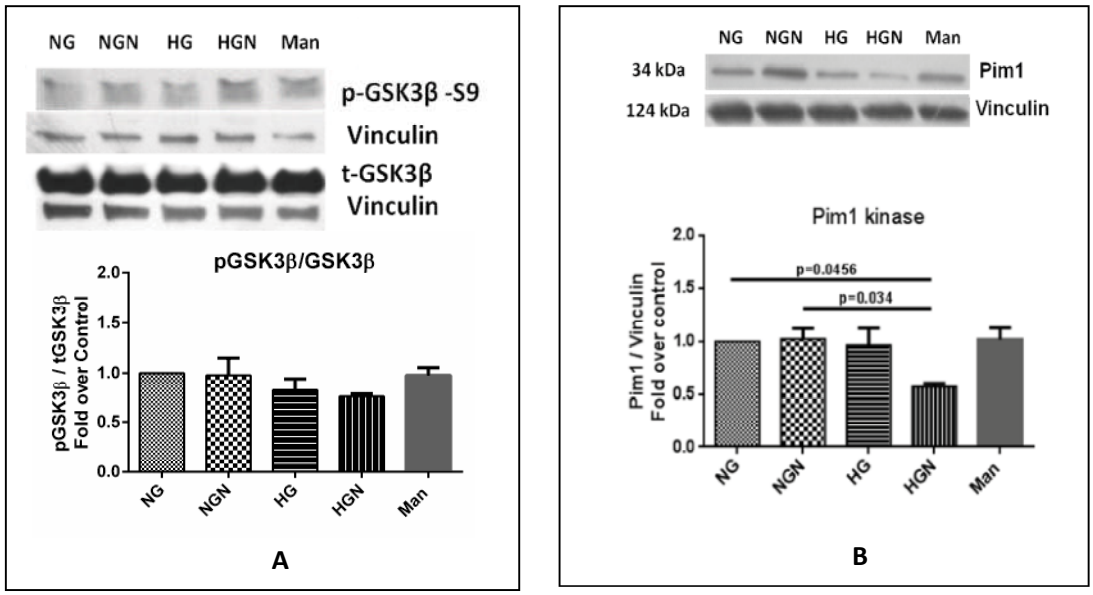

Fig. IV.25. Levels of p-GSK3β Ser9 levels and Pim1 kinase levels in H9c2 on HG/nitrite exposures.
The downstream kinases of Akt1, GSK3β (A) and Pim1 kinase (B) were analyzed for their activation or protein expression levels respectively. The bar graphs represent mean values from 4 independent experiments and error bars denote the SEM.

IV.16. Opa1 expression in H9c2 is altered under HG, only on SNAP treatment and not on nitrite treatment

As Drp1 activity is enhanced by nitrite and SNAP treatments under HG indicating augmented mitochondrial fission, its counterpart OPA1, involved in regulation of mitochondrial fusion was also examined at protein level. OPA1, a regulator of inner mitochondrial membrane fusion was downregulated in H9c2 cells treated with SNAP

under HG in comparison with those treated under NG (Fig. IV.26. A). Nevertheless, OPA1 was also not altered by nitrite under HG with respect to control (Fig. IV.26. B).

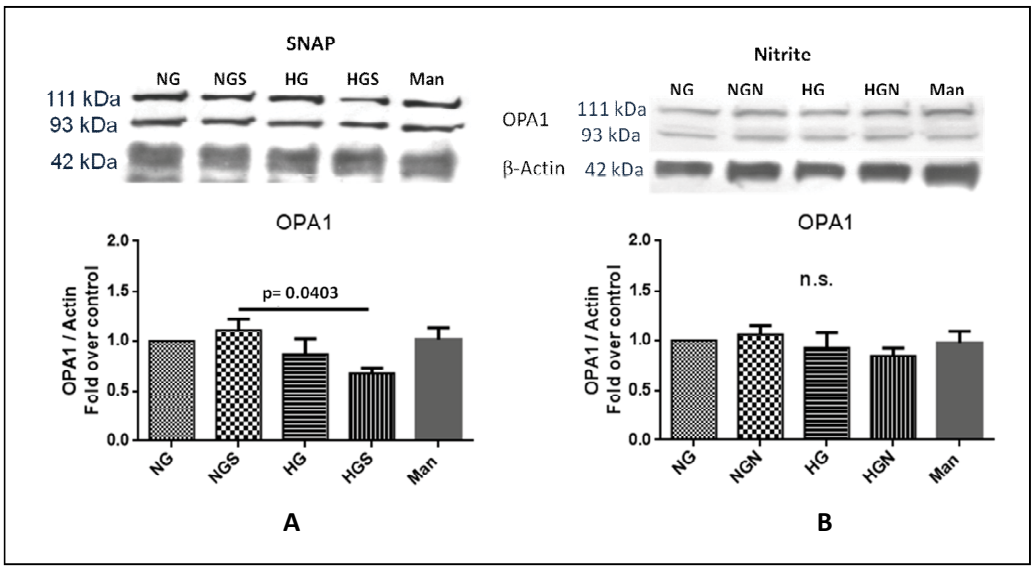

Fig. IV.26. Levels of OPA1 in H9c2 cells treated with HG, SNAP and nitrite.

The H9c2 cell lysates after HG/SNAP (A) and HG/nitrite (B) treatments along with respective controls were probed for OPA1 and β-actin. The relative protein levels are represented as bar graphs depicting mean ± SEM, n=4.

IV.17. Silencing of Drp1 in H9c2 using siRNA

The influence of nitrite treatment under HG on Drp1 activity warranted the examination of effects of the same treatment on Drp1-silenced cells. Also since, Drp1 is a key point of contention in mitochondria-mediated cell death processes (Breitzig et al., 2018; Estaquier and Arnoult, 2007; Vantaggiato et al., 2019; Xie et al., 2018), the effects of its silencing on some of the apoptosis and mitophagy markers were examined.

The H9c2 cells were exposed to Drp1 siRNA at different concentrations of 50, 100 and 200 nM and scrambled siRNA at 100 nM as per the 'methods' section and the expression of Drp1 was checked after 48 h and 72 h of transfection. It was found that the maximum inhibition was observed at 50 nM concentrations particularly in the 48 h incubation period (Fig. IV.27.). So 50 nM siRNA, with a 48 h transfection period was used for ensuing experiments.

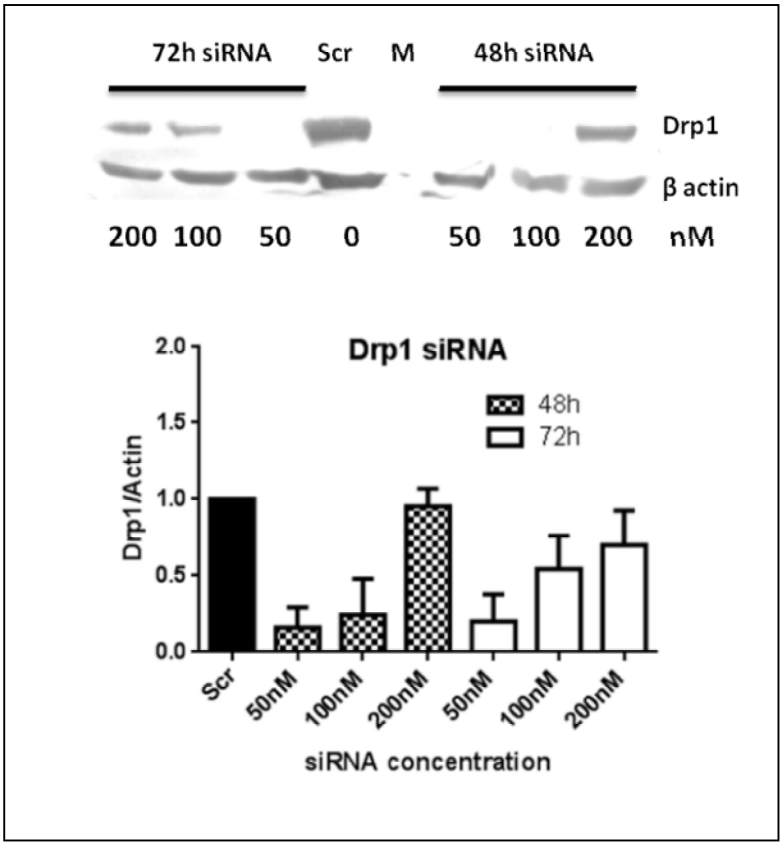

Fig. IV.27. Validation of Drp1 knockdown using siRNA in H9c2 cells

H9c2 cells were transiently transfected with Drp1 siRNA (5 pmol) or scrambled siRNA (Control groups), as described under 'methods'. Total Drp1 levels were assessed by western blot analysis, using β-actin as loading control, n=2.

IV.18. Differential effects of Drp1 silencing on OPA1 levels

The H9c2 cells were exposed to Drp1 siRNA as above and for the final 24 h treated with nitrite under NG and HG conditions. H9c2 cells treated with scrambled siRNA followed with 24 h NG, HG and mannitol exposures served as different controls. The OPA1 levels were elevated on Drp1 silencing under normoglycemia with/without nitrite treatment. Meanwhile under HG, Drp1 silencing rendered no significant change in OPA1 expression (Fig. IV.28.). Hyperglycemia thus suppressed the elevation of OPA1 on Drp1 silencing irrespective of nitrite treatment.

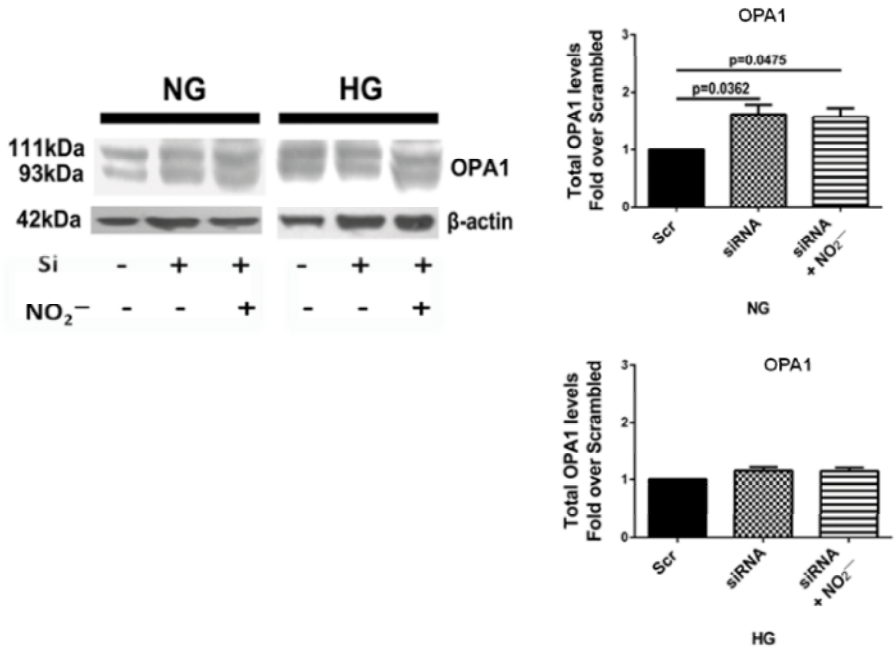

Fig. IV.28. Levels of OPA1 in H9c2 cells after Drp1 silencing

The H9c2 cell lysates after Drp1 silencing and nitrite treatments under NG and HG along with negative and mannitol controls were probed for OPA1 and β-actin. The bar graphs depicts mean ± SEM, n=3.

IV.19. Effect of Drp1 silencing on mitochondrial respiration

The H9c2 cells were exposed to Drp1 siRNA and 24 h after transfection cells were treated with nitrite under NG and HG conditions for 48 h. H9c2 cells treated with scrambled siRNA along with 48 h NG and HG exposures as above, served as controls. The mitochondrial respiration was measured using Oxygraph as described in 'methods' and the respiratory ratios were estimated.

IV.19.1. Effect on mitochondrial coupling efficiency

The coupling efficiency was calculated from the measurements of Basal and Leak respirations as described in IV.9. It was observed that nitrite treatment enhances mitochondrial coupling efficiency of Drp1 silenced cells under normoglycemia while the silencing itself did not exert any effect. However under hyperglycemia, the coupling efficiency was decreased by Drp1 silencing while nitrite did not have any additional effect (Fig. IV.29. A).

IV.19.2. Effect on mitochondrial routine control ratio

The routine control ratio is the fraction of basal (routine) respiration with respect to the ETS capacity, R/E. The routine control ratio of Drp1 silenced cells gets reduced on nitrite treatment under NG, while Drp1 silencing *per se* did not affect it. But under HG, Drp1 silencing significantly increased the R/E ratio and nitrite also had an additive effect (Fig. IV.29. B)

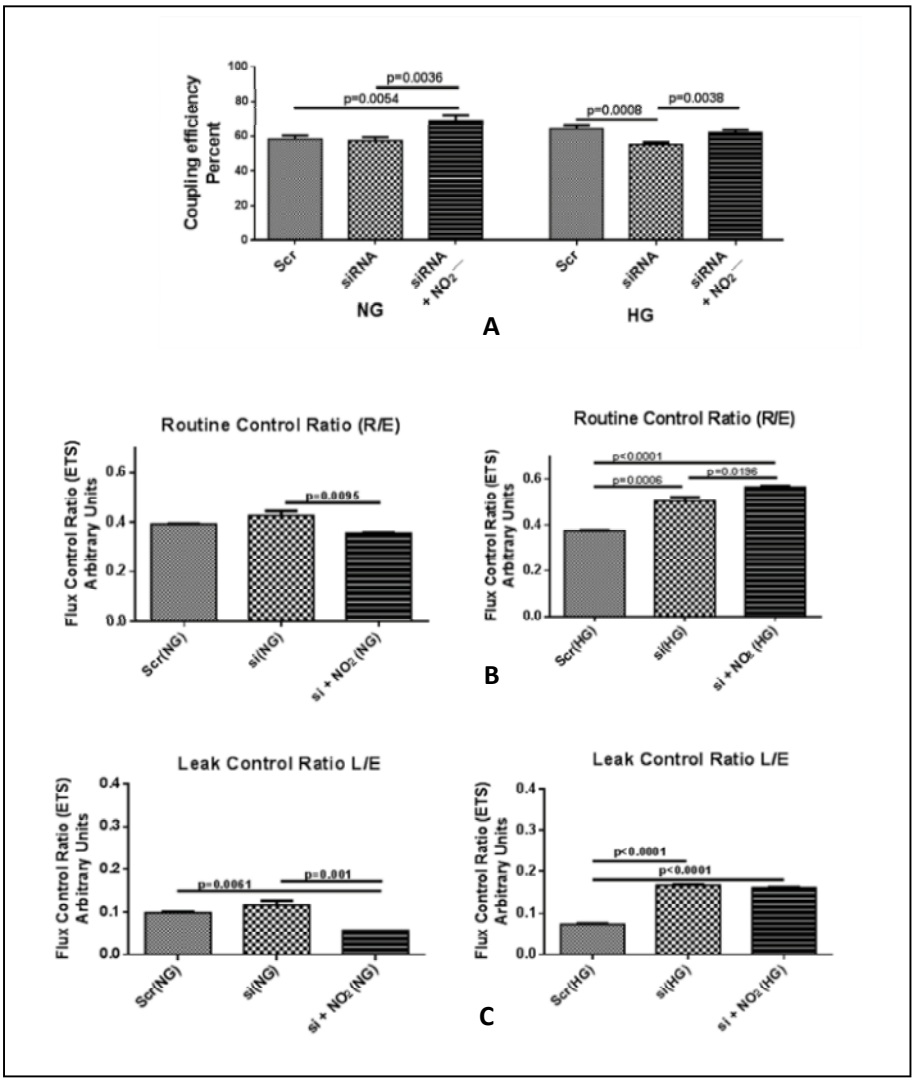

Fig. IV.29. Bar graphs representing the mitochondrial respiration in H9c2 cells after Drp1 silencing

Bar graphs representing the coupling efficiency (A), routine control ratio (B) and leak control ratio (C) in H9c2 cells after Drp1 silencing under NG and HG with or without nitrite treatments. Data represented as mean ± SEM, n=3.

IV.19.3. Effect on mitochondrial leak control ratio

The leak control ratio is the fraction of leak respiration with respect to the ETS capacity, L/E. Under NG conditions, Drp1 silencing *per se* did not have any effect but on nitrite treatment the leak control ratio declined considerably. The leak control ratio of Drp1 silenced cells increased in HG treated groups irrespective of nitrite treatments (Fig.IV.29. C).

The increase in coupling efficiency in nitrite treated Drp1-silenced cells under NG is due to almost a 40% reduction in leak respiration compared to control which might be beneficial to the cells. Collectively, the above observations indicate a differential effect of Drp1 silencing depending on the glycemic levels which needs further elucidation.

IV.20. Effect of Drp1 silencing on apoptosis and mitophagy markers

Drp1-silenced H9c2 cells were examined for the protein levels of molecules involved in apoptosis and mitophagy, two processes that are closely related to mitochondrial fission. H9c2 cells were given treatments as in IV.18., and the levels of cleaved PARP, cleaved Caspase7, Bcl2, Pink1 and Parkin were analyzed. There are already reports in other cell lines that inhibition of Drp1 impairs intrinsic apoptosis, and also decrease mitophagy (Estaquier and Arnoult, 2007; Twig et al., 2008). PARP is a protein involved in DNA repair which is cleaved by caspases during apoptosis into an 89 kDa fragment. The cleaved PARP level was decreased by nitrite treatment in NG/Drp1 silenced group while no significant change occurred in any of the HG treated groups (Fig.IV.30.). So, Drp1 silencing *per s*e did not show any influence on cleaved PARP levels.

Caspase7 is an effector caspase in apoptotic signaling, and is downregulated in Drp1 silenced H9c2 cells under HG irrespective of nitrite supplementation, whereas no significant change was observed under NG among any groups (Fig. IV.31. A). Bcl2 is an anti-apoptotic protein that as a consequence of inhibition of apoptotic factors can indirectly inhibit autophagy too (Lindqvist et al., 2014).

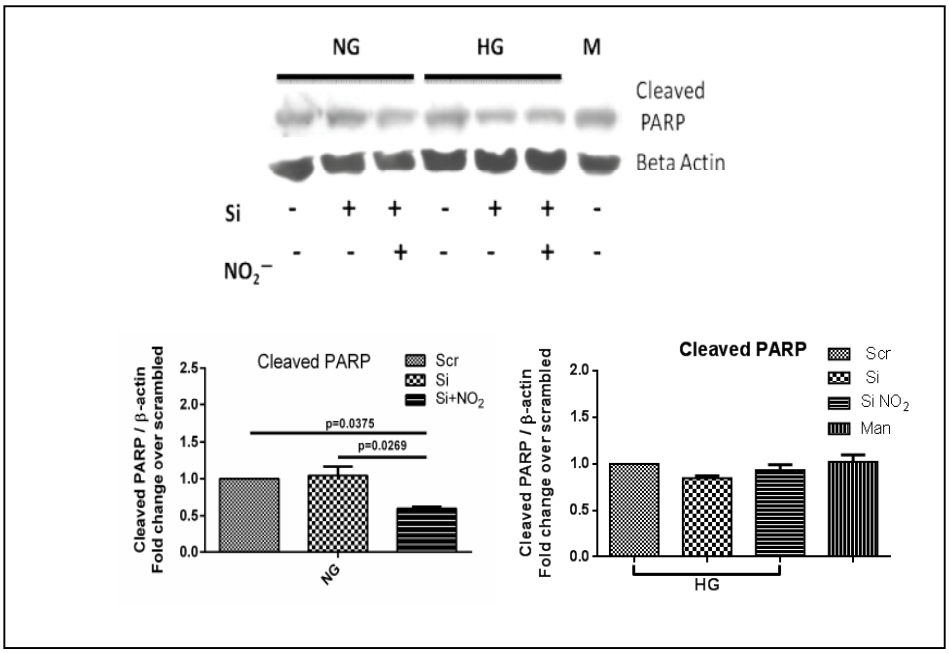

Fig. IV.30. Cleaved PARP levels in Drp1 silenced cells

The bands of cleaved PARP were normalized to β-actin. Data represented as mean ± SEM, n=3.

Bcl2 levels are reduced in Drp1 silenced cells under HG with/without nitrite supplementation while under NG no change was observed in any of the treatment groups (Fig. IV.31. B). Thus, Drp1 silencing reduces the apoptosis inhibitory signals under HG.

In the case of mitophagy regulators, PTEN induced kinase 1 (Pink1) is a serine-threonine kinase that is degraded by mitochondrial proteases when the MMP is intact. Disruption of MMP leads to accumulation of the protein (Narendra et al., 2010). Parkin is the regulatory ubiquitin E3 ligase partner of Pink1 and a mitophagy promoter. Parkin is critical for maintaining mitochondrial integrity and is reported to be upregulated on cardiac-specific ablation of Drp1 in mice (Breitzig et al., 2018; Song Moshi et al., 2015). Pink1 (55 kDa fragment) is reduced in Drp1 silenced cells under both glycemic levels irrespective of nitrite treatment (Fig. IV.32. A). This fragment of Pink1 has been reported to form in depolarized mitochondria (low MMP)(Becker et al., 2012) and Drp1 suppression is characterized by a low MMP (Choi et al., 2013).

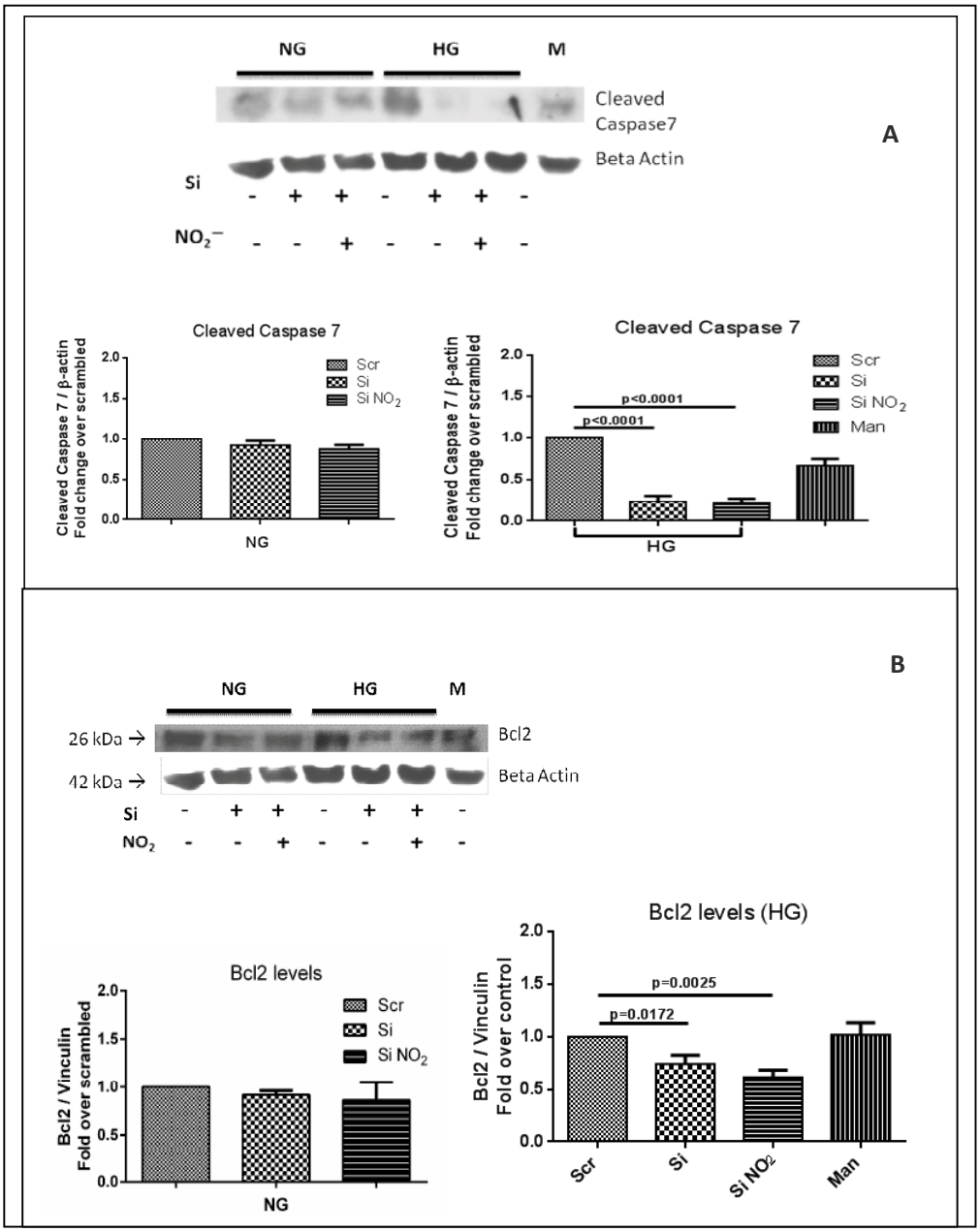

Fig. IV.31. Cleaved Caspase 7 and Bcl2 levels in Drp1 silenced cells

The bands of cleaved Caspase 7 (A) and Bcl2 (B) were densitometrically measured and normalized to β-actin. Data represented as mean ± SEM from 3 independent experiments.

Meanwhile Parkin is accumulated in the Drp1-silenced cells under NG and nitrite treatment imparts an additive effect on Parkin levels. Nevertheless, the HG treated cells

showed no significant difference in Parkin levels in the Drp1-silenced groups compared to the HG-scrambled siRNA control. Interestingly, all the HG treated groups had higher Parkin levels than the Mannitol control (Fig. IV.32. B). This observation implies that the effect of HG on Parkin levels overrides that of Drp1 silencing. There are contrasting reports revealing the role of Drp1 in regulation of mitophagy.

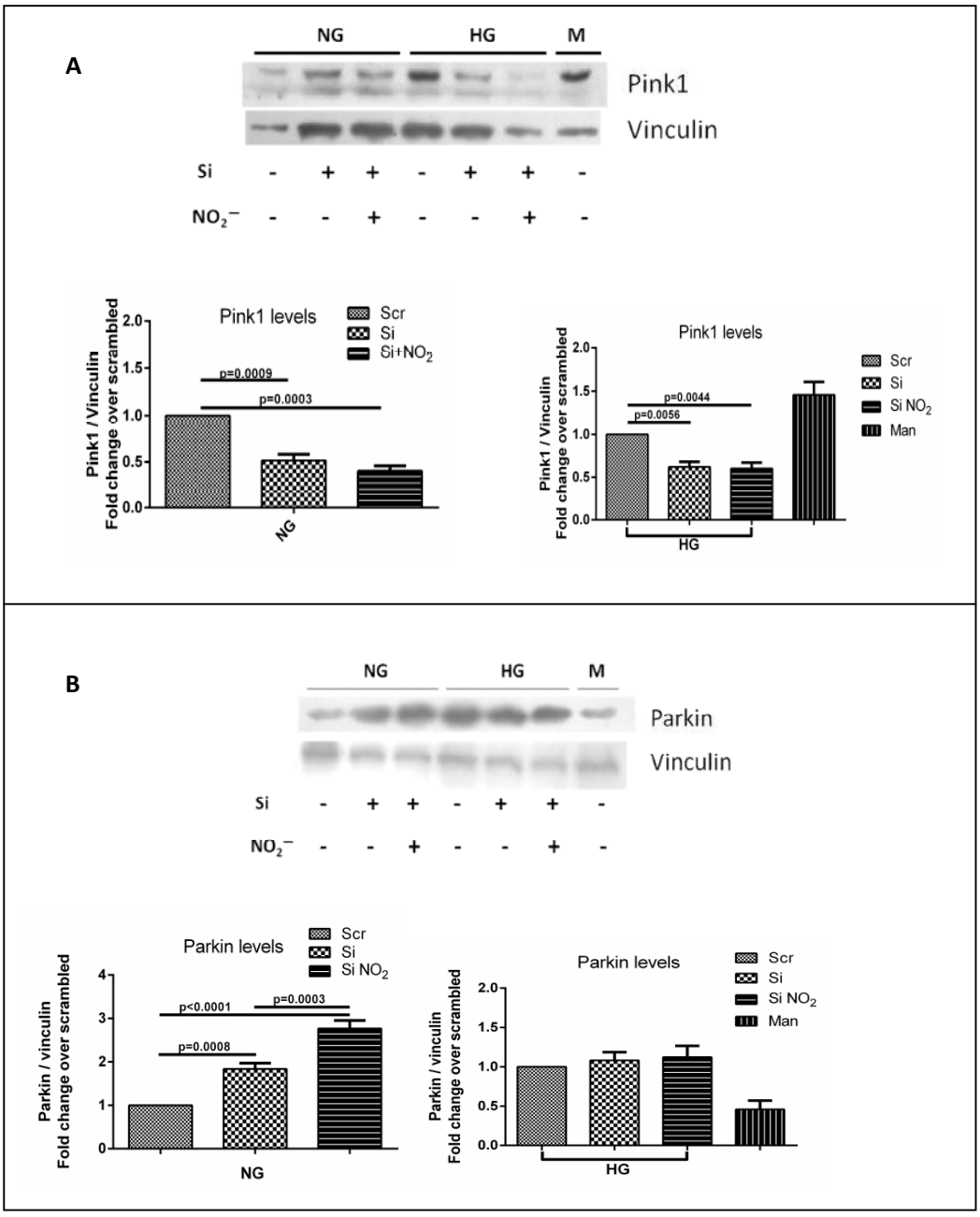

Fig. IV.32. Pink1 and Parkin levels in Drp1 silenced cells

The bands of Pink1 (A) and Parkin (B) were normalized to Vinculin. Data represented as mean ± SEM from 3 independent experiments.

In one scenario it has been displayed as the key regulator of Pink1-Parkin mediated mitophagy whereas other reports present Drp1 activity to protect healthy mitochondrial domains from elimination by unchecked Pink1–Parkin activity (Breitzig et al., 2018; Burman et al., 2017). From the above results, it can be corroborated that hyperglycemia and nitrite can act as additional determinants of Drp1's role in apoptosis and mitophagy or mitochondrial dynamics in general.

IV.B Key findings (Broad Objective B)

- Nitrite /SNAP activated Drp1 under high glucose and concomitantly decreased the Akt1 activity in H9c2 cells.
- Akt inactivation was not associated with a significant change in the GSK3β phosphorylation
- The inactivation of Akt under HG-nitrite was associated with reduced expression of Pim1 kinase
- Silencing of Drp1 leads to differential effects by nitrite under NG vs. HG conditions, mainly pertaining to mitochondrial respiration and markers of mitochondria-related processes like apoptosis and mitophagy.

V. Discussion

Inorganic nitrite is reported to increase mitochondrial fusion in cardiomyocytes by modulating the Drp1 activity. This is rendered by increasing the inhibitory phosphorylation on Drp1 at Ser637 residue and thereby abridging its translocation to mitochondria (Pride et al., 2014). Subsequently, this leads to the enhancement of mitochondrial membrane potential and superoxide generation from the fused mitochondria (Pride et al., 2014). These events have been demonstrated under normoxic conditions where there are basal levels of ROS being generated. However, the presence of high levels of ROS in the setting of hyperglycemia exhibit a new challenge for the nitrite mediated cytoprotection. In the present study, we addressed the same and investigated the effects and mechanisms of nitrite mediated modulations on H9c2 mitochondria under hyperglycemia. Interestingly, it was observed that nitrite reduced, albeit non-significantly, the ROS levels that are elevated in high glucose (HG) condition as opposed to the effect seen under normoxia/normoglycemia. There was a contrast in the associated events too. The mitochondrial membrane potential (MMP) was diminished with a simultaneous increase in mitochondrial fission in H9c2 cells under hyperglycemia. The addition of nitrite in this condition further reduced the diminished MMP inflicted by HG as indicated by less tubular mitochondria on JC1 staining. Concomitantly, nitrite treatment under HG leads to enhanced expression of mitochondrial membrane proteins, uncoupling protein 3 (UCP3) and adenine nucleotide translocase 1 (ANT1) and alterations in levels of the antioxidant enzymes GPx4 and mitochondrial SOD (SOD2). This is in contrast to the results of a human study where the oral nitrate supplementation decreased the levels of ANT1 and UCP3 in skeletal muscle tissue (Larsen et al., 2011). The results of the present study also indicate that nitrite is abrogating the high glucose-induced mitochondrial fragmentation and MPT opening albeit without a concomitant increase in ROS levels. In order to check whether the modulations in mitochondrial ROS and membrane potential have any repercussions on mitochondrial morphology, the aspect ratio, form factor and interconnectedness of the mitochondrial populations were analyzed. A decrease in ARs and FFs indicate less elongated mitochondria. While, high glucose treatment had a negative impact on the aspect ratio and form factor of the mitochondria, none of the morphological parameters significantly differed between the high glucose-nitrite treated group and the group treated with high glucose alone. All these observations

show that nitrite under hyperglycemic conditions are not exerting any additional effect on the mitochondrial morphology, despite minimally reducing the membrane potential. The membrane potential greatly impacts the ATP-linked respiration in mitochondria and hence the mitochondrial coupling efficiency was measured. The aforementioned human study had also reported an improved mitochondrial efficiency in skeletal muscle on oral nitrate supplementation (Larsen et al., 2011), but in the current study the coupling efficiency was not altered by nitrite/SNAP under HG. Coupling efficiency essentially means the percent of oxygen consumption driven by the ATP production to the total basal respiration of intact cells at 37°C. The absence of changes in coupling efficiency even at 48 h incubations under HG suggests a maintained mitochondrial function pertaining to oxygen consumption despite changes in membrane potential. Increase in substrate utilization by mitochondria has been associated to increased mitochondrial biogenesis (Hey-Mogensen and Clausen, 2017). Also, reports show that nitrite supplementation can facilitate mitochondrial biogenesis in vivo (Mo et al., 2012). In the present study, for analyzing the effects on mitochondrial biogenesis, the mRNA levels of TFAM, one of the major determinants of the mitochondrial copy number were quantified and further the overall mitochondrial mass was determined by MitoTracker Red staining. Both the above parameters were found to be unaffected by nitrite treatment under normal and high glucose conditions which substantiates the unaltered mitochondrial respiratory quotients observed. TFAM mRNA levels slightly declined under HG on nitrite treatment in comparison to the NGN group, indicating a slight indirect brunt of glycemic levels on biogenesis regulation.

The mitochondrial dynamics is yet another key factor that determines the mitochondrial homeostasis in cells. This is regulated by the opposing processes of mitochondrial fission and fusion. When the alterations in phosphorylation levels of key regulators of mitochondrial form through immunoblot analysis significant changes were found in the HG/SNAP or HG/nitrite treated groups. Both nitrite and SNAP treatments caused Akt1 inactivation (reduction in the activation phosphorylation at Ser473) under HG and a concomitant Drp1 activation leading to altered mitochondrial morphology (less reticulate mitochondria). When the effect of the nitrite anion under HG was further analyzed for changes in downstream kinases of Akt1, it was observed that there is a reduction in the

expression of a pro-survival kinase, Pim1. This protein has been reported to increase the inactivation phosphorylation at Ser-637 residue of Drp1 (Din et al., 2013). Pim1 is proto-oncogene which has been implicated in vascular diseases and particularly in hyperglycemia, it is found to mediate vascular smooth muscle cell (VSMC) proliferation (Wang et al., 2017). Another kinase that is downstream of Akt and upstream of Drp1 is the GSK3β whose kinase domain is rendered inactive by phosphorylation at Ser-9 by an activated Akt1 (Beurel et al., 2015; Nitulescu et al., 2018). Nevertheless, the Ser-9 phosphorylation was non-significantly reduced in HG-nitrite group indicating the action of other kinases on GSK3β (Beurel et al., 2015). A reduced GSK3β phosphorylation has been associated with impaired insulin signaling (pro-survival) in rodent models (Zhang et al., 2012); hence the preservation of an inactive GSK3β in HG-nitrite group indicates the existence of other survival mechanisms. Optic atrophy 1 (OPA1), a regulator of inner mitochondrial membrane fusion was also not altered by either nitrite or SNAP under HG implying absence of repercussions on fusion machinery, though fission is being upregulated. Moreover, the decrease in the inhibitory phosphorylation of Drp1 and a concomitant decrease in Akt1 activity and Pim1 kinase expression bestow a possible mechanism behind the above changes in regulators of mitochondrial fission and MMP.

In the next part of the study, nitrite and HG treatments with Drp1-silenced H9c2 cells revealed a differential effect of nitrite on cardiomyoblasts depending on the glycemic levels. Drp1 silencing elevated the expression of OPA1 in normoglycemia with/without nitrite treatment whereas in HG, Drp1 silencing rendered a non-significant change in OPA1 expression. OPA1, like Drp1 is known to interact with pro-apoptotic Bcl2 family proteins and also plays a role in cytochrome c release during apoptosis (Knowlton and Liu, 2015; Nan et al., 2017). When the mitochondrial respiration was measured after Drp1 silencing, it was found that nitrite supplementation enhances mitochondrial coupling efficiency of Drp1-silenced cells under NG but not under HG. Further, on analyzing the protein levels of molecules involved in apoptosis and mitophagy, two processes that are closely related to mitochondrial fission, significant alterations were observed. Caspase 7, an effector caspase in apoptotic signaling, is downregulated in Drp1 silenced cells under HG with/without nitrite supplementation, whereas no significant change was observed under NG. However, the apoptotic marker cleaved PARP levels

were not altered by Drp1 silencing under HG. Anti-apoptotic protein, Bcl2 is reduced in Drp1 silenced cells under HG with/without nitrite supplementation but not under NG. In the case of mitophagy regulators, PTEN induced kinase 1 (Pink1) is reduced in Drp1 silenced cells under both glycemic levels irrespective of nitrite treatment. Another molecule involved maintaining mitochondrial integrity and autophagy is Parkin. The Parkin levels are elevated from endogenous levels in Drp1 silenced cells only under normoglycemia with/without nitrite supplementation. The supplementation of nitrite in the presence of high glucose not only deteriorates the mitochondrial derangements pertaining to the fission machinery but also does not improve the respiratory efficiency as reported in previous literature (Larsen et al., 2011). Moreover, downregulation of pro-survival pathways reveals the deleterious effects imparted by the anion. These observations, albeit requiring further validation, also underscore the key role played by Drp1 in determining the effects of nitrite and HG on myoblasts.

V. 1. Significance of the study

Massive production of reactive species derived from oxygen or nitrogen, which trigger oxidative and nitrosative stress is considered a possible side effect of elevated nitrite levels. Our data substantiate the need of addressing the systemic effect of nitrite/nitrate therapy covering individual organs so as to validate the reported benefits in the setting of metabolic disorders. The above findings uphold a pressing need for addressing any inexactitude of optimistic outcomes from clinical trials pertaining to cardiovascular health in metabolic syndrome. In a scenario where a dichotomy prevails in the current stance of the scientific community about the use of nitrite/nitrate as supplements to patients with metabolic syndrome, there is a need for delving deep into their molecular and biochemical targets and the changes effected by them.

V.2. Limitations of the study

- The cell line model provides information only about the *in vitro* effects of nitrite anion/SNAP.
- High glucose simulates only hyperglycemia, not the multitude of manifestations during diabetes or metabolic syndrome.

- The myoblasts are metabolically different from the differentiated adult myocytes.
- The *in vivo* changes in cardiac mitochondrial function and physiology could not be assessed

VI. Summary

The major findings from this study are:

- Nitrite has differential effects on cellular redox status of myocytes based on the ROS environment already prevailing in the cells.
- Both SNAP & Nitrite treatments decrease mitochondrial membrane potential of H9c2 myoblasts under high glucose conditions.
- UCP3 & ANT1 levels are increased under HG conditions and by SNAP correlating to the decreased mitochondrial membrane potential.
- Mitochondrial coupling efficiency and the mitochondrial mass as well as biogenesis are unchanged under HG on SNAP or nitrite treatments.
- Nitrite /SNAP activated Drp1 under high glucose and concomitantly decreased the Akt1 activity in H9c2 cells.
- Akt inactivation was not associated with a significant change in the GSK3β phosphorylation
- The inactivation of Akt under HG-nitrite was associated with reduced expression of Pim1 kinase, indicating a possible crosstalk with Drp1 activity.
- Silencing of Drp1 leads to differential effects by nitrite under NG vs. HG conditions, mainly pertaining to mitochondrial respiration and markers of mitochondria-related processes like apoptosis and mitophagy.

Take home message:

The present study found potentially harmful molecular changes imparted by inorganic nitrite or an NO donor in cardiac myoblasts, under high glucose conditions. This gives a cautionary note to the clinical trials investigating the beneficial effects of inorganic nitrite supplementation to human subjects with metabolic syndrome

Summary Diagram

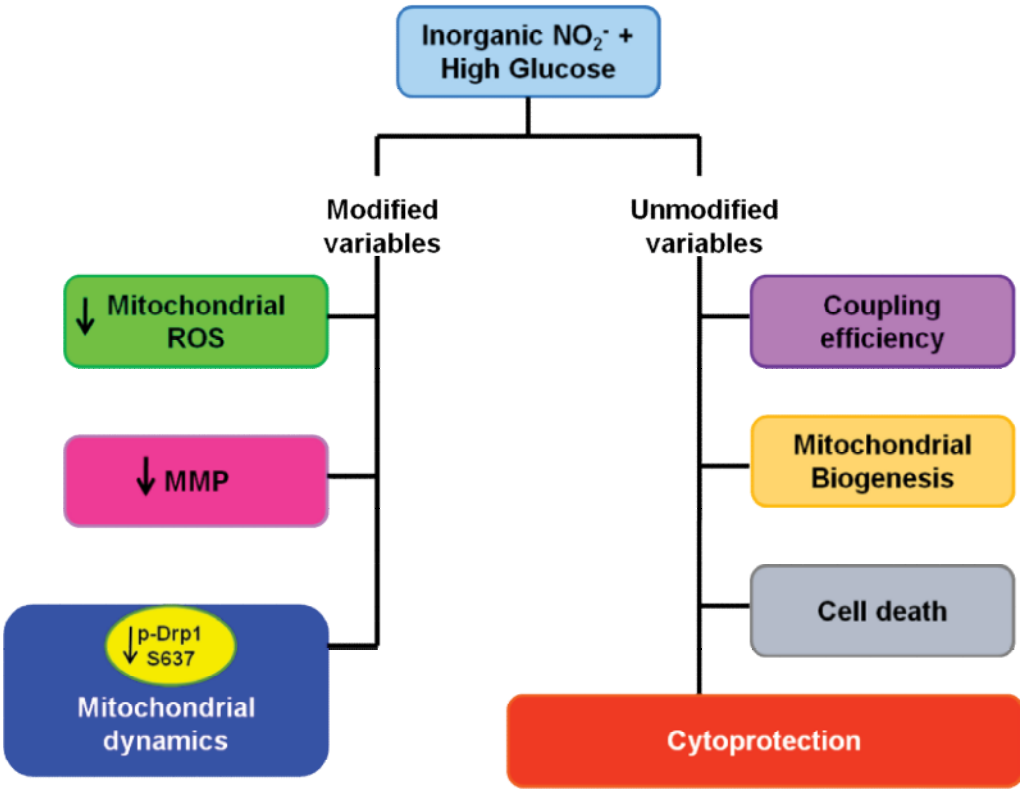

Fig. VI.1. Summary of the effects of nitrite in H9c2 under HG

VII. Publications and Abstracts

Articles

1. **Inorganic nitrite alters mitochondrial dynamics without overt changes in cell death and mitochondrial respiration in cardiomyoblasts under hyperglycemia**

   CR Anand, B Bhavya, VS Harikrishnan, K Jayakumar, Srinivas Gopala

   ***Toxicology in Vitro (2020)**, Volume 70, https://doi.org/10.1016/j.tiv.2020.105048*

2. **MutT Homolog1 has multifaceted role in glioma and is under the apparent orchestration by Hypoxia Inducible factor1 alpha**

   *Bharathan Bhavya, HV Easwer, GC Vilanilam, **CR Anand**, K Sreelakshmi, U Madhusoodanan, P Rajalakshmi, I Neena, CJ Padmakrishnan, GR Menon, K Krishnakumar, AN Deepti, Srinivas Gopala*

   ***Life Sciences (2020)**, In Press, https://doi.org/10.1016/j.lfs.2020.118673*

Reviews

1. **Are Nirtic oxide- mediated protein modifications of functional significance in diabetic heart? ye'S, -NO', wh-'Y-NO't?**

   *Nandini Ravikumar Jayakumari, **Anand Chellappan Reghuvaran**, Raji Sasikala Rajendran, Vivek Velayudhan Pillai, Jayakumar Karunakaran, Harikrishnan Vijayakumar Sreelatha, Srinivas Gopala*

   ***Nitric Oxide** 43 (2014) 35-44.*

2. **To be Wild or Mutant: Role of isocitrate dehydrogenase1 (IDH1) and 2-hydroxy glutarate (2-HG) in gliomagenesis and treatment outcome in glioma**

   *Bharathan Bhavya, **CR Anand**, UK Madhusoodanan, P Rajalakshmi,*

K Krishnakumar, HV Easwer, AN Deepti, Srinivas Gopala

***Cellular and Molecular Neurobiology** (2019) Volume 40(1):53-63.*

Articles under revision

1. **Honokiol regulates mitochondrial substrate utilization and cellular fatty acid metabolism in diabetic mice heart**

   *Nandini RJ, Raji SR, Ashok S, Sulfath TP, **Anand CR**, Harikrishnan VS, Srinivas Gopala*

   European Journal of Pharmacology (2021)

2. **Diminished substrate-mediated cardiac mitochondrial respiration and elevated autophagy in adult male offspring of gestational diabetic rats**

   *Raji Sasikala Rajendran, Nandini Ravikumar Jayakumari, Ashok Sivasailam, **Anand Chellappan Reghuvaran**, Vivek Velayudhan Pillai, Jayakumar Karunakaran, Harikrishnan Vijayakumar Sreelatha, Shankarappa Manjunatha, Srinivas Gopala*

   IUBMB Life (2021)

Oral Presentations

1. **Mitochondria-mediated Effects Imparted By NO-donors To Cardiomyocytes in the setting of Hyperglycemia**

   ***Anand C R** & G. Srinivas. **International Conference on advances in degenerative diseases and molecular interventions (ADDMI)** organized by*

   Society for Research on Degenerative diseases (SODD) on November 23-24th,

2017 at Hycinth by Sparsa, Thiruvanthapuram.

2. ***Role of Dynamin related protein 1 (Drp1) in cardiomyoblasts on nitrite supplementation under hyperglycemia***

   Anand C R *& G. Srinivas "**Biochemistry Talks**" on August 2, 2019, Sree Chitra Tirunal Institute for Medical Sciences and Technology, Trivandrum*

Posters

1. **Modulatory effects of nitric oxide on mitochondrial fission regulators during hyperglycemia**

   Anand C R *& G. Srinivas Recent Advances in Biochemical Therapeutics (RBAT IV) organized by Department of Biochemistry, University of Kerala, Kariyavattom on January 23-25th, 2018.*

VIII. References

Ansley DM, Wang B (2013) Oxidative stress and myocardial injury in the diabetic heart. J. Pathol. **229**: 232–241. doi:10.1002/path.4113.
Apostoli GL, Solomon A, Smallwood MJ, Winyard PG, Emerson M (2014) Role of inorganic nitrate and nitrite in driving nitric oxide-cGMP-mediated inhibition of platelet aggregation in vitro and in vivo. J. Thromb. Haemost. JTH **12**: 1880–1889. doi:10.1111/jth.12711.
Ashmore T, Roberts LD, Morash AJ, Kotwica AO, Finnerty J, West JA, Murfitt SA, Fernandez BO, Branco C, Cowburn AS, Clarke K, Johnson RS, Feelisch M, Griffin JL, Murray AJ (2015) Nitrate enhances skeletal muscle fatty acid oxidation via a nitric oxide-cGMP-PPAR-mediated mechanism. BMC Biol. **13**: 1–17. doi:10.1186/s12915-015-0221-6.
Ashrafi G, Schwarz TL (2013) The pathways of mitophagy for quality control and clearance of mitochondria. Cell Death Differ. **20**: 31–42. doi:10.1038/cdd.2012.81.
Babykutty S, Suboj P, Srinivas P, Nair AS, Chandramohan K, Gopala S (2012) Insidious role of nitric oxide in migration/invasion of colon cancer cells by upregulating MMP-2/9 via activation of cGMP-PKG-ERK signaling pathways. Clin. Exp. Metastasis **29**: 471–492. doi:10.1007/s10585-012-9464-6.
Bailey JC, Feelisch M, Horowitz JD, Frenneaux MP, Madhani M (2014) Pharmacology and therapeutic role of inorganic nitrite and nitrate in vasodilatation. Pharmacol. Ther. **144**: 303–320. doi:10.1016/j.pharmthera.2014.06.009.
Baliga RS, Milsom AB, Ghosh SM, Trinder SL, Macallister RJ, Ahluwalia A, Hobbs AJ (2012) Dietary nitrate ameliorates pulmonary hypertension: cytoprotective role for endothelial nitric oxide synthase and xanthine oxidoreductase. Circulation **125**: 2922–2932. doi:10.1161/CIRCULATIONAHA.112.100586.
Balog J, Mehta SL, Vemuganti R (2016) Mitochondrial fission and fusion in secondary brain damage after CNS insults. J. Cereb. Blood Flow Metab. **36**: 2022–2033. doi:10.1177/0271678X16671528.
Becker D, Richter J, Tocilescu MA, Przedborski S, Voos W (2012) Pink1 Kinase and Its Membrane Potential (Δψ)-dependent Cleavage Product Both Localize to Outer Mitochondrial Membrane by Unique Targeting Mode. J. Biol. Chem. **287**: 22969–22987. doi:10.1074/jbc.M112.365700.
Benjamin N, O'Driscoll F, Dougall H, Duncan C, Smith L, Golden M, McKenzie H (1994) Stomach NO synthesis. Nature **368**: 502. doi:10.1038/368502a0.
Bereiter-Hahn J, Vöth M (1994) Dynamics of mitochondria in living cells: shape changes, dislocations, fusion, and fission of mitochondria. Microsc. Res. Tech. **27**: 198–219. doi:10.1002/jemt.1070270303.
Beurel E, Grieco SF, Jope RS (2015) Glycogen synthase kinase-3 (GSK3): regulation, actions, and diseases. Pharmacol. Ther. **0**: 114–131. doi:10.1016/j.pharmthera.2014.11.016.
Bleazard W, McCaffery JM, King EJ, Bale S, Mozdy A, Tieu Q, Nunnari J, Shaw JM (1999) The dynamin-related GTPase Dnm1 regulates mitochondrial fission in yeast. Nat. Cell Biol. **1**: 298–304. doi:10.1038/13014.
Bleier L, Dröse S (2013) Superoxide generation by complex III: from mechanistic rationales to functional consequences. Biochim. Biophys. Acta **1827**: 1320–1331. doi:10.1016/j.bbabio.2012.12.002.
Bliek AM van der, Shen Q, Kawajiri S (2013) Mechanisms of Mitochondrial Fission and Fusion. Cold Spring Harb. Perspect. Biol. **5**: a011072. doi:10.1101/cshperspect.a011072.

Borillo Gwynngelle A., Mason Matt, Quijada Pearl, Völkers Mirko, Cottage Christopher, McGregor Michael, Din Shabana, Fischer Kimberlee, Gude Natalie, Avitabile Daniele, Barlow Steven, Alvarez Roberto, Truffa Silvia, Whittaker Ross, Glassy Matthew S., Gustafsson Asa B., Miyamoto Shigeki, Glembotski Christopher C., Gottlieb Roberta A., Brown Joan Heller, Sussman Mark A. (2010a) Pim-1 Kinase Protects Mitochondrial Integrity in Cardiomyocytes. Circ. Res. **106**: 1265–1274. doi:10.1161/CIRCRESAHA.109.212035.

Borillo Gwynngelle A., Mason Matt, Quijada Pearl, Völkers Mirko, Cottage Christopher, McGregor Michael, Din Shabana, Fischer Kimberlee, Gude Natalie, Avitabile Daniele, Barlow Steven, Alvarez Roberto, Truffa Silvia, Whittaker Ross, Glassy Matthew S., Gustafsson Asa B., Miyamoto Shigeki, Glembotski Christopher C., Gottlieb Roberta A., Brown Joan Heller, Sussman Mark A. (2010b) Pim-1 Kinase Protects Mitochondrial Integrity in Cardiomyocytes. Circ. Res. **106**: 1265–1274. doi:10.1161/CIRCRESAHA.109.212035.

Brand MD (2010) The sites and topology of mitochondrial superoxide production. Exp. Gerontol. **45**: 466–472. doi:10.1016/j.exger.2010.01.003.

Brault L, Gasser C, Bracher F, Huber K, Knapp S, Schwaller J (2010) PIM serine/threonine kinases in the pathogenesis and therapy of hematologic malignancies and solid cancers. Haematologica **95**: 1004–1015. doi:10.3324/haematol.2009.017079.

Breitzig MT, Alleyn MD, Lockey RF, Kolliputi N (2018) A mitochondrial delicacy: dynamin-related protein 1 and mitochondrial dynamics. Am. J. Physiol. Cell Physiol. **315**: C80–C90. doi:10.1152/ajpcell.00042.2018.

Bryan NS, Calvert JW, Elrod JW, Gundewar S, Ji SY, Lefer DJ (2007) Dietary nitrite supplementation protects against myocardial ischemia-reperfusion injury. Proc. Natl. Acad. Sci. U. S. A. **104**: 19144–19149. doi:10.1073/pnas.0706579104.

Bugger H, Abel ED (2010) Mitochondria in the diabetic heart. Cardiovasc. Res. **88**: 229–240. doi:10.1093/cvr/cvq239.

Bullock AN, Debreczeni J, Amos AL, Knapp S, Turk BE (2005) Structure and substrate specificity of the Pim-1 kinase. J. Biol. Chem. **280**: 41675–41682. doi:10.1074/jbc.M510711200.

Burman JL, Pickles S, Wang C, Sekine S, Vargas JNS, Zhang Z, Youle AM, Nezich CL, Wu X, Hammer JA, Youle RJ (2017) Mitochondrial fission facilitates the selective mitophagy of protein aggregates. J. Cell Biol. **216**: 3231–3247. doi:10.1083/jcb.201612106.

Burnette WN (1981) "Western blotting": electrophoretic transfer of proteins from sodium dodecyl sulfate--polyacrylamide gels to unmodified nitrocellulose and radiographic detection with antibody and radioiodinated protein A. Anal. Biochem. **112**: 195–203. doi:10.1016/0003-2697(81)90281-5.

Butler L, Cros C, Oldman KL, Harmer AR, Pointon A, Pollard CE, Abi-Gerges N (2015) Enhanced characterization of contractility in cardiomyocytes during early drug safety assessment. Toxicol. Sci. Off. J. Soc. Toxicol. **145**: 396–406. doi:10.1093/toxsci/kfv062.

Calvert JW, Lefer DJ (2009) Myocardial protection by nitrite. Cardiovasc. Res. **83**: 195–203. doi:10.1093/cvr/cvp079.

Camara AKS, Bienengraeber M, Stowe DF (2011) Mitochondrial approaches to protect against cardiac ischemia and reperfusion injury. Physiology **2**: 13. doi:10.3389/fphys.2011.00013.

Cantu D, Schaack J, Patel M (2009) Oxidative Inactivation of Mitochondrial Aconitase Results in Iron and H2O2-Mediated Neurotoxicity in Rat Primary Mesencephalic

Cultures. PLoS ONE **4**. doi:10.1371/journal.pone.0007095. http://www.ncbi.nlm.nih.gov/pmc/articles/PMC2738973/.
Carlström M, Larsen FJ, Nyström T, Hezel M, Borniquel S, Weitzberg E, Lundberg JO (2010) Dietary inorganic nitrate reverses features of metabolic syndrome in endothelial nitric oxide synthase-deficient mice. Proc. Natl. Acad. Sci. U. S. A. **107**: 17716–17720. doi:10.1073/pnas.1008872107.
Carlström M, Liu M, Yang T, Zollbrecht C, Huang L, Peleli M, Borniquel S, Kishikawa H, Hezel M, Persson AEG, Weitzberg E, Lundberg JO (2013) Cross-talk Between Nitrate-Nitrite-NO and NO Synthase Pathways in Control of Vascular NO Homeostasis. Antioxid. Redox Signal. **23**: 295–306. doi:10.1089/ars.2013.5481.
Carlström M, Persson AEG, Larsson E, Hezel M, Scheffer PG, Teerlink T, Weitzberg E, Lundberg JO (2011) Dietary nitrate attenuates oxidative stress, prevents cardiac and renal injuries, and reduces blood pressure in salt-induced hypertension. Cardiovasc. Res. **89**: 574–585. doi:10.1093/cvr/cvq366.
Carreira RS, Lee P, Gottlieb RA (2011) Mitochondrial Therapeutics for Cardioprotection. Curr. Pharm. Des. **17**: 2017–2035.
Cassidy-Stone A, Chipuk JE, Ingerman E, Song C, Yoo C, Kuwana T, Kurth MJ, Shaw JT, Hinshaw JE, Green DR, Nunnari J (2008) Chemical inhibition of the mitochondrial division dynamin reveals its role in Bax/Bak-dependent mitochondrial outer membrane permeabilization. Dev. Cell **14**: 193–204. doi:10.1016/j.devcel.2007.11.019.
Chandel NS (2018) Mitochondria: back to the future. Nat. Rev. Mol. Cell Biol. **19**: 76–76. doi:10.1038/nrm.2017.133.
Chen H, Chan DC (2005) Emerging functions of mammalian mitochondrial fusion and fission. Hum. Mol. Genet. **14 Spec No. 2**: R283-289. doi:10.1093/hmg/ddi270.
Cho B, Choi SY, Cho HM, Kim HJ, Sun W (2013) Physiological and pathological significance of dynamin-related protein 1 (drp1)-dependent mitochondrial fission in the nervous system. Exp. Neurobiol. **22**: 149–157. doi:10.5607/en.2013.22.3.149.
Choi SY, Kim JY, Kim H-W, Cho B, Cho HM, Oppenheim RW, Kim H, Rhyu IJ, Sun W (2013) Drp1-mediated mitochondrial dynamics and survival of developing chick motoneurons during the period of normal programmed cell death. FASEB J. **27**: 51–62. doi:10.1096/fj.12-211920.
Cnop M, Welsh N, Jonas J-C, Jörns A, Lenzen S, Eizirik DL (2005) Mechanisms of Pancreatic β-Cell Death in Type 1 and Type 2 Diabetes: Many Differences, Few Similarities. Diabetes **54**: S97–S107. doi:10.2337/diabetes.54.suppl_2.S97.
Cross DAE, Alessi DR, Cohen P, Andjelkovich M, Hemmings BA (1995) Inhibition of glycogen synthase kinase-3 by insulin mediated by protein kinase B. Nature **378**: 785–789. doi:10.1038/378785a0.
Dagda RK, Cherra SJ, Kulich SM, Tandon A, Park D, Chu CT (2009) Loss of PINK1 Function Promotes Mitophagy through Effects on Oxidative Stress and Mitochondrial Fission. J. Biol. Chem. **284**: 13843–13855. doi:10.1074/jbc.M808515200.
Damacena-Angelis C, Oliveira-Paula GH, Pinheiro LC, Crevelin EJ, Portella RL, Moraes LAB, Tanus-Santos JE (2017) Nitrate decreases xanthine oxidoreductase-mediated nitrite reductase activity and attenuates vascular and blood pressure responses to nitrite. Redox Biol. **12**: 291–299. doi:10.1016/j.redox.2017.03.003.
Dimmeler S, Fleming I, Fisslthaler B, Hermann C, Busse R, Zeiher AM (1999) Activation of nitric oxide synthase in endothelial cells by Akt-dependent phosphorylation. Nature **399**: 601–605. doi:10.1038/21224.

Din S, Mason M, Völkers M, Johnson B, Cottage CT, Wang Z, Joyo AY, Quijada P, Erhardt P, Magnuson NS, Konstandin MH, Sussman MA (2013) Pim-1 preserves mitochondrial morphology by inhibiting dynamin-related protein 1 translocation. Proc. Natl. Acad. Sci. U. S. A. **110**: 5969–5974. doi:10.1073/pnas.1213294110.

Doganci S, Yildirim V, Bolcal C, Korkusuz P, Gumusel B, Demirkilic U, Aydin A (2012) Sodium nitrite and cardioprotective effect in pig regional myocardial ischemia-reperfusion injury model. Adv. Clin. Exp. Med. Off. Organ Wroclaw Med. Univ. **21**: 713–726.

Duranski MR, Greer JJM, Dejam A, Jaganmohan S, Hogg N, Langston W, Patel RP, Yet S-F, Wang X, Kevil CG, Gladwin MT, Lefer DJ (2005) Cytoprotective effects of nitrite during in vivo ischemia-reperfusion of the heart and liver. J. Clin. Invest. **115**: 1232–1240. doi:10.1172/JCI200522493.

Düssmann H, Kögel D, Rehm M, Prehn JHM (2003) Mitochondrial Membrane Permeabilization and Superoxide Production during Apoptosis A SINGLE-CELL ANALYSIS. J. Biol. Chem. **278**: 12645–12649. doi:10.1074/jbc.M210826200.

Estaquier J, Arnoult D (2007) Inhibiting Drp1-mediated mitochondrial fission selectively prevents the release of cytochrome c during apoptosis. Cell Death Differ. **14**: 1086–1094. doi:10.1038/sj.cdd.4402107.

Federici Massimo, Menghini Rossella, Mauriello Alessandro, Hribal Marta Letizia, Ferrelli Francesca, Lauro Davide, Sbraccia Paolo, Spagnoli Luigi Giusto, Sesti Giorgio, Lauro Renato (2002) Insulin-Dependent Activation of Endothelial Nitric Oxide Synthase Is Impaired by O-Linked Glycosylation Modification of Signaling Proteins in Human Coronary Endothelial Cells. Circulation **106**: 466–472. doi:10.1161/01.CIR.0000023043.02648.51.

Ferree A, Shirihai O (2012) Mitochondrial Dynamics: The Intersection of Form and Function. Adv. Exp. Med. Biol. **748**: 13–40. doi:10.1007/978-1-4614-3573-0_2.

Flynn JM, Melov S (2013) SOD2 in Mitochondrial Dysfunction and Neurodegeneration. Free Radic. Biol. Med. **62**. doi:10.1016/j.freeradbiomed.2013.05.027. https://www.ncbi.nlm.nih.gov/pmc/articles/PMC3811078/.

Fonseca TB, Sánchez-Guerrero Á, Milosevic I, Raimundo N (2019) Mitochondrial fission requires DRP1 but not dynamins. Nature **570**: E34–E42. doi:10.1038/s41586-019-1296-y.

Fox CJ, Hammerman PS, Cinalli RM, Master SR, Chodosh LA, Thompson CB (2003) The serine/threonine kinase Pim-2 is a transcriptionally regulated apoptotic inhibitor. Genes Dev. **17**: 1841–1854. doi:10.1101/gad.1105003.

Frank S, Gaume B, Bergmann-Leitner ES, Leitner WW, Robert EG, Catez F, Smith CL, Youle RJ (2001) The role of dynamin-related protein 1, a mediator of mitochondrial fission, in apoptosis. Dev. Cell **1**: 515–525.

Frezza C, Cipolat S, Martins de Brito O, Micaroni M, Beznoussenko GV, Rudka T, Bartoli D, Polishuck RS, Danial NN, De Strooper B, Scorrano L (2006) OPA1 controls apoptotic cristae remodeling independently from mitochondrial fusion. Cell **126**: 177–189. doi:10.1016/j.cell.2006.06.025.

Frohman MA (2015) Role of mitochondrial lipids in guiding fission and fusion. J. Mol. Med. **93**: 263–269. doi:10.1007/s00109-014-1237-z.

Fulton D, Gratton JP, McCabe TJ, Fontana J, Fujio Y, Walsh K, Franke TF, Papapetropoulos A, Sessa WC (1999) Regulation of endothelium-derived nitric oxide production by the protein kinase Akt. Nature **399**: 597–601. doi:10.1038/21218.

García-Martinez C, Sibille B, Solanes G, Darimont C, Macé K, Villarroya F, Gómez-Foix AM (2001) Overexpression of UCP3 in cultured human muscle lowers mitochondrial membrane potential, raises ATP/ADP ratio, and favors fatty acid vs. glucose oxidation. FASEB J. Off. Publ. Fed. Am. Soc. Exp. Biol. **15**: 2033–2035. doi:10.1096/fj.00-0828fje.
Garner DL, Thomas CA (1999) Organelle-specific probe JC-1 identifies membrane potential differences in the mitochondrial function of bovine sperm. Mol. Reprod. Dev. **53**: 222–229. doi:10.1002/(SICI)1098-2795(199906)53:2<222::AID-MRD11>3.0.CO;2-L.
Ghasemi A, Zahediasl S (2013) Potential Therapeutic Effects of Nitrate/Nitrite and Type 2 Diabetes Mellitus. Int. J. Endocrinol. Metab. **11**: 63–64. doi:10.5812/ijem.9103.
Gheibi S, Bakhtiarzadeh F, Jeddi S, Farrokhfall K, Zardooz H, Ghasemi A (2017) Nitrite increases glucose-stimulated insulin secretion and islet insulin content in obese type 2 diabetic male rats. Nitric Oxide Biol. Chem. **64**: 39–51. doi:10.1016/j.niox.2017.01.003.
Giacco F, Brownlee M (2010) Oxidative stress and diabetic complications. Circ. Res. **107**: 1058–1070. doi:10.1161/CIRCRESAHA.110.223545.
Gilchrist M, Shore AC, Benjamin N (2011a) Inorganic nitrate and nitrite and control of blood pressure. Cardiovasc. Res. **89**: 492–498. doi:10.1093/cvr/cvq309.
Gilchrist M, Shore AC, Benjamin N (2011b) Inorganic nitrate and nitrite and control of blood pressure. Cardiovasc. Res. **89**: 492–498. doi:10.1093/cvr/cvq309.
Gilchrist M, Winyard PG, Aizawa K, Anning C, Shore A, Benjamin N (2013) Effect of dietary nitrate on blood pressure, endothelial function, and insulin sensitivity in type 2 diabetes. Free Radic. Biol. Med. **60**: 89–97. doi:10.1016/j.freeradbiomed.2013.01.024.
Gladwin MT, Grubina R, Doyle MP (2009) The new chemical biology of nitrite reactions with hemoglobin: R-state catalysis, oxidative denitrosylation, and nitrite reductase/anhydrase. Acc. Chem. Res. **42**: 157–167. doi:10.1021/ar800089j.
Godber BLJ, Doel JJ, Sapkota GP, Blake DR, Stevens CR, Eisenthal R, Harrison R (2000) Reduction of Nitrite to Nitric Oxide Catalyzed by Xanthine Oxidoreductase. J. Biol. Chem. **275**: 7757–7763. doi:10.1074/jbc.275.11.7757.
Green K, Brand MD, Murphy MP (2004) Prevention of Mitochondrial Oxidative Damage as a Therapeutic Strategy in Diabetes. Diabetes **53**: S110–S118. doi:10.2337/diabetes.53.2007.S110.
Gurgul-Convey E, Lenzen S (2015) Is Nitric Oxide Really the Primary Mediator of Pancreatic β-Cell Death in Type 1 Diabetes? J. Biol. Chem. **290**: 10570–10570. doi:10.1074/jbc.L115.648089.
Halestrap AP, Kerr PM, Javadov S, Woodfield K-Y (1998) Elucidating the molecular mechanism of the permeability transition pore and its role in reperfusion injury of the heart. Biochim. Biophys. Acta BBA - Bioenerg. **1366**: 79–94. doi:10.1016/S0005-2728(98)00122-4.
Hall JL (2014) Glycogen Synthase Kinase–3 and the Heart∗. J. Am. Coll. Cardiol. **64**: 707–709. doi:10.1016/j.jacc.2014.06.1142.
Hansen MN, Lundberg JO, Filice M, Fago A, Christensen NMG, Jensen FB (2016) The roles of tissue nitrate reductase activity and myoglobin in securing nitric oxide availability in deeply hypoxic crucian carp. J. Exp. Biol. **219**: 3875–3883. doi:10.1242/jeb.149195.
He C, Zhu H, Li H, Zou M-H, Xie Z (2013) Dissociation of Bcl-2–Beclin1 Complex by Activated AMPK Enhances Cardiac Autophagy and Protects Against Cardiomyocyte Apoptosis in Diabetes. Diabetes **62**: 1270–1281. doi:10.2337/db12-0533.

He C, Hart PC, Germain D, Bonini MG (2016) SOD2 and the mitochondrial UPR: partners regulating cellular phenotypic transitions. Trends Biochem. Sci. **41**: 568–577. doi:10.1016/j.tibs.2016.04.004.
Hecht SS, Hoffmann D (1998) N-nitroso compounds and man: sources of exposure, endogenous formation and occurrence in body fluids. Eur. J. Cancer Prev. Off. J. Eur. Cancer Prev. Organ. ECP **7**: 165–166.
Heger J, Lynetskiy O, Euler G, Schlueter K-D, Schulz R, Doerner A (2018) P269Hearts subjected to ischemia-reperfusion benefit from adenine nucleotide translocase 1 overexpression. Cardiovasc. Res. **114**: S69–S69. doi:10.1093/cvr/cvy060.189.
Hemmings BA, Restuccia DF (2012) PI3K-PKB/Akt Pathway. Cold Spring Harb. Perspect. Biol. **4**. doi:10.1101/cshperspect.a011189. https://www.ncbi.nlm.nih.gov/pmc/articles/PMC3428770/.
Hendgen-Cotta UB, Merx MW, Shiva S, Schmitz J, Becher S, Klare JP, Steinhoff H-J, Goedecke A, Schrader J, Gladwin MT, Kelm M, Rassaf T (2008) Nitrite reductase activity of myoglobin regulates respiration and cellular viability in myocardial ischemia-reperfusion injury. Proc. Natl. Acad. Sci. **105**: 10256–10261. doi:10.1073/pnas.0801336105.
Hey-Mogensen M, Clausen TR (2017) Targeting Mitochondrial Biogenesis and Mitochondrial Substrate Utilization to Treat Obesity and Insulin Resistance, Respectively - Two Data-Driven Hypotheses. Curr. Diabetes Rev. **13**: 395–404. doi:10.2174/1573399812666160217122827.
Horscroft JA, O'Brien KA, Clark AD, Lindsay RT, Steel AS, Procter NEK, Devaux J, Frenneaux M, Harridge SDR, Murray AJ (2019) Inorganic nitrate, hypoxia, and the regulation of cardiac mitochondrial respiration—probing the role of PPARα. FASEB J. **33**: 7563–7577. doi:10.1096/fj.201900067R.
Inoue-Yamauchi A, Oda H (2012) Depletion of mitochondrial fission factor DRP1 causes increased apoptosis in human colon cancer cells. Biochem. Biophys. Res. Commun. **421**: 81–85. doi:10.1016/j.bbrc.2012.03.118.
Jang J-Y, Choi Y, Jeon Y-K, Aung KC aYu, Kim C-W (2008) Over-expression of Adenine Nucleotide Translocase 1 (ANT1) Induces Apoptosis and Tumor Regression in vivo. BMC Cancer **8**. doi:10.1186/1471-2407-8-160. http://bmccancer.biomedcentral.com/articles/10.1186/1471-2407-8-160.
Jansson EA, Huang L, Malkey R, Govoni M, Nihlén C, Olsson A, Stensdotter M, Petersson J, Holm L, Weitzberg E, Lundberg JO (2008) A mammalian functional nitrate reductase that regulates nitrite and nitric oxide homeostasis. Nat. Chem. Biol. **4**: 411–417. doi:10.1038/nchembio.92.
Jia G, Sowers JR (2014) New Thoughts in an Old Player: Role of Nitrite in the Treatment of Ischemic Revascularization. Diabetes **63**: 39–41. doi:10.2337/db13-1530.
Jiang H, Torregrossa AC, Potts A, Pierini D, Aranke M, Garg HK, Bryan NS (2014) Dietary nitrite improves insulin signaling through GLUT4 translocation. Free Radic. Biol. Med. **67**: 51–57. doi:10.1016/j.freeradbiomed.2013.10.809.
Johnson G, Tsao P, Lefer AM (1990) Synergism between superoxide dismutase and sodium nitrite in cardioprotection following ischemia and reperfusion. Am. Heart J. **119**: 530–537. doi:10.1016/s0002-8703(05)80275-3.
Kasahara A, Cipolat S, Chen Y, Dorn GW, Scorrano L (2013) Mitochondrial Fusion Directs Cardiomyocyte Differentiation via Calcineurin and Notch Signaling. Science **342**: 734–737. doi:10.1126/science.1241359.

Kim B, Kim J-S, Yoon Y, Santiago MC, Brown MD, Park J-Y (2013) Inhibition of Drp1-dependent mitochondrial division impairs myogenic differentiation. Am. J. Physiol.-Regul. Integr. Comp. Physiol. **305**: R927–R938. doi:10.1152/ajpregu.00502.2012.
Kim-Shapiro DB, Gladwin MT (2014) Mechanisms of nitrite bioactivation. Nitric Oxide **38**: 58–68. doi:10.1016/j.niox.2013.11.002.
Knowlton AA, Liu TT (2015) Mitochondrial Dynamics and Heart Failure. Compr. Physiol. **6**: 507–526. doi:10.1002/cphy.c150022.
Kojima H, Nakatsubo N, Kikuchi K, Kawahara S, Kirino Y, Nagoshi H, Hirata Y, Nagano T (1998a) Detection and imaging of nitric oxide with novel fluorescent indicators: diaminofluoresceins. Anal. Chem. **70**: 2446–2453. doi:10.1021/ac9801723.
Kojima H, Sakurai K, Kikuchi K, Kawahara S, Kirino Y, Nagoshi H, Hirata Y, Nagano T (1998b) Development of a fluorescent indicator for nitric oxide based on the fluorescein chromophore. Chem. Pharm. Bull. (Tokyo) **46**: 373–375. doi:10.1248/cpb.46.373.
Korshunov SS, Skulachev VP, Starkov AA (1997) High protonic potential actuates a mechanism of production of reactive oxygen species in mitochondria. FEBS Lett. **416**: 15–18. doi:10.1016/s0014-5793(97)01159-9.
Krebiehl G, Ruckerbauer S, Burbulla LF, Kieper N, Maurer B, Waak J, Wolburg H, Gizatullina Z, Gellerich FN, Woitalla D, Riess O, Kahle PJ, Proikas-Cezanne T, Krüger R (2010) Reduced Basal Autophagy and Impaired Mitochondrial Dynamics Due to Loss of Parkinson's Disease-Associated Protein DJ-1. PLOS ONE **5**: e9367. doi:10.1371/journal.pone.0009367.
Kuznetsov AV, Mayboroda O, Kunz D, Winkler K, Schubert W, Kunz WS (1998) Functional Imaging of Mitochondria in Saponin-permeabilized Mice Muscle Fibers. J. Cell Biol. **140**: 1091–1099.
Kuznetsov AV, Veksler V, Gellerich FN, Saks V, Margreiter R, Kunz WS (2008) Analysis of mitochondrial function in situ in permeabilized muscle fibers, tissues and cells. Nat. Protoc. **3**: 965–976. doi:10.1038/nprot.2008.61.
Kuzuya T, Nishida M (2000) Role of NO in Myocardial Injury Induced by Oxidative Stress: Ischemia, Myocarditis, Cardiomyopathy, and Heart Failure. In Heart Fail., ed. Akira Kitabatake, Shigetake Sasayama, Gary S. Francis, Hiroshi Okamoto, 81–87. Springer Japan. doi:10.1007/978-4-431-68331-5_7.
Lal H, Ahmad F, Woodgett J, Force T (2015) The GSK-3 family as therapeutic target for myocardial diseases. Circ. Res. **116**: 138–149. doi:10.1161/CIRCRESAHA.116.303613.
Landino LM (2008) Protein Thiol Modification by Peroxynitrite Anion and Nitric Oxide Donors. In Methods Enzymol., ed. Enrique Cadenas and Lester Packer, **Volume 440**95–109. Academic Press. http://www.sciencedirect.com/science/article/pii/S0076687907008051.
Larsen FJ, Schiffer TA, Borniquel S, Sahlin K, Ekblom B, Lundberg JO, Weitzberg E (2011) Dietary inorganic nitrate improves mitochondrial efficiency in humans. Cell Metab. **13**: 149–159. doi:10.1016/j.cmet.2011.01.004.
Layec G, Bringard A, Le Fur Y, Micallef J-P, Vilmen C, Perrey S, Cozzone PJ, Bendahan D (2016) Mitochondrial Coupling and Contractile Efficiency in Humans with High and Low VO2 peak. Med. Sci. Sports Exerc. **48**: 811–821. doi:10.1249/MSS.0000000000000858.
Lee H, Smith SB, Yoon Y (2017) The Short Variant of the Mitochondrial Dynamin OPA1 Maintains Mitochondrial Energetics and Cristae Structure. J. Biol. Chem.: jbc.M116.762567. doi:10.1074/jbc.M116.762567.

Lee JE, Westrate LM, Wu H, Page C, Voeltz GK (2016) Multiple dynamin family members collaborate to drive mitochondrial division. Nature **540**: 139–143. doi:10.1038/nature20555.
Lee Y, Jeong S-Y, Karbowski M, Smith CL, Youle RJ (2004) Roles of the mammalian mitochondrial fission and fusion mediators Fis1, Drp1, and Opa1 in apoptosis. Mol. Biol. Cell **15**: 5001–5011. doi:10.1091/mbc.e04-04-0294.
Li C-J, Elsasser TH, Kahl S (2009) AKT/eNOS signaling module functions as a potential feedback loop in the growth hormone signaling pathway. J. Mol. Signal. **4**: 1. doi:10.1186/1750-2187-4-1.
Li H, Samouilov A, Liu X, Zweier JL (2003) Characterization of the magnitude and kinetics of xanthine oxidase-catalyzed nitrate reduction: evaluation of its role in nitrite and nitric oxide generation in anoxic tissues. Biochemistry **42**: 1150–1159. doi:10.1021/bi026385a.
Li L, Tan J, Miao Y, Lei P, Zhang Q (2015) ROS and Autophagy: Interactions and Molecular Regulatory Mechanisms. Cell. Mol. Neurobiol. **35**: 615–621. doi:10.1007/s10571-015-0166-x.
Li S-Y, Fang CX, Aberle NS, Ren BH, Ceylan-Isik AF, Ren J (2019) Inhibition of PI-3 kinase/Akt/mTOR, but not calcineurin signaling, reverses insulin-like growth factor I-induced protection against glucose toxicity in cardiomyocyte contractile function. J. Endocrinol. **186**: 491–503. doi:10.1677/joe.1.06168.
Liang C, Li Y-Y (2014) Use of regulators and inhibitors of Pim-1, a serine/threonine kinase, for tumour therapy (Review). Mol. Med. Rep. **9**: 2051–2060. doi:10.3892/mmr.2014.2139.
Lima AR, Santos L, Correia M, Soares P, Sobrinho-Simões M, Melo M, Máximo V (2018) Dynamin-Related Protein 1 at the Crossroads of Cancer. Genes **9**. doi:10.3390/genes9020115. https://www.ncbi.nlm.nih.gov/pmc/articles/PMC5852611/.
Lin G, Brownsey RW, MacLeod KM (2009) Regulation of mitochondrial aconitase by phosphorylation in diabetic rat heart. Cell. Mol. Life Sci. **66**: 919–932. doi:10.1007/s00018-009-8696-3.
Lindqvist LM, Heinlein M, Huang DCS, Vaux DL (2014) Prosurvival Bcl-2 family members affect autophagy only indirectly, by inhibiting Bax and Bak. Proc. Natl. Acad. Sci. **111**: 8512–8517. doi:10.1073/pnas.1406425111.
Lundberg JO, Weitzberg E, Lundberg JM, Alving K (1994) Intragastric nitric oxide production in humans: measurements in expelled air. Gut **35**: 1543–1546. doi:10.1136/gut.35.11.1543.
Lundberg JO, Carlström M, Larsen FJ, Weitzberg E (2011a) Roles of dietary inorganic nitrate in cardiovascular health and disease. Cardiovasc. Res. **89**: 525–532. doi:10.1093/cvr/cvq325.
Lundberg JO, Gladwin MT, Ahluwalia A, Benjamin N, Bryan NS, Butler A, Cabrales P, Fago A, Feelisch M, Ford PC, Freeman BA, Frenneaux M, Friedman J, Kelm M, Kevil CG, Kim-Shapiro DB, Kozlov AV, Lancaster JR, Lefer DJ, McColl K, McCurry K, Patel RP, Petersson J, Rassaf T, Reutov VP, Richter-Addo GB, Schechter A, Shiva S, Tsuchiya K, van Faassen EE, Webb AJ, Zuckerbraun BS, Zweier JL, Weitzberg E (2009) Nitrate and nitrite in biology, nutrition and therapeutics. Nat. Chem. Biol. **5**: 865–869. doi:10.1038/nchembio.260.
Lundberg JO, Weitzberg E, Gladwin MT (2008) The nitrate–nitrite–nitric oxide pathway in physiology and therapeutics. Nat. Rev. Drug Discov. **7**: 156–167. doi:10.1038/nrd2466.

Lundberg JO, Weitzberg E, Shiva S, Gladwin MT (2011b) The Nitrate–Nitrite–Nitric Oxide Pathway in Mammals. In Nitrite Nitrate Hum. Health Dis., ed. Nathan S. Bryan, Joseph Loscalzo, 21–48. Totowa, NJ: Humana Press. Nutrition and Health. doi:10.1007/978-1-60761-616-0_3. https://doi.org/10.1007/978-1-60761-616-0_3.

Lushchak OV, Piroddi M, Galli F, Lushchak VI (2014a) Aconitase post-translational modification as a key in linkage between Krebs cycle, iron homeostasis, redox signaling, and metabolism of reactive oxygen species. Redox Rep. Commun. Free Radic. Res. **19**: 8–15. doi:10.1179/1351000213Y.0000000073.

Lushchak OV, Piroddi M, Galli F, Lushchak VI (2014b) Aconitase post-translational modification as a key in linkage between Krebs cycle, iron homeostasis, redox signaling, and metabolism of reactive oxygen species. Redox Rep. **19**: 8–15. doi:10.1179/1351000213Y.0000000073.

MacVicar T, Langer T (2016) OPA1 processing in cell death and disease – the long and short of it. J. Cell Sci. **129**: 2297–2306. doi:10.1242/jcs.159186.

Marsboom Glenn, Toth Peter T., Ryan John J., Hong Zhigang, Wu Xichen, Fang Yong-Hu, Thenappan Thenappan, Piao Lin, Zhang Hannah J., Pogoriler Jennifer, Chen Yimei, Morrow Erik, Weir E. Kenneth, Rehman Jalees, Archer Stephen L. (2012) Dynamin-Related Protein 1–Mediated Mitochondrial Mitotic Fission Permits Hyperproliferation of Vascular Smooth Muscle Cells and Offers a Novel Therapeutic Target in Pulmonary Hypertension. Circ. Res. **110**: 1484–1497. doi:10.1161/CIRCRESAHA.111.263848.

Martínez-Ruiz A, Cadenas S, Lamas S (2011) Nitric oxide signaling: Classical, less classical, and nonclassical mechanisms. Free Radic. Biol. Med. **51**: 17–29. doi:10.1016/j.freeradbiomed.2011.04.010.

Menezes EF, Peixoto LG, Teixeira RR, Justino AB, Puga GM, Espindola FS (2019) Potential Benefits of Nitrate Supplementation on Antioxidant Defense System and Blood Pressure Responses after Exercise Performance. Research article. Oxid. Med. Cell. Longev. doi:10.1155/2019/7218936. https://www.hindawi.com/journals/omcl/2019/7218936/.

Mo L, Wang Y, Geary L, Corey C, Alef MJ, Beer-Stolz D, Zuckerbraun BS, Shiva S (2012) Nitrite Activates AMP Kinase to Stimulate Mitochondrial Biogenesis Independent of soluble Guanylate Cyclase. Free Radic. Biol. Med. **53**: 1440–1450. doi:10.1016/j.freeradbiomed.2012.07.080.

Moe IT, Pham TA, Hagelin EMV, Ahmed MS, Attramadal H (2013) CCN2 exerts direct cytoprotective actions in adult cardiac myocytes by activation of the PI3-kinase/Akt/GSK-3β signaling pathway. J. Cell Commun. Signal. **7**: 31–47. doi:10.1007/s12079-012-0183-1.

Mohler ER, Hiatt WR, Gornik HL, Kevil CG, Quyyumi A, Haynes WG, Annex BH (2014) Sodium nitrite in patients with peripheral artery disease and diabetes mellitus: Safety, walking distance and endothelial function. Vasc. Med. **19**: 9–17. doi:10.1177/1358863X13515043.

Muraski JA, Rota M, Misao Y, Fransioli J, Cottage C, Gude N, Esposito G, Delucchi F, Arcarese M, Alvarez R, Siddiqi S, Emmanuel GN, Wu W, Fischer K, Martindale JJ, Glembotski CC, Leri A, Kajstura J, Magnuson N, Berns A, Beretta RM, Houser SR, Schaefer EM, Anversa P, Sussman MA (2007) Pim-1 regulates cardiomyocyte survival downstream of Akt. Nat. Med. **13**: 1467–1475. doi:10.1038/nm1671.

Murrell W (1879) NITRO-GLYCERINE AS A REMEDY FOR ANGINA PECTORIS. The Lancet **113**. Originally published as Volume 1, Issue 2890: 80–81. doi:10.1016/S0140-6736(02)46032-1.

Nan J, Zhu W, Rahman MS, Liu M, Li D, Su S, Zhang N, Hu X, Yu H, Gupta MP, Wang J (2017) Molecular regulation of mitochondrial dynamics in cardiac disease. Biochim. Biophys. Acta Mol. Cell Res. **1864**: 1260–1273. doi:10.1016/j.bbamcr.2017.03.006.
Narendra DP, Jin SM, Tanaka A, Suen D-F, Gautier CA, Shen J, Cookson MR, Youle RJ (2010) PINK1 Is Selectively Stabilized on Impaired Mitochondria to Activate Parkin. PLoS Biol. **8**. doi:10.1371/journal.pbio.1000298. http://www.ncbi.nlm.nih.gov/pmc/articles/PMC2811155/.
Nitulescu GM, Van De Venter M, Nitulescu G, Ungurianu A, Juzenas P, Peng Q, Olaru OT, Grădinaru D, Tsatsakis A, Tsoukalas D, Spandidos DA, Margina D (2018) The Akt pathway in oncology therapy and beyond (Review). Int. J. Oncol. **53**: 2319–2331. doi:10.3892/ijo.2018.4597.
O'Brien KA, Horscroft JA, Devaux J, Lindsay RT, Steel AS, Clark AD, Philp A, Harridge SDR, Murray AJ (2019) PPARα-independent effects of nitrate supplementation on skeletal muscle metabolism in hypoxia. Biochim. Biophys. Acta BBA - Mol. Basis Dis. **1865**. The power of metabolism: Linking energy supply and demand to contractile function: 844–853. doi:10.1016/j.bbadis.2018.07.027.
Ohtake K, Nakano G, Ehara N, Sonoda K, Ito J, Uchida H, Kobayashi J (2015) Dietary nitrite supplementation improves insulin resistance in type 2 diabetic KKA(y) mice. Nitric Oxide Biol. Chem. Off. J. Nitric Oxide Soc. **44**: 31–38. doi:10.1016/j.niox.2014.11.009.
Okada M, Morioka S, Kanazawa H, Yamawaki H (2016) Canstatin inhibits isoproterenol-induced apoptosis through preserving mitochondrial morphology in differentiated H9c2 cardiomyoblasts. Apoptosis **21**: 887–895. doi:10.1007/s10495-016-1262-1.
Omar SA, Webb AJ, Lundberg JO, Weitzberg E (2016) Therapeutic effects of inorganic nitrate and nitrite in cardiovascular and metabolic diseases. J. Intern. Med. **279**: 315–336. doi:10.1111/joim.12441.
Omar SA, Webb AJ (2014) Nitrite reduction and cardiovascular protection. J. Mol. Cell. Cardiol. **73**. Redox Signalling in the Cardiovascular System: 57–69. doi:10.1016/j.yjmcc.2014.01.012.
Ong S-B, Hall AR, Hausenloy DJ (2013) Mitochondrial dynamics in cardiovascular health and disease. Antioxid. Redox Signal. **19**: 400–414. doi:10.1089/ars.2012.4777.
Ong S-B, Kalkhoran SB, Cabrera-Fuentes HA, Hausenloy DJ (2015) Mitochondrial fusion and fission proteins as novel therapeutic targets for treating cardiovascular disease. Eur. J. Pharmacol. **763**: 104–114. doi:10.1016/j.ejphar.2015.04.056.
Osaki M, Oshimura M, Ito H (2004) PI3K-Akt pathway: its functions and alterations in human cancer. Apoptosis Int. J. Program. Cell Death **9**: 667–676. doi:10.1023/B:APPT.0000045801.15585.dd.
Ott M, Gogvadze V, Orrenius S, Zhivotovsky B (2007) Mitochondria, oxidative stress and cell death. Apoptosis **12**: 913–922. doi:10.1007/s10495-007-0756-2.
PACHER P, BECKMAN JS, LIAUDET L (2007) Nitric Oxide and Peroxynitrite in Health and Disease. Physiol. Rev. **87**: 315–424. doi:10.1152/physrev.00029.2006.
Pagliuso A, Tham TN, Stevens JK, Lagache T, Persson R, Salles A, Olivo-Marin J, Oddos S, Spang A, Cossart P, Stavru F (2016) A role for septin 2 in Drp1-mediated mitochondrial fission. EMBO Rep. **17**: 858–873. doi:10.15252/embr.201541612.
Palmeira CM, Rolo AP, Berthiaume J, Bjork JA, Wallace KB (2007) Hyperglycemia decreases mitochondrial function: the regulatory role of mitochondrial biogenesis. Toxicol. Appl. Pharmacol. **225**: 214–220. doi:10.1016/j.taap.2007.07.015.

Park YS, Choi SE, Koh HC (2018) PGAM5 regulates PINK1/Parkin-mediated mitophagy via DRP1 in CCCP-induced mitochondrial dysfunction. Toxicol. Lett. **284**: 120–128. doi:10.1016/j.toxlet.2017.12.004.
Parker JD, Gori T (2009) Nitrate-induced tolerance, toxicity and preconditioning: a rationale for reconsidering the use of these drugs. BMC Pharmacol. **9**: S30. doi:10.1186/1471-2210-9-S1-S30.
Patel RP, McAndrew J, Sellak H, White CR, Jo H, Freeman BA, Darley-Usmar VM (1999) Biological aspects of reactive nitrogen species. Biochim. Biophys. Acta BBA - Bioenerg. **1411**: 385–400. doi:10.1016/S0005-2728(99)00028-6.
Perelman A, Wachtel C, Cohen M, Haupt S, Shapiro H, Tzur A (2012) JC-1: alternative excitation wavelengths facilitate mitochondrial membrane potential cytometry. Cell Death Dis. **3**: e430–e430. doi:10.1038/cddis.2012.171.
Pieme CA, Tatangmo JA, Simo G, Biapa Nya PC, Ama Moor VJ, Moukette Moukette B, Tankeu Nzufo F, Njinkio Nono BL, Sobngwi E (2017) Relationship between hyperglycemia, antioxidant capacity and some enzymatic and non-enzymatic antioxidants in African patients with type 2 diabetes. BMC Res. Notes **10**. doi:10.1186/s13104-017-2463-6.
https://www.ncbi.nlm.nih.gov/pmc/articles/PMC5372257/.
Pinheiro LC, Montenegro MF, Amaral JH, Ferreira GC, Oliveira AM, Tanus-Santos JE (2012) Increase in gastric pH reduces hypotensive effect of oral sodium nitrite in rats. Free Radic. Biol. Med. **53**: 701–709. doi:10.1016/j.freeradbiomed.2012.06.001.
Pride CK, Mo L, Quesnelle K, Dagda RK, Murillo D, Geary L, Corey C, Portella R, Zharikov S, Croix CS, Maniar S, Chu CT, Khoo NKH, Shiva S (2014) Nitrite activates protein kinase A in normoxia to mediate mitochondrial fusion and tolerance to ischaemia/reperfusion. Cardiovasc. Res. **101**: 57–68. doi:10.1093/cvr/cvt224.
Pushpa-Rekha TR, Burdsall AL, Oleksa LM, Chisolm GM, Driscoll DM (1995) Rat phospholipid-hydroperoxide glutathione peroxidase. cDNA cloning and identification of multiple transcription and translation start sites. J. Biol. Chem. **270**: 26993–26999. doi:10.1074/jbc.270.45.26993.
Rana P, Nadanaciva S, Will Y (2011) Mitochondrial membrane potential measurement of H9c2 cells grown in high-glucose and galactose-containing media does not provide additional predictivity towards mitochondrial assessment. Toxicol. In Vitro **25**: 580–587. doi:10.1016/j.tiv.2010.11.016.
Raubenheimer K, Hickey D, Leveritt M, Fassett R, Ortiz de Zevallos Munoz J, Allen JD, Briskey D, Parker TJ, Kerr G, Peake JM, Pecheniuk NM, Neubauer O (2017) Acute Effects of Nitrate-Rich Beetroot Juice on Blood Pressure, Hemostasis and Vascular Inflammation Markers in Healthy Older Adults: A Randomized, Placebo-Controlled Crossover Study. Nutrients **9**. doi:10.3390/nu9111270.
Reers M, Smith TW, Chen LB (1991) J-aggregate formation of a carbocyanine as a quantitative fluorescent indicator of membrane potential. Biochemistry **30**: 4480–4486. doi:10.1021/bi00232a015.
Rehman J, Zhang HJ, Toth PT, Zhang Y, Marsboom G, Hong Z, Salgia R, Husain AN, Wietholt C, Archer SL (2012) Inhibition of mitochondrial fission prevents cell cycle progression in lung cancer. FASEB J. Off. Publ. Fed. Am. Soc. Exp. Biol. **26**: 2175–2186. doi:10.1096/fj.11-196543.

d'El-Rei J, Cunha AR, Trindade M, Neves MF (2016) Beneficial Effects of Dietary Nitrate on Endothelial Function and Blood Pressure Levels. Int. J. Hypertens. **2016**. doi:10.1155/2016/6791519. http://www.ncbi.nlm.nih.gov/pmc/articles/PMC4819099/.

Roberts LD, Ashmore T, McNally BD, Murfitt SA, Fernandez BO, Feelisch M, Lindsay R, Siervo M, Williams EA, Murray AJ, Griffin JL (2017) Inorganic Nitrate Mimics Exercise-Stimulated Muscular Fiber-Type Switching and Myokine and γ-Aminobutyric Acid Release. Diabetes **66**: 674–688. doi:10.2337/db16-0843.

Rouschop KM, Dubois LJ, Keulers TG, van den Beucken T, Lambin P, Bussink J, van der Kogel AJ, Koritzinsky M, Wouters BG (2013) PERK/eIF2α signaling protects therapy resistant hypoxic cells through induction of glutathione synthesis and protection against ROS. Proc. Natl. Acad. Sci. U. S. A. **110**: 4622–4627. doi:10.1073/pnas.1210633110.

Saks VA, Kuznetsov AV, Vendelin M, Guerrero K, Kay L, Seppet EK (2004) Functional coupling as a basic mechanism of feedback regulation of cardiac energy metabolism. Mol. Cell. Biochem. **256–257**: 185–199. doi:10.1023/b:mcbi.0000009868.92189.fb.

Scandroglio F, Tórtora V, Radi R, Castro L (2014) Metabolic control analysis of mitochondrial aconitase: influence over respiration and mitochondrial superoxide and hydrogen peroxide production. Free Radic. Res. **48**: 684–693. doi:10.3109/10715762.2014.900175.

Shannon OM, McGawley K, Nybäck L, Duckworth L, Barlow MJ, Woods D, Siervo M, O'Hara JP (2017) "Beet-ing" the Mountain: A Review of the Physiological and Performance Effects of Dietary Nitrate Supplementation at Simulated and Terrestrial Altitude. Sports Med. Auckl. Nz **47**: 2155–2169. doi:10.1007/s40279-017-0744-9.

Sharp WW (2015) Dynamin-related protein 1 as a therapeutic target in cardiac arrest. J. Mol. Med. **93**: 243–252. doi:10.1007/s00109-015-1257-3.

Sharp WW, Archer SL (2015) Mitochondrial dynamics in cardiovascular disease: fission and fusion foretell form and function. J. Mol. Med. **93**: 225–228. doi:10.1007/s00109-015-1258-2.

Shen X, Zheng S, Metreveli NS, Epstein PN (2006) Protection of Cardiac Mitochondria by Overexpression of MnSOD Reduces Diabetic Cardiomyopathy. Diabetes **55**: 798–805. doi:10.2337/diabetes.55.03.06.db05-1039.

Shimabukuro M, Ohneda M, Lee Y, Unger RH (1997) Role of nitric oxide in obesity-induced beta cell disease. J. Clin. Invest. **100**: 290–295.

Shiva S, Wang X, Ringwood LA, Xu X, Yuditskaya S, Annavajjhala V, Miyajima H, Hogg N, Harris ZL, Gladwin MT (2006) Ceruloplasmin is a NO oxidase and nitrite synthase that determines endocrine NO homeostasis. Nat. Chem. Biol. **2**: 486–493. doi:10.1038/nchembio813.

Siervo M, Scialò F, Shannon OM, Stephan BCM, Ashor AW (2018) Does dietary nitrate say NO to cardiovascular ageing? Current evidence and implications for research. Proc. Nutr. Soc. **77**: 112–123. doi:10.1017/S0029665118000058.

da Silva AF, Mariotti FR, Máximo V, Campello S (2014) Mitochondria dynamism: of shape, transport and cell migration. Cell. Mol. Life Sci. **71**: 2313–2324. doi:10.1007/s00018-014-1557-8.

Sivandzade F, Bhalerao A, Cucullo L (2019) Analysis of the Mitochondrial Membrane Potential Using the Cationic JC-1 Dye as a Sensitive Fluorescent Probe. Bio-Protoc. **9**. doi:10.21769/BioProtoc.3128.
http://www.ncbi.nlm.nih.gov/pmc/articles/PMC6343665/.

Skárka L, Bardová K, Brauner P, Flachs P, Jarkovská D, Kopecký J, Ostádal B (2003) Expression of mitochondrial uncoupling protein 3 and adenine nucleotide translocase 1 genes in developing rat heart: putative involvement in control of mitochondrial membrane potential. J. Mol. Cell. Cardiol. **35**: 321–330. doi:10.1016/s0022-2828(03)00016-6.
Skulachev VP (1996) Role of uncoupled and non-coupled oxidations in maintenance of safely low levels of oxygen and its one-electron reductants. Q. Rev. Biophys. **29**: 169–202.
Smiley ST, Reers M, Mottola-Hartshorn C, Lin M, Chen A, Smith TW, Steele GD, Chen LB (1991) Intracellular heterogeneity in mitochondrial membrane potentials revealed by a J-aggregate-forming lipophilic cation JC-1. Proc. Natl. Acad. Sci. U. S. A. **88**: 3671–3675.
Smirnova E, Shurland D-L, Ryazantsev SN, van der Bliek AM (1998) A Human Dynamin-related Protein Controls the Distribution of Mitochondria. J. Cell Biol. **143**: 351–358.
Smith PK, Krohn RI, Hermanson GT, Mallia AK, Gartner FH, Provenzano MD, Fujimoto EK, Goeke NM, Olson BJ, Klenk DC (1985) Measurement of protein using bicinchoninic acid. Anal. Biochem. **150**: 76–85. doi:10.1016/0003-2697(85)90442-7.
Song Moshi, Gong Guohua, Burelle Yan, Gustafsson Åsa B., Kitsis Richard N., Matkovich Scot J., Dorn Gerald W. (2015) Interdependence of Parkin-Mediated Mitophagy and Mitochondrial Fission in Adult Mouse Hearts. Circ. Res. **117**: 346–351. doi:10.1161/CIRCRESAHA.117.306859.
Sparacino-Watkins CE, Tejero J, Sun B, Gauthier MC, Thomas J, Ragireddy V, Merchant BA, Wang J, Azarov I, Basu P, Gladwin MT (2014) Nitrite Reductase and Nitric-oxide Synthase Activity of the Mitochondrial Molybdopterin Enzymes mARC1 and mARC2. J. Biol. Chem. **289**: 10345–10358. doi:10.1074/jbc.M114.555177.
Steinberg HO, Brechtel G, Johnson A, Fineberg N, Baron AD (1994) Insulin-mediated skeletal muscle vasodilation is nitric oxide dependent. A novel action of insulin to increase nitric oxide release. J. Clin. Invest. **94**: 1172–1179. doi:10.1172/JCI117433.
Suski J, Lebiedzinska M, Bonora M, Pinton P, Duszynski J, Wieckowski MR (2018) Relation Between Mitochondrial Membrane Potential and ROS Formation. Methods Mol. Biol. Clifton NJ **1782**: 357–381. doi:10.1007/978-1-4939-7831-1_22.
Suski JM, Lebiedzinska M, Bonora M, Pinton P, Duszynski J, Wieckowski MR (2012) Relation between mitochondrial membrane potential and ROS formation. Methods Mol. Biol. Clifton NJ **810**: 183–205. doi:10.1007/978-1-61779-382-0_12.
Symons JD, McMillin SL, Riehle C, Tanner J, Palionyte M, Hillas E, Jones D, Cooksey RC, Birnbaum MJ, McClain DA, Zhang Q-J, Gale D, Wilson LJ, Abel ED (2009) Contribution of Insulin and Akt1 Signaling to Endothelial Nitric Oxide Synthase in the Regulation of Endothelial Function and Blood Pressure. Circ. Res. **104**: 1085–1094. doi:10.1161/CIRCRESAHA.108.189316.
Taguchi N, Ishihara N, Jofuku A, Oka T, Mihara K (2007) Mitotic Phosphorylation of Dynamin-related GTPase Drp1 Participates in Mitochondrial Fission. J. Biol. Chem. **282**: 11521–11529. doi:10.1074/jbc.M607279200.
Tait SWG, Green DR (2012) Mitochondria and cell signalling. J. Cell Sci. **125**: 807–815. doi:10.1242/jcs.099234.
Thadani U, Rodgers T (2006) Side effects of using nitrates to treat angina. Expert Opin. Drug Saf. **5**: 667–674. doi:10.1517/14740338.5.5.667.
Tilokani L, Nagashima S, Paupe V, Prudent J (2018) Mitochondrial dynamics: overview of molecular mechanisms. Essays Biochem. **62**: 341–360. doi:10.1042/EBC20170104.

Tomer D, Chippalkatti R, Mitra K, Rikhy R (2018) ERK regulates mitochondrial membrane potential in fission deficient Drosophila follicle cells during differentiation. Dev. Biol. **434**: 48–62. doi:10.1016/j.ydbio.2017.11.009.
Tórtora V, Quijano C, Freeman B, Radi R, Castro L (2007) Mitochondrial aconitase reaction with nitric oxide, S-nitrosoglutathione, and peroxynitrite: Mechanisms and relative contributions to aconitase inactivation. Free Radic. Biol. Med. **42**: 1075–1088. doi:10.1016/j.freeradbiomed.2007.01.007.
Tricker AR (1997) N-nitroso compounds and man: sources of exposure, endogenous formation and occurrence in body fluids. Eur. J. Cancer Prev. Off. J. Eur. Cancer Prev. Organ. ECP **6**: 226–268.
Truitt R, Mu A, Corbin EA, Vite A, Brandimarto J, Ky B, Margulies KB (2018) Increased Afterload Augments Sunitinib-Induced Cardiotoxicity in an Engineered Cardiac Microtissue Model. JACC Basic Transl. Sci. **3**: 265–276. doi:10.1016/j.jacbts.2017.12.007.
Twig G, Elorza A, Molina AJA, Mohamed H, Wikstrom JD, Walzer G, Stiles L, Haigh SE, Katz S, Las G, Alroy J, Wu M, Py BF, Yuan J, Deeney JT, Corkey BE, Shirihai OS (2008) Fission and selective fusion govern mitochondrial segregation and elimination by autophagy. EMBO J. **27**: 433–446. doi:10.1038/sj.emboj.7601963.
Valdivieso ÁG, Dugour AV, Sotomayor V, Clauzure M, Figueroa JM, Santa-Coloma TA (2018) N-acetyl cysteine reverts the proinflammatory state induced by cigarette smoke extract in lung Calu-3 cells. Redox Biol. **16**: 294–302. doi:10.1016/j.redox.2018.03.006.
Vanderpool Rebecca, Gladwin Mark T. (2015) Harnessing the Nitrate–Nitrite–Nitric Oxide Pathway for Therapy of Heart Failure With Preserved Ejection Fraction. Circulation **131**: 334–336. doi:10.1161/CIRCULATIONAHA.114.014149.
Vanhatalo A, Bailey SJ, Blackwell JR, DiMenna FJ, Pavey TG, Wilkerson DP, Benjamin N, Winyard PG, Jones AM (2010) Acute and chronic effects of dietary nitrate supplementation on blood pressure and the physiological responses to moderate-intensity and incremental exercise. Am. J. Physiol.-Regul. Integr. Comp. Physiol. **299**: R1121–R1131. doi:10.1152/ajpregu.00206.2010.
Vantaggiato C, Castelli M, Giovarelli M, Orso G, Bassi MT, Clementi E, De Palma C (2019) The Fine Tuning of Drp1-Dependent Mitochondrial Remodeling and Autophagy Controls Neuronal Differentiation. Cell. Neurosci.: 120. doi:10.3389/fncel.2019.00120.
Varanita T, Soriano ME, Romanello V, Zaglia T, Quintana-Cabrera R, Semenzato M, Menabò R, Costa V, Civiletto G, Pesce P, Viscomi C, Zeviani M, Di Lisa F, Mongillo M, Sandri M, Scorrano L (2015) The Opa1-Dependent Mitochondrial Cristae Remodeling Pathway Controls Atrophic, Apoptotic, and Ischemic Tissue Damage. Cell Metab. **21**: 834–844. doi:10.1016/j.cmet.2015.05.007.
Velmurugan S, Gan JM, Rathod KS, Khambata RS, Ghosh SM, Hartley A, Eijl SV, Sagi-Kiss V, Chowdhury TA, Curtis M, Kuhnle GG, Wade WG, Ahluwalia A (2015) Dietary nitrate improves vascular function in patients with hypercholesterolemia: a randomized, double-blind, placebo-controlled study. Am. J. Clin. Nutr.: ajcn116244. doi:10.3945/ajcn.115.116244.
Velmurugan S, Kapil V, Ghosh SM, Davies S, McKnight A, Aboud Z, Khambata RS, Webb AJ, Poole A, Ahluwalia A (2013) Antiplatelet effects of dietary nitrate in healthy volunteers: Involvement of cGMP and influence of sex. Free Radic. Biol. Med. **65**: 1521–1532. doi:10.1016/j.freeradbiomed.2013.06.031.

Villa-Abrille MC, Sidor A, O'Rourke B (2008) Insulin Effects on Cardiac Na+/Ca2+ Exchanger Activity ROLE OF THE CYTOPLASMIC REGULATORY LOOP. J. Biol. Chem. **283**: 16505–16513. doi:10.1074/jbc.M801424200.

Wai T, Langer T (2016) Mitochondrial Dynamics and Metabolic Regulation. Trends Endocrinol. Metab. **27**: 105–117. doi:10.1016/j.tem.2015.12.001.

Walker MA, Bailey TG, McIlvenna L, Allen JD, Green DJ, Askew CD (2019) Acute Dietary Nitrate Supplementation Improves Flow Mediated Dilatation of the Superficial Femoral Artery in Healthy Older Males. Nutrients **11**. doi:10.3390/nu11050954. http://www.ncbi.nlm.nih.gov/pmc/articles/PMC6566150/.

Wang K, Deng X, Shen Z, Jia Y, Ding R, Li R, Liao X, Wang S, Ha Y, Kong Y, Wu Y, Guo J, Jie W (2017) High glucose promotes vascular smooth muscle cell proliferation by upregulating proto-oncogene serine/threonine-protein kinase Pim-1 expression. Oncotarget **8**: 88320–88331. doi:10.18632/oncotarget.19368.

Wang Y, Feng W, Xue W, Tan Y, Hein DW, Li X-K, Cai L (2009) Inactivation of GSK-3β by Metallothionein Prevents Diabetes-Related Changes in Cardiac Energy Metabolism, Inflammation, Nitrosative Damage, and Remodeling. Diabetes **58**: 1391–1402. doi:10.2337/db08-1697.

Wang Z, Bhattacharya N, Mixter PF, Wei W, Sedivy J, Magnuson NS (2002) Phosphorylation of the cell cycle inhibitor p21Cip1/WAF1 by Pim-1 kinase. Biochim. Biophys. Acta **1593**: 45–55. doi:10.1016/s0167-4889(02)00347-6.

Wang Z, Yin F, Xu J, Zhang T, Wang G, Mao M, Wang Z, Sun W, Han J, Yang M, Jiang Y, Hua Y, Cai Z (2019) CYT997(Lexibulin) induces apoptosis and autophagy through the activation of mutually reinforced ER stress and ROS in osteosarcoma. J. Exp. Clin. Cancer Res. **38**: 44. doi:10.1186/s13046-019-1047-9.

Webb AJ, Milsom AB, Rathod KS, Chu WL, Qureshi S, Lovell MJ, Lecomte FMJ, Perrett D, Raimondo C, Khoshbin E, Ahmed Z, Uppal R, Benjamin N, Hobbs AJ, Ahluwalia A (2008) Mechanisms Underlying Erythrocyte and Endothelial Nitrite Reduction to Nitric Oxide in Hypoxia Role for Xanthine Oxidoreductase and Endothelial Nitric Oxide Synthase. Circ. Res. **103**: 957–964. doi:10.1161/CIRCRESAHA.108.175810.

Wei YH, Lu CY, Wei CY, Ma YS, Lee HC (2001) Oxidative stress in human aging and mitochondrial disease-consequences of defective mitochondrial respiration and impaired antioxidant enzyme system. Chin. J. Physiol. **44**: 1–11.

Weitzberg E, Hezel M, Lundberg JO (2010) Nitrate-Nitrite-Nitric Oxide PathwayImplications for Anesthesiology and Intensive Care. Anesthesiol. J. Am. Soc. Anesthesiol. **113**: 1460–1475. doi:10.1097/ALN.0b013e3181fcf3cc.

Whang YE, Yuan X-J, Liu Y, Majumder S, Lewis TD (2004) Regulation of Sensitivity to TRAIL by the PTEN Tumor Suppressor. In Vitam. Horm., **67**409–426. Academic Press, January 1. TRAIL (TNF-Related Apoptosis-Inducing Ligand). doi:10.1016/S0083-6729(04)67021-X.
http://www.sciencedirect.com/science/article/pii/S008367290467021X.

Wiemerslage L, Lee D (2016) Quantification of Mitochondrial Morphology in Neurites of Dopaminergic Neurons using Multiple Parameters. J. Neurosci. Methods **262**: 56–65. doi:10.1016/j.jneumeth.2016.01.008.

Wong H-S, Dighe PA, Mezera V, Monternier P-A, Brand MD (2017) Production of superoxide and hydrogen peroxide from specific mitochondrial sites under different bioenergetic conditions. J. Biol. Chem.: jbc.R117.789271. doi:10.1074/jbc.R117.789271.

Wu G, Meininger CJ (2009) Nitric oxide and vascular insulin resistance. BioFactors Oxf. Engl. **35**: 21–27. doi:10.1002/biof.3.
Wylie LJ, Park JW, Vanhatalo A, Kadach S, Black MI, Stoyanov Z, Schechter AN, Jones AM, Piknova B (2019) Human skeletal muscle nitrate store: influence of dietary nitrate supplementation and exercise. J. Physiol. doi:10.1113/JP278076.
Xie L, Shi F, Tan Z, Li Y, Bode AM, Cao Y (2018) Mitochondrial network structure homeostasis and cell death. Cancer Sci. **109**: 3686–3694. doi:10.1111/cas.13830.
Xie Z, Zhang J, Wu J, Viollet B, Zou M-H (2008) Upregulation of Mitochondrial Uncoupling Protein-2 by the AMP-Activated Protein Kinase in Endothelial Cells Attenuates Oxidative Stress in Diabetes. Diabetes **57**: 3222–3230. doi:10.2337/db08-0610.
Yang K, Chen Z, Gao J, Shi W, Li L, Jiang S, Hu H, Liu Z, Xu D, Wu L (2017) The Key Roles of GSK-3β in Regulating Mitochondrial Activity. Cell. Physiol. Biochem. **44**: 1445–1459. doi:10.1159/000485580.
Yoshii SR, Kishi C, Ishihara N, Mizushima N (2011) Parkin Mediates Proteasome-dependent Protein Degradation and Rupture of the Outer Mitochondrial Membrane. J. Biol. Chem. **286**: 19630–19640. doi:10.1074/jbc.M110.209338.
Youle RJ, Narendra DP (2011) Mechanisms of mitophagy. Nat. Rev. Mol. Cell Biol. **12**: 9–14. doi:10.1038/nrm3028.
Yu T, Robotham JL, Yoon Y (2006) Increased production of reactive oxygen species in hyperglycemic conditions requires dynamic change of mitochondrial morphology. Proc. Natl. Acad. Sci. U. S. A. **103**: 2653–2658. doi:10.1073/pnas.0511154103.
Yu T, Sheu S-S, Robotham JL, Yoon Y (2008) Mitochondrial fission mediates high glucose-induced cell death through elevated production of reactive oxygen species. Cardiovasc. Res. **79**: 341–351. doi:10.1093/cvr/cvn104.
Zeballos GA, Bernstein RD, Thompson CI, Forfia PR, Seyedi N, Shen W, Kaminiski PM, Wolin MS, Hintze TH (1995) Pharmacodynamics of plasma nitrate/nitrite as an indication of nitric oxide formation in conscious dogs. Circulation **91**: 2982–2988.
Zhai P, Gao S, Holle E, Yu X, Yatani A, Wagner T, Sadoshima J (2007) Glycogen Synthase Kinase-3α Reduces Cardiac Growth and Pressure Overload-induced Cardiac Hypertrophy by Inhibition of Extracellular Signal-regulated Kinases. J. Biol. Chem. **282**: 33181–33191. doi:10.1074/jbc.M705133200.
Zhang Y, Babcock SA, Hu N, Maris JR, Wang H, Ren J (2012) Mitochondrial aldehyde dehydrogenase (ALDH2) protects against streptozotocin-induced diabetic cardiomyopathy: role of GSK3β and mitochondrial function. BMC Med. **10**: 40. doi:10.1186/1741-7015-10-40.
Zhao R, Jiang S, Zhang L, Yu Z (2019) Mitochondrial electron transport chain, ROS generation and uncoupling (Review). Int. J. Mol. Med. doi:10.3892/ijmm.2019.4188. http://www.spandidos-publications.com/10.3892/ijmm.2019.4188.
Zhou J, Lal H, Chen X, Shang X, Song J, Li Y, Kerkela R, Doble BW, MacAulay K, DeCaul M, Koch WJ, Farber J, Woodgett J, Gao E, Force T (2010) GSK-3α directly regulates β-adrenergic signaling and the response of the heart to hemodynamic stress in mice. J. Clin. Invest. **120**: 2280–2291. doi:10.1172/JCI41407.
Zhu T, Chen J-L, Wang Q, Shao W, Qi B (2018) Modulation of Mitochondrial Dynamics in Neurodegenerative Diseases: An Insight Into Prion Diseases. Front. Aging Neurosci.: 336. doi:10.3389/fnagi.2018.00336.

Zou P, Liu L, Zheng LD, Payne KK, Manjili MH, Idowu MO, Zhang J, Schmelz EM, Cheng Z (2016) Coordinated Upregulation of Mitochondrial Biogenesis and Autophagy in Breast Cancer Cells: The Role of Dynamin Related Protein-1 and Implication for Breast Cancer Treatment. Oxid. Med. Cell. Longev. **2016**: 4085727. doi:10.1155/2016/4085727.
Zweier JL, Wang P, Samouilov A, Kuppusamy P (1995) Enzyme-independent formation of nitric oxide in biological tissues. Nat. Med. **1**: 804–809. doi:10.1038/nm0895-804.

IX. Annexures

Urkund Analysis Result

Analysed Document: thesis until results.pdf (D57596165)
Submitted: 10/24/2019 3:06:00 PM
Submitted By: srinivasg@sctimst.ac.in
Significance: 0 %

Sources included in the report:

THESIS - Theodore Lemuel Mathuram.pdf (D24506531)
https://www.researchgate.net/publication/11293227_Microarray_Analysis_of_the_Mycobacterium_tuberculosis_Transcriptional_Response_to_the_Acidic_Conditions_Found_in_Phagosomes

Instances where selected sources appear:

3